AD

TECHNICAL REPORT

73-7-FL

ACCELERATOR RADIATION PROTECTION

Edited by

THOMAS G. MARTIN, III

Radiation Sources Division

Project Reference: 1T061101A91A07

1972

UNITED STATES ARMY
NATICK LABORATORIES
Natick, Massachusetts 01760

Food Laboratory

FL—169

Approved for public release; distribution unlimited.

Citation of trade names in this report does not constitute an official indorsement or approval of the use of such items.

Destroy this report when no longer needed. Do not return it to the originator.

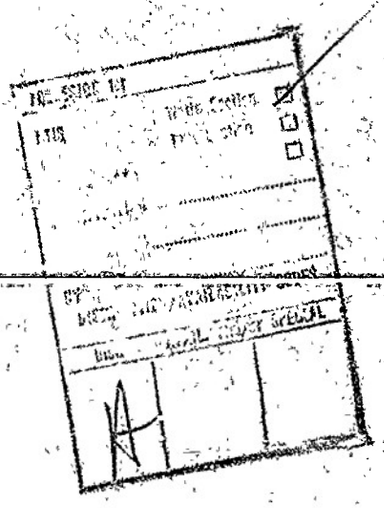

UNCLASSIFIED
Security Classification

DOCUMENT CONTROL DATA - R & D

(Security classification of title, body of abstract and indexing annotation must be entered when the overall report is classified)

1 ORIGINATING ACTIVITY (Corporate author) US Army Natick Laboratories Natick, Massachusetts 01760	2a. REPORT SECURITY CLASSIFICATION Unclassified 2b. GROUP

3 REPORT TITLE
Accelerator Radiation Protection

4. DESCRIPTIVE NOTES (Type of report and inclusive dates)

5 AUTHOR(S) (First name, middle initial, last name)
Thomas G. Martin, III

6. REPORT DATE June 1972	7a. TOTAL NO. OF PAGES 250 / 95	7b. NO. OF REFS 200
8a. CONTRACT OR GRANT NO. b. PROJECT NO. 1T061101A91A07 c. d.	9a. ORIGINATOR'S REPORT NUMBER(S) 9b. OTHER REPORT NO(S) (Any other numbers that may be assigned this report) FL-169	

10. DISTRIBUTION STATEMENT
Approved for public release, Distribution unlimited.

11. SUPPLEMENTARY NOTES	12. SPONSORING MILITARY ACTIVITY US Army Natick Laboratories Natick, Massachusetts 01760

13. ABSTRACT

The eight chapters of this report cover much of the material needed in the evaluation of design and operational safety for particle accelerators below 40-50 MeV. Each chapter deals with a phase of the problem such as x-ray shielding (Chapter II) neutron shielding (Chapter III) and induced radioactivity (Chapter IV).

I-a

DD FORM 1 NOV 65 1473 REPLACES DD FORM 1473, 1 JAN 64, WHICH IS OBSOLETE FOR ARMY USE.

Unclassified
Security Classification

14 KEY WORDS	LINK A		LINK B		LINK C	
	ROLE	WT	ROLE	WT	ROLE	WT
Design	8		4			
Construction	8		4			
Safe Handling	8		4			
Particle Accelerators	9		9			
Cyclotrons	9		9			
Low Energy	0		0			
40-50 MeV	0		0			
Shielding			8			
Radiation Shielding			8			
X-Ray Shielding			8			
Neutron Shielding			8			
Radioactivity			8			
Induced Radioactivity			8			
Elevation			4			

I-f

Distribution of this
document is unlimited

AD_____

Technical Report
TR–73–7

ACCELERATOR RADIATION PROTECTION

Edited by

THOMAS G. MARTIN, III

Radiation Sources Division

Project Reference:
1T061101A91A07

FL–169

1972

Food Laboratory
U. S. ARMY NATICK LABORATORIES
Natick, Massachusetts

I-C

FOREWORD

In April 1969 a request to provide the U. S. Army Material Command guidance in the preparation of an army regulation on particle accelerator radiation protection prompted an examination of the need for a reference publication on this subject. The need was apparent and no suitable reference combined the vast amounts of information available in the literature. Though no single publication will ever contain all that is required to enable the design, construction and safe operation of all types of low energy particle accelerators, this report is intended to direct the reader along the right path.

This report was prepared under the support of the U. S. Army Natick Laboratories In-House Laboratory Independent Research program. The several authors were all members of the U. S. Army Natick Laboratories, Food Laboratory staff during the initial preparations of the various chapters.

Many scientists and engineers were of significant help in the preparation of this report. Helpful suggestions were received from Mr. Warren Ramler, Milan Oselka, George Mavriogenes, Preston Smith and Thomas Klippert of the Argonne National Laboratory, John Handloser, Cecil Sandifer and Austin O'Dell of Edgerton Germeshausin and Greer, Santa Barbara, California; Niel Norris, G. Tremblin and Brian Williams of General Atomics, San Diego, California; Norman Austin and Donald Lawrence of Varian Associates, Richard Meyer of Lawrence Radiation Laboratory; Don White and Harry Harrison of The U. S. Army White Sands Missile Range.

Special appreciation goes to the Staff of the Stanford Linear Accelerator Center, Dr. Richard McCall, Dr. Gorin Svensson, W. R. Nelson, Donald Busick and Kenneth Kase whose constructive criticism did much to help make the report of practical value.

Permission has been obtained for the use of copyrighted material from McGraw-Hill Book Company and The American Society of Mechanical Engineers.

ABSTRACT

The eight chapters of this report cover much of the material needed in the evaluation of design and operational safety for particle accelerators below 40-50 MeV. Each chapter deals with a phase of the problem such as x-ray shielding (Chapter II), neutron shielding (Chapter III), and induced radioactivity (Chapter IV).

TABLE OF CONTENTS

Chapter I

Accelerator Radiation Protection

Thomas G. Martin, III

Introduction

Few scientific and engineering accomplishments have had a more rapid growth then particle accelerators. The construction of the initial proton accelerator by Cockcroft and Walton in the early thirties was to usher in an era which would soon result in the development of such giants as the two mile Stanford Linear Accelerator, the 28 GeV CERN Proton Synchrotron in Switzerland and France, and the 200 GeV synchrotron at the National Accelerator Laboratory near Batavia, Illinois, U.S.A.

Along with a quest for higher energy there evolved new uses for low energy accelerators which indicated a need for machines capable of delivering large amounts of radiation for various purposes. It is the purpose of this chapter to examine some of these purposes, to quote some of the problem areas and in so doing to introduce subsequent chapters.

History

Experimental nuclear physics had its birth in 1919 with Rutherford's discovery that alpha particles from radium or thorium could disintegrate the nucleus of the nitrogen atom. Thereafter a search began to create tools which would enable experimenters to examine the structure of the nucleus. It was not until the early thirties that the particle accelerator was born. Cockcroft and Walton reported in 1932 that they had successfully disintegrated lithium with the 700 keV protons produced by their voltage multiplier in the Cavendish Laboratory[1].

Around the same time at Princeton University, R. J. Van de Graaff began his work on the silk belt charged electrostatic generator. In 1931 he described his first generator which developed about 1.5 MeV. At MIT after nearly 10 years of development, Professor Van de Graaff's accelerator produced dependable beams of electrons and positive ions of 2.75 MeV. The present day electrostatic generator is a "work horse" of the accelerator field.

Professor Ernest O. Lawrence proposed another approach to the acceleration of charged particles. His method produced acceleration in circular orbits with a high frequency magnetic field. The first cyclotron developed by Lawrence and Livingston at the University of California, produced 1.2 MeV protons in 1932[2]. Professor Lawrence received the Nobel Prize in Physics in 1939 for the development of the cyclotron.

By 1940 particles of 20 MeV were obtained which approached the practical limit for the fixed frequency cyclotron. With new designs higher and higher energies were obtained permitting further study of the structure of the nucleus and creation of new nuclear particles.

The development of higher energy machines was paralleled by the improvement of the dependability and capability of the lower energy machines. Requirements for intense (high current) beams developed. The population of machines producing radiation of energy less than 100 MeV has grown with a rate of about 10%/year from 1935 to 1969 to a total of more than 2400[3].

There were two general areas of utilization which accounted for most of the rapid growth of the low energy accelerator. The first was the interest of the medical field in the clinical applications of radiation (deep radiation therapy) strengthened by a more recent interest by nuclear medicine specialists in short lived radioisotope production by cyclotrons[4]. The second was the development of industrial radiation processing for certain biological and chemical effects (e.g., sterilization of medical supplies and radiation induced polymerization). Burrill[3] estimated that 34.9% of the low energy accelerators in the U. S. in 1969 were medical and 6.5% were employed in industrial processing. The growth rate for the industrial use, however, was approximately 30% between 1958 and 1970.

In his review of the shielding problem with low energy particle accelerators, Burrill[5] effectively classified the types of accelerators with which this book is concerned. His concluding paragraph expresses a hope that that article would "serve as a foundation for an effectual course of action". Though this work was well underway before Burrill's article appeared, the editor feels that enough of a foundation is laid in his article to warrant special reference here. A single publication which provides all of the information necessary to determine all that must be done to provide safety in the operation of all possible types of accelerators does not yet exist. This book, even over the limited energy span intended, also does not provide such complete information. It is the intent here to provide enough information to serve as a starter in the evaluation of a particular accelerator facility.

It is important to note that there can be no universal solution to all accelerator radiation problems and therefore it can not be over emphasized that each facility with all of its peculiar problems must be evaluated individually. Example problems have been worked for each chapter where practical. The problems are simple examples and not intended to reflect, except in a general way, the complexities in the design and evaluation of a particular accelerator installation.

Types of Accelerators

The goal of this book is to include all types of particle accelerators below about 50 MeV. Probably this may be too ambitious for a single short publication but at least by grouping and being a little general the goal may be suitably attained.

The choice of energy range to be considered here was dictated by several important parameters. Certainly the availability of highly competent personnel at the major high energy facilities reduces the requirement for a publication such as this for these installations.

Furthermore with increasing energy (above about 40 to 60 MeV) the documentation of behavior becomes progressively more difficult and less suitable to presentation in a simplified and condensed manner.

One of the most significant reasons for the low energy choice was the rapid growth in the population of accelerators in this range.

Table I-1 lists some of the types of particle accelerators which may operate in this energy range. Table I-2 lists some examples of the present uses of these accelerators.

In each of the following chapters some phase of the radiation protection problem is discussed.

For example the chapter dealing with X-ray production and shielding (II) notes that this problem although universally applicable to all machines is predominantly a problem of the electron accelerators. There is no intent to slight the positive ion accelerators but in these cases the significance of X-ray production is generally masked by the overwhelming significance of the neutron production.

A similar statement may be made (with somewhat less conviction) when discussing the neutron production of electron accelerators. That neutrons are produced provided sufficient energy is present is accepted as well as the general isotropy of their distribution. However, their significance is masked by the production of bremsstrahlung (X-ray) and this secondary radiation generally determines the shielding and other radiation protection procedures.

There are problems which are common to all types and sizes of accelerators. All accelerators require some area to be of restricted access. This area may vary from a small shielded box with an interlocked lid to large experimental halls with flight paths of many meters and complex beam handling systems. The means of limiting access and the techniques of determining which areas at any specific time require limiting access

TABLE I-1

Accelerator	Examples	Particles	Energy Range MeV
Potential Drop	Van de Graaf Cockcroft-Walton Dynamitron Resonant Transformer Insulating Core Transformer	e, p, d, α, He^+ H^3 and heavy ions	0.1 – $\simeq$ 20
Linear Accelerators	Electron Positive ion	electrons p,d, He^+H^3 and heavy ions	0.1 – > 50 0.1 – > 50
Cyclotrons	Fixed Frequency Frequency Modulated Variable Frequency	α, p, d, He^+ H^3	1 – > 50
Betatrons		electrons	1 – > 50

TABLE I-2

Some Uses of Low Energy Particle Accelerators

Field	Use	Advantages
Industry	Radiography — X-ray	Higher energy than isotopes enables examination of thick metal samples.
	Radiography — neutrons	Density resolution not available by standard means even isotopic resolution in some cases. (Low density materials inside of high density (rubber gaskets in steel)).
	Sterilization	Medical supplies may be sterilized without subject to excess heat, toxic chemicals or repackaging.
	Sprout inhibition	Potatoes may be stored for extended periods without growth of sprouts.
	Polymerization	Improved wood characteristics produced by polymerizing monomer-impregnated in the wood.
Medicine	Deep therapy (x-ray)	Betatron and linac produced x-rays of relatively high energy permit deep penetration.
	Deep therapy (charged particle)	Increased effectiveness of high LET radiation coupled with a reduced oxygen effect enhances therapeutic effect of charged particles ([7]).
	Deep therapy (neutrons)	Also have low oxygen enhancement ratio and produce lower bone doses than x-rays ([7,8]).
	Radioisotope Production	Short lived radioisotopes for nuclear medical applications produced on site.

TABLE I-2 (continued)

Some Uses of Low Energy Particle Accelerators

Field	Use	Advantages
Medicine (continued)	Activation Analysis	Forensic Medicine — permits analysis of trace elements nondestructively.
Education & Research	Nuclear Science	Relatively inexpensive source of particles to study nuclear scattering, nuclear reactions and nuclear structure.
	Activation Analysis	Versatile source for all types of A.A. neutron, photonuclear, and charged particles.
	Atomic physics	Permits the stripping of heavy ions and the study of atomic collisions of heavy ions ([9]).
	Radiation Chemistry	Use of pulse radiolysis techniques permits study of the kinetics of free radicals.

are nearly as varied as the number of facilities which consider these problems. A discussion of some of the available means of limiting access as well as monitoring systems for determining which areas require access limitation, is presented in chapters VI and VII.

Under this subject, interlock systems serving to provide effective control of areas, are described in a general way with specific attention to some limitations of certain systems.

During the operation of particle accelerators there are by-products produced which themselves require consideration in order to prevent hazardous conditions. Such products are toxic gases such as ozone and oxides of nitrogen; radioactive gases, such as ^{15}O, ^{13}N, ^{41}A and ^{3}H and induced radioactivity in shielding and accelerator parts. Some discussion on the rates of production of these products is presented in addition to an examination of the associated waste disposal problems in Chapters IV and VIII.

Study Committees

Several committees of distinguished scientists have addressed the problems of accelerator radiation protection. The International Commission on Radiological Protection (ICRP) was organized in 1928 under the auspices of the Second International Congress of Radiology, held in Stockholm, to deal with the problems of X-ray protection. The ICRP has several subcommittees which deal with the problems associated with the radiation from particle accelerators. Of particular interest here is a report of subcommittee 3, ICRP, on Calculation of Radiation Dose from Protons and Neutrons to 400 MeV[10].

The International Commission on Radiation Units and Measurements (ICRU), the oldest of these noted committees, has as its principle goal the development of internationally accepted recommendations concerning:

1. Quantities and units of radiation and radioactivity.

2. Procedures suitable for measuring and application of the quantities.

3. Physical data needed in the application of these procedures. ICRU reports on the dosimetry of X and gamma rays from 0.6 to 50 MeV (ICRU Report 14) and on Neutron Fluence, Energy Fluence, Neutron Spectra and Kerma (ICRU Report 13) are of particular interest here.

The National Council on Radiation Protection and Measurements (NCRP) grew from its original "Advisory Committee on X-Ray and Radium Protection" formed in 1929 as a recommendation of the ICRP, to its present size of 65 council members and 140 other participants. The council consists of a Board of Directors and 33 technical subcommittees. Of special interest are the subcommittees which deal with Heavy Particles (NCRP

Report 20), Electron Protection (NCRP Report 31), Radiation Shielding for Particle Accelerators (no reports issued as yet), Radiation Protection in the Use of Small Neutron Generators (no reports issued as yet) and High-Energy X-Ray Dosimetry (no reports issued as yet).

More recently another organization of highly competent personnel undertook to standardize the approach to solving accelerator radiation protection problems. The United States of American Standards Institute (USASI) have proposed, reviewed and accepted a new standard entitled Radiological Safety in the Design and Operation of Particle Accelerators.

Accidents and Their Prevention

Serious accidents involving over-exposures to radiation have been infrequent in the history of particle accelerators yet those that have occurred have been such that everything possible must be done to prevent their reoccurrence.

The first serious accident involving an accelerator happened at a large hospital in December 1944[11]. This accident resulted in severe skin burns from the scattered 1 MeV electron beam of an electrostatic generator. The cause of this accident was a genuine lack of knowledge concerning the dangers of the scattered beam. In general this lack of knowledge concerning the potential danger was not common to the accidents which happened more recently.

Most accidents which have been recorded since 1944 have had one of two common threads. Either a lack of education of the nonaccelerator worker (e.g., maintenance personnel) or the short circuiting of established radiation safety procedures. The recorded cases in which potentially lethal doses of radiation have been received have all involved highly experienced personnel. This accents the need for continuous education programs to remind all personnel of the hazards.

There can be no substitute for the vigilance of personnel. Automatic devices, interlocks and remote area monitoring systems are essential but insufficient to do the job without personnel training.

Administration of Radiation Protection

The program for radiation protection must begin with the conception of the accelerator facility. The funding, design and construction phases must include comprehensive consideration of the radiation protection problems. It is well accepted that if proper safeguards are incorporated into the construction of the accelerator facility the cost of safety will be significantly lower then if such safeguards are superimposed upon already existing facilities.

The recommendations of those radiation safety committees described will serve as a basis for a suitable radiation protection policy. There is no way to fix a universally acceptable procedure which will be completely effective and workable in all operations. It is on this basis that emphasis is placed on the need to consider, in detail, each operation individually.

There are two separate directions which must be followed in the initial phases of a facility design. One is the structure of the f cility and equipment and the second is the structure of the staff responsibilities. The decision to structure the facilities a specific way must be a result of consideration of the successful and safe performance of the job for which the facility is designed.

"How much protection is necessary" is the question which must be answered. The concept of risk vs. benefit is easy to invoke but extremely difficult to convert to quantitative terms. Not too long ago it seemed likely that the decision to allow radiation workers higher permissible exposures than members of the general public would go unquestioned. Yet this approach is now under fire from many quarters. To design a facility which will result in no radiation exposure to anyone is probably an impossible task, however, it is possible to live well within the limits recommended by those committees cited above.

The philosophy of a radiation protection program must be to limit the exposure of personnel to radiation at the lowest practical level. This practical level must routinely be in keeping with the recommended limits. The maximum permissible dose (MPD) concept is discussed further in Chapter V. Terms which include such words as "permissible, allowable or tolerance", however, are frequently misused. Dunster[12] said that it is clear that the MPD cannot represent a sudden transition from a condition of safety on one side to a position of danger on the other. This must be kept in mind in the application of these guides.

The following chapters are intended to aid in the decisions concerning the structure of the facility and equipment, the determination of amount and type of shielding necessary to establish predetermined radiation levels, the amount of induced radioactivity expected under given conditions and the exhaust rate required for particular conditions in a target area are the types of input factors which make this type of decision possible.

The structure of staff responsibilities concerning the radiation protection program is no less important then the facility structure. However, it is somewhat less straightforward since there is no inverse square law or absorption coefficients for responsibility.

In general it is the practice of those organizations able to afford it, to establish a health physics staff which serves in an advisory role to the operations staff. The

responsibility for radiation safety remains with the operational supervisor. This technique divorces the advisory group from the unpleasant role of "policemen" and places responsibility with the supervisor most closely related with the problem areas.

Such an arrangement is frequently not possible in small organizations where it may be necessary for the operations staff to act as the health physics staff as well. Though less then ideal, this condition will frequently be a "way of life". Under these conditions, it is of paramount importance to define responsibilities and priorities.

Emergency Planning

The need for an emergency plan is common to all major operations. The industrial type hazards (fire, high voltage, toxic chemicals, etc.) are present in all accelerator facilities, however, in addition there may be the potentially lethal radiation hazard. The design of the shielding, the access limitation and the monitoring and interlock systems may incorporate the state of the art in protection yet the potential disaster can still occur due to carelessness, or a series of coincidences.

In some ways the radiation present in such intense levels serves to increase some of the other hazards. For example, the presence of quantities of ozone produced by the action of radiation on oxygen can result in an explosion hazard in addition to its toxicity. This is particularly characteristic of operations which routinely irradiate material cooled by liquid nitrogen. The oxygen from the air condensed in the liquid nitrogen, radiolyzed to ozone and left in concentrated form after the evaporation of the nitrogen presents a significant explosion hazard. Ozone production is discussed in Chapter VIII.

Radiation Damage to electrical insulation also increases hazards due to fire and electrical shock. Insulation damage due to normal wear is considered in routine preventative maintenance of electrical facilities, the presence of radiation warrants more frequent inspection.

The need for fire drills, and other building evacuation procedures has long been accepted by the public. Such drills are necessary in insuring the effectiveness of an emergency procedure at an accelerator as well.

An important step in the preparation of an emergency plan, particularly for an accelerator facility, is the careful and comprehensive preparation of a medical treatment procedure for a serious radiation exposure victim. Recently it was shown that by a well planned and executed procedure, patients who had received exposures which previously would certainly have been lethal, were saved[13]. It is important that the potential accident be discussed with the resident medical personnel when applicable as well as the staff of the nearest hospital. The assumption that a nearby hospital will be ready and willing to accept a seriously over exposed patient is dangerous. The unusual character of such an accident indicates the need for special procedural planning on the part of medical personnel.

A plan for emergency actions should establish a line of command which will place the properly qualified person in charge during the emergency. The procedure should allow for various contingencies which might arise during emergency conditions. Generally, radioactive contamination of major proportions is not characteristic of an accelerator accident, however, the accidental destruction of a target could result in such a condition. Certainly emergency procedures must allow for this.

It is a management responsibility to insure that all employees and visitors are made aware of the hazards and the expected behavior on site. Emergency plans and procedures must be published and evidence obtained indicating that all personnel are thoroughly familiar with them. Communications channels for medical treatment, and fire fighting aid should be immediately evident should the need for either arise.

Emergency procedures must be well planned; they must be familiar to all involved and they must be tested if they are to be effective when they must be put into action.

References

1. Cockcroft, J. D. and Walton, E. T. S., Proc. Roy. Soc. (London), A137, 229 (1932).

2. Livingston, M. S. and Blewett, J. P., Particle Accelerators, p. 5, McGraw-Hill Book Co., Inc. (1962).

3. Burrill, E. A., The Low Energy Accelerator Industry, Nuclear News **13**, No. 4, p. 58-62 (April 1970).

4. Clark, J. C., Matthews, C. M. E., Silvester, D. J., and Vonberg, D. D. Using cyclotron-produced Isotopes at Hammersmith Hospital, Nucleonics **25**, No. 6 (June 1967).

5. Burrill, E. A., The Shielding Problem with Low-Energy Particle Accelerators, Nuclear Safety **9**, No. 6, p. 457 (Nov–Dec 1968).

6. Barton, J. P. Role of Accelerators in Neutron Radiography. Proc. of Second Conf. on the Uses of Small Accelerators for Teaching and Research, CONF 700322, p 321-344, ORAU Oak Ridge, Tenn. (March 23–25, 1970).

7. Cleland, M. R. and Morganstern, K. H., Applications of Low-Voltage, High-Current Accelerators in Tumor Therapy Research, Proc. of Conf. on the Uses of Small Accelerators for Teaching and Research, CONF 680411, p. 390-414, ORAU, Oak Ridge, Tenn. (April 8–10, 1968).

8. Boone, M. L. M. and Hevezi, J. M. Fast Neutron Radiobiology and Radiotherapy Proc. of Second Conf. on the Uses of Small Accelerators for Teaching and Research, CONF 700322, p. 393-406, ORAU, Oak Ridge, Tenn. (March 23–25, 1970).

9. Ryding, G. Atomic Physics with a Low Voltage Tandem, Proc. of The Second Conf. on the Uses of Small Accelerators for Teaching and Research, CONF 700322, p. 259-280, ORAU, Oak Ridge, Tenn. (March 23–25, 1970).

10. Cowan, F. P., Recent Work of NCRP, ICRU and ICRP of Interest to Accelerator Health Physicists, Second International Conference on Accelerator Dosimetry and Experience, CONF 691101, p. 21, Stanford, Calif. (Nov 5–7, 1969).

11. Robbins, L., Superficial "Burns" of Skin and Eyes from Scattered Cathode Rays, Radiology **46**, No. 1 (1946).

12. Dunster, H. J., Maximum Permissible Doses of Radiation, Their Concept and Application, J. Brit. Nucl. Energy Soc. 9, p. 41–44, (Jan 1970).

13 Koval, B., McGraw-Hill World News, Pittsburg, Chemical Engineering (April 22, 1968).

Chapter II

X-Ray Production and Shielding

A. Brynjolfsson and T. G. Martin

Introduction

The principle shielding problem associated with particle accelerators is frequently not the primary accelerated charged particles. Secondary radiations produced as a result of the interaction of the primary beam with a target, portion of the accelerator, or the shielding most often determine the type and magnitude of the shielding.

The secondary radiations which are of significance in the energy range under consideration are neutrons and X-ray or bremsstrahlung. When electrons are stopped in a material, X-rays are emitted.

As a further consequence of their interaction with matter these X-rays and to a lesser extent the primary electrons can produce neutrons provided they posses sufficient energy (photoneutron production).

The problem of X-ray shielding is most severe with electron accelerating machines therefore this chapter will deal principally with this type of accelerator. Applicable comments will be made concerning other types of accelerators.

In addition, since only concrete shielding is considered here, for electron machines it is reasonable to assume that, for the energy range under consideration (< MeV), when sufficient shielding has been provided to protect against X-rays there is also sufficient shielding to protect against the neutrons. More detail on neutron production and shielding is presented in Chapter III.

Some details are presented concerning the angular distribution and the photon spectra of bremsstrahlung.

In general mathematical derivations have been limited to presentation of imperical formulae to enable the calculation of the data presented graphically. Several example problems are presented with their solutions to illustrate the use of the figures.

X-Ray Production in Electron Accelerators

As they are slowed down in matter electrons, with energies above a few MeV, lose significant amounts of their energy by radiation. This radiation, a continuous spectrum, is called bremsstrahlung. Not well explained by classical means, Bethe and Heitler[1] presented quantum mechanical theory for this radiative process in 1934.

Several methods for calculating the rate of production of bremsstrahlung have been proposed and are discussed in detail in the comprehensive work of Koch and Motz[2].

The fraction of the electron energy that is emitted as bremsstrahlung depends on the initial electron energy and the atomic number of the stopping material. Table II-1 presents X-ray production yields for several materials as a function of initial electron energy. Further discussion and data on approximately forty materials have been presented in the tables of Berger and Seltzer[3].

Table II-1. The % of the electron energy that is converted to X-rays upon complete stopping of the electrons in a few materials as a function of the electron energy [2]

Electron energy in MeV	Total X-ray production in % of Electron power				
	Water	Al	Fe	W	U
0.5	0.265	0.59	1.34	4.77	6.21
1.0	0.486	1.06	2.31	7.63	9.75
5.0	2.08	4.08	8.20	21.17	25.17
10.0	4.16	7.72	14.40	31.78	36.21
20.0	8.31	14.45	24.44	45.04	49.40
30.0	12.21	20.26	32.11	53.23	57.39
50.0	19.03	29.51	43.08	63.41	66.97

The Angular Distribution

The angular distribution of the X-rays from the target varies mainly with the electron energy, the atomic number of the target material, and the thickness of the target. At very low electron energy (few keV), the intrinsic angular distribution is the same as from a radio-antenna, i.e., the intensity is greatest perpendicular to the direction of the electron beam. At high electron energy the intrinsic angular distribution is then as shown theoretically by Heitler[1] and experimentally by Lanzl and Hanson[4], given by

$$I(\theta) = I(0) \left[1 + \frac{E\theta^2}{m_o c^2} \right]^{-2} \qquad \text{(II-1)}$$

where

$I(\theta)$ = the X-ray intensity at the angle θ.

$E = (T + m_0c^2)$ = total energy of the electron in MeV.

m_0c^2 = rest energy of the electron in MeV.

θ = angle. in radians, between the incoming electron and the X-rays.

A convenient unit is the radiation length or that path length of material which will result in high energy electrons losing $\frac{1}{e}$ of their energy by radiation. The radiation length X_0[1] may be defined as

$$\frac{1}{X_0} = 4 \alpha [N/A] Z^2 r_0^2 \ln(183 Z^{-1/3}) \qquad \text{(II-2)}$$

where

α = fine structure constant (1/137)

N = Avagadros number (6.02×10^{23})

A = atomic weight of material

Z = atomic number of material

r_0 = classical radius of an electron (2.82×10^{-13} cm)

or

$$\frac{1}{X_0} = 1.398 \times 10^{-3} \frac{Z^2}{A} \ln(183 Z^{-1/3}) \qquad \text{(II-2a)}$$

A plot of X_0 vs. Z is given in Fig. II-1. Target thicknesses are frequently expressed in radiation lengths and the concept is important in the determination of conditions of operations.

The angular distribution of the X-ray intensity is governed by this intrinsic distribution when the target is less than 0.0005 radiation lengths. One radiation length is 6.265 g/cm^2 of tungsten and 44.6 g/cm^2 of water.

As the electrons penetrate a thick target they are increasingly scattered. The angular distribution of the X-rays is then (for target thickness greater than 0.002 radiation lengths) governed by the angular distribution of the electrons. For thick targets the expression by Muirhead, et al.[5], which is similar to the one deduced by Lawson[6], is used

$$F(\theta) = \frac{E^2\tau}{440\cdot\pi}\left[\mathrm{Ei}\left(-\frac{(E\cdot\theta)^2}{1.781 m_0c^2}\right) - \mathrm{Ei}\left(\frac{-E\cdot\theta)^2\cdot 1n(183\cdot Z^{-1/3})}{1510.8}\right)\right] \quad \text{(II-3)}$$

where

$F(\theta)$ = is the fraction of the electron energy radiated per unit solid angle at angle θ in radians from the direction of incident electron.

E = total energy of the electrons in MeV.

τ = fraction of the electron energy which is radiated per radiation length, see Table II-2.

m_0c^2 = 0.511 MeV = rest energy of the electron in MeV.

Z = atomic number of the target material.

t = target thickness in radiation length.

Ei(x) is the exponential integral function[7]

Table II-2 τ, fraction of the radiated electron energy that is radiated per radiation length

Medium	Radiation length in g/cm²	Energy in MeV			
		5	10	20	40
water	44.6	.74	.82	.90	.99
aluminum	26.3	.69	.75	.83	.90
iron	14.4	.72	.76	.82	.88
tungsten	6.3	.75	.75	.76	.80

However, although Eq. (II-3) is frequently referred to, it should be used with caution because, in its derivation, only small angle scattering of the electrons was considered. Therefore, it may not be valid for angles greater than 10°, nor target thicknesses greater than 0.1 radiation length. In shielding problems these limitations are unsatisfactory, because all angles up to 180° must be considered and the target must be thick enough to stop the beam completely. Brynjolfsson and Martin[8] have measured the X-ray intensity at several angles including very large angles for 8, 10, 12 and 20 MeV electrons (from a linear accelerator) stopped in a tungsten target .062" thick -- 3.04 g/cm^2. The results are shown in Fig. II-2 together with the experimental results of Buechner, et al.[9], Lanzl and Hanson[4] and Kirn and Kennedy[10]. Fig. II-3 shows the data obtained including larger angles. For comparison, also shown in the angular distribution according to Eq. (II-3) for t = 0.1 and Z = 74.

FORWARD X-RAY INTENSITY

The forward intensity may be obtained from Eq. (II-3) which for $\theta = 0$ reduces to

$$F(0) = \frac{E^2 \tau}{440 \cdot \pi} \ln \frac{3250t}{\ln(183\ Z^{-1/3})} \qquad \text{(II-4)}$$

where F(0) is the fraction of the electron energy that is radiated in the forward direction per unit solid angle. Eq. (II-4) is equivalent to

$$I(0) = \frac{723 \cdot \tau (T+0.511)^2 \cdot T \cdot i}{d^2} \cdot \ln\left(\frac{3250t}{\ln(183 \cdot Z^{-1/3})}\right) \qquad \text{(II-5)}$$

where

I(0) = forward X-ray intensity flux in units of watts/cm^2

T = kinetic energy of the electrons in MeV

i = the beam current in ampere.

d = distance from the X-ray target in cm.

Dose rate R(0) in units of rads per hour is obtained by multiplying Eq. (II-5) by $3.6 \cdot 10^8 (\mu_k/\rho)_{av}$, where $(\mu_k/\rho)_{av}$ is the energy transfer coefficient in air in cm^2/gm weighted with the X-ray intensity spectrum f(T,k) as defined in Eq. (II-10).

$$R(0) = 2.604 \cdot 10^{11} \left(\frac{\mu_k}{\rho}\right)_{av} \frac{\tau (T+0.511)^2 \cdot T \cdot i}{d^2} \ln\left(\frac{3250t}{\ln(183 \cdot Z^{-1/3})}\right) \qquad \text{(II-6)}$$

The forward intensity increases according to equations (II-4) to (II 6) logarithmically with t. However, in the deduction of Eq. (II-3) the decrease in electron energy T, and the reduction in the current i of high energy electrons were not considered; nor was the X-ray absorption in the target included. Variation of the relative X-ray intensity with the thickness of a gold target was measured by Lanzl and Hanson[4] at 16.93 MeV (See Fig. II-4). They found a maximum intensity at a thickness of 1.7 g/cm^2. At this thickness the electrons have lost approximately 30% of their energy. The contribution to the forward intensity from electrons that have lost 30% of their energy is small. To obtain a maximum X-ray intensity at any energy T the correspondent t in Eq. (II-6) should vary with the initial electron energy. Set

$$t = \frac{0.3T}{(a + b \cdot T) \cdot t_z} \qquad (II\text{-}7)$$

where

t_z = one radiation length in g/cm^2 in a material with atomic number Z (for tungsten it is 6.3).

t = target thickness in radiation lengths.

T = initial kinetic energy of the electrons in MeV.

a = stopping power in MeV/g for electronic collision (approximately 1.2 in tungsten).

$b \cdot T$ = stopping power in MeV/g for radiation (approximately $0.12 \cdot T$ for tungsten).

The stopping powers a and $b \cdot T$ may be found in the Tables by Berger and Seltzer[3]. Fig. II-5 shows the forward intensity in rads per hour at 1 m distance from the target per kwatt output from the accelerator. The curve was obtained from Eq. (II-6) using Z = 74 and t given by Eq. (II-7). The experimental points are from Buechner, et al.[9], Miller[11] and the authors[8].

Had the X-ray emission been isotropic the radiation intensity in all directions from the target would be given by

$$R_{iso} = 3.6 \cdot 10^{14} \cdot \frac{\mu_k}{\rho} \cdot \frac{q(E,Z)}{4\pi d^2} \cdot T \cdot i \qquad (II\text{-}8)$$

where

R_{iso} = the isotropic radiation intensity in rads per hour.

$q(E,Z)$ = the fraction of the electron energy converted to X-rays. This quantity is given in % in Table I.

Other quantities are the same as in Eq. (II-6) and (II-7).

X-Ray Spectra

The forward X-ray spectrum for a thick heavy target is similar to that from a thin target, because the greatest contribution to the forward intensity is from the first layers of the target, while the impinging electrons are still well collimated. Fig. II-4 shows that half of the forward intensity from a 10.93 MeV electron is produced in the first 0.1 g of the gold target. To calculate the shielding in the forward direction, the thin target spectrum is used.

The normalized spectrum, f(T,k), (the number of photons of energy k per energy interval (MeV) times the photon energy k) is shown in Fig. II-5 and II-6 for 1, 2.5, 5, 10, 15, 20, 30 and 40 Mev.

The X-ray intensity at large angles is due to single, plural, and multiple electron scattering processes. The differential cross section for the single scattering process is given by

$$I \cdot 2\pi \cdot \sin\theta d\theta = \frac{N_o}{A} \frac{Z^2 \cdot e^4}{4(T+m_o c^2)^2 \beta^4} \cdot \frac{2\pi \sin\theta d\theta}{\sin^4(\theta/2)} \cdot R \qquad \text{(II-9)}$$

where

N_o = $6.02 \cdot 10^{23}$

A = atomic weight

e = charge of the electrons

β = ratio of electron velocity to that of light

R = the correction factor to the Rutherford Scattering

This ratio R has been evaluated by Duggett and Spencer[12], among others.

The Rutherford Scattering and the ratio R decrease sharply with increasing energy. The scattering into large angles is therefore very small until the electrons have lost most of their energy, and the X-ray spectrum at large angles (>60°) is very soft. Using Eq. (II-9) we have made rough calculations of the photon spectrum from a tungsten target. The results are shown in Fig. II-8. Although the soft part of the spectrum dominates the small concrete thicknesses, it is the hard part of the spectrum that determines the adequate shielding thickness at large angles.

Calculations of the Shielding Thickness (electron accelerators)

The dose D in rads/hour after penetrating a concrete thickness of x cm is given by

$$D = 2.604 \cdot 10^{11} \frac{\tau(T+0.511)^2 \cdot T \cdot i}{d^2} \ln\left[\frac{3250t}{\ln(185 \cdot Z^{-1/3})}\right] \cdot \sum_{k=0}^{T} \frac{\mu_k}{\rho} \cdot f(Tk) \cdot B(kx) \left[\exp-(\mu_t(k)x)\right] dk \qquad (II\text{-}10)$$

where

τ = fraction of electron energy radiation per radiation length (Table II-2)

T = electron energy in MeV.

i = beam current in Ampere.

d = distance in cm from X-ray target to the detector.

t = target thickness in radiation lengths (Eq. II-7).

μ_k/ρ = energy transfer coefficient in cm^2/g.

f(T,k) = normalized photon spectrum given in Fig. II-5, II-6, and II-7.

B(k,x) = dose buildup factor given in Fig. II-9

$\mu_t(k)$ = total absorption coefficient in concrete in cm^{-1} is shown in Fig. II-10.

x = thickness of concrete in cm.

Eq. (II-10) was integrated numerically. The results are shown in Fig. II-11 and Table II-3. For permissible dose rate of $D = 10^{-4}$ rad/hr the adequate shielding thickness is a function of electron energy (Fig. II-12).

Table II-3. The dose rates behind a concrete shielding. The dose rate D in rads per hour is obtained by multiplying the values in the Table by W/R^2, where W is the electron beam power in kwatt and R is the distance in m to the detector from the X-ray target

Electron energy T MeV / concrete thickness in m	5.51	10.51	15.51	20.51	25.51	30.51	40.51
0	4.66+5 *	2.73+6	8.95+6	2.01+7	3.78+7	6.41+7	1.48+7
50	2.64+2	5.84+4	3.04+5	8.00+5	1.82+6	3.22+6	8.40+6
100	4.44+1	2.38+3	1.55+4	5.01+4	1.16+5	2.24+5	6.77+5
200	3.34+0	5.90+0	6.10+1	2.40+2	6.13+2	1.24+3	3.32+3
300	1.74-4	1.73-3	2.82-1	1.29 0	3.48-0	7.22 0	1.93+1
400	7.58-6	5.71-5	1.37-3	7.18-3	2.05-2	3.29-2	9.21-2

*4.66×10^5

X-Rays from Positive ion Accelerators

The x-ray production from heavy ion accelerators below 50 MeV is usually not important. The bremsstrahlung is approximately inversally proportional to the M^2 where M is the mass of the incident particle. It is therefore usually insignificant for heavy particles. More important are the x-rays from deexcitation of atoms and nuclei and the bremmstrahlung from stray electrons. When an electron is removed from an inner shell of the atom and the vacancy is filled again the emitted x-ray may become important. This radiation is soft and the shielding problem small. It is however important to be remindful of its existance and importance even at low energies of the incident particle. Instruments must be able to detect and measure this soft radiation. At higher energies the nuclear excitations become more important because of the greater penetration of the harder x-rays emitted. Most important are usually the x-rays that are to be emitted from

the positive end of the accelerator due to a back streaming of electrons. The great variation in design makes it difficult to give useful guidelines. If we assume that the ion current "I" results in a reverse directed electron current of magnitude 0.2·I that is accelerated through 1/3 the terminal voltage we would usually get a very considerable x-ray production. These electrons may be produced when stray ions are lost from the beam and hit the inside surface of the accelerator usually where the field is appreciable, or they may be produced by ionization of the residual gas in the accelerator tube. These assumptions are unreliable estimates. Still they indicate that the shielding requirement for heavy ion accelerator may not be so much less than the shielding requirement for comparable electron accelerators. Exact estimate will require specification of design and usage. As a rough estimate we offer that shielding which is required at 90° from the beam axis of an electron accelerator, with the same beam current and energy.

References

1. Heitler, W., the Quantum Theory of Radiation, p. 247, 3rd Edition, Oxford, Clarendon Press (1954).

2. Koch, H. W. and Motz, J. W., Rev. Mod. Phys. 31, 920 (1959).

3. Berger, M. J. and Seltzer, S. M., NASA SP-3012 (1964).

4. Lanzl, L. H. and Hanson, A. O., Phys. Rev. 83, 959 (1951).

5. Muirhead, E. G., Spicer, B. M., and Lichtblau, H., Proc. Phys. Soc. (London), 65A, 59 (1952)

6. Lawson, J. D., Nucleonics, 10, No. 11 (1952)

7. Jahnke, E. and Emde, F., Tables of Functions, P. 1, Fourth Edition, Dover Publication (1945).

8. Brynjolfsson, A. and Martin, T. G., Intern. J. Appl. Rad. Isotop. 22, p. 29 (1971).

9. Buechner, W. W., Van de Graaff, R. J. Burrill, E. A. and Sperduto, A., Phys. Rev. 74, No. 10, p. 1348 (1948).

10. Kirn, F. S. and Kennedy, R. J., Nucleonics 12, No. 6, p. 44 (1954).

11. Miller, C. W., J. Brit. Ind. Inst. of Rad. Eng., 14, No. 8 (1954).

12. Doggett, J. A. and Spencer, L. V., Phys. Rev. 103, 1957 (1956).

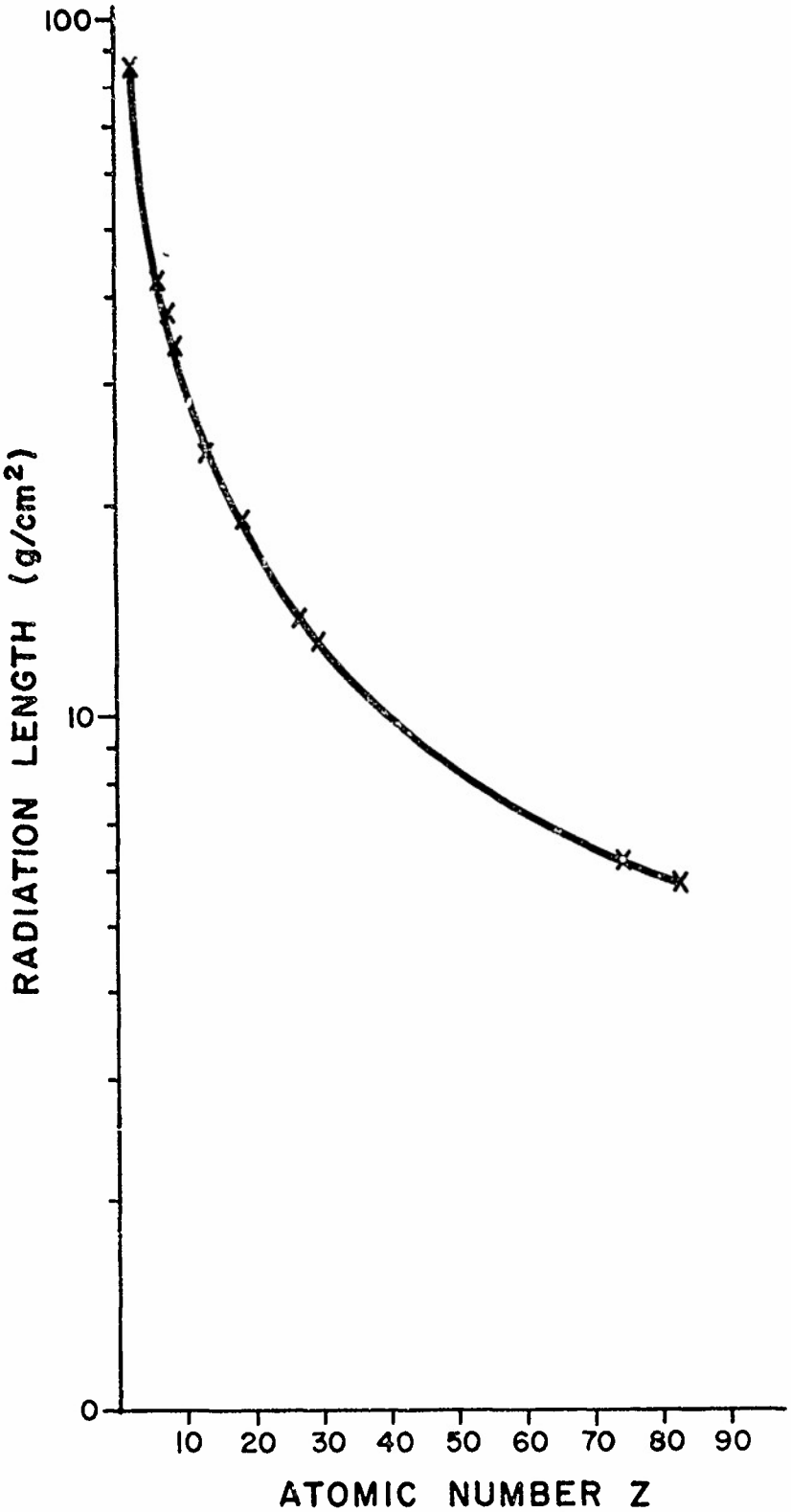

Figure II-1 - Value of radiation length (cm^2/g) vs. target atomic number.

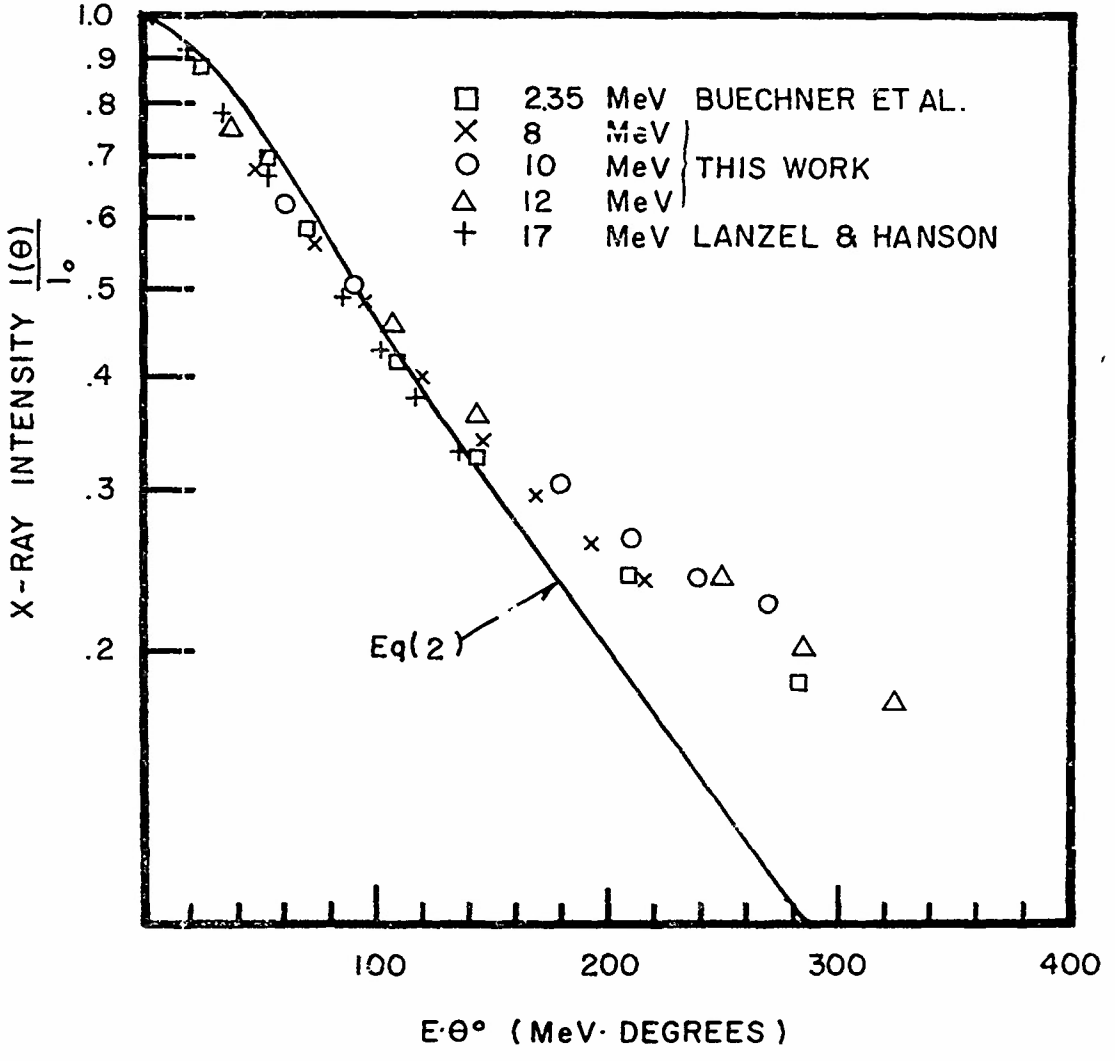

Figure II-2 - Relative X-ray intensity vs. angle θ from electron beam. The abscissa shows the angle θ in degrees times the energy of the initial electron.

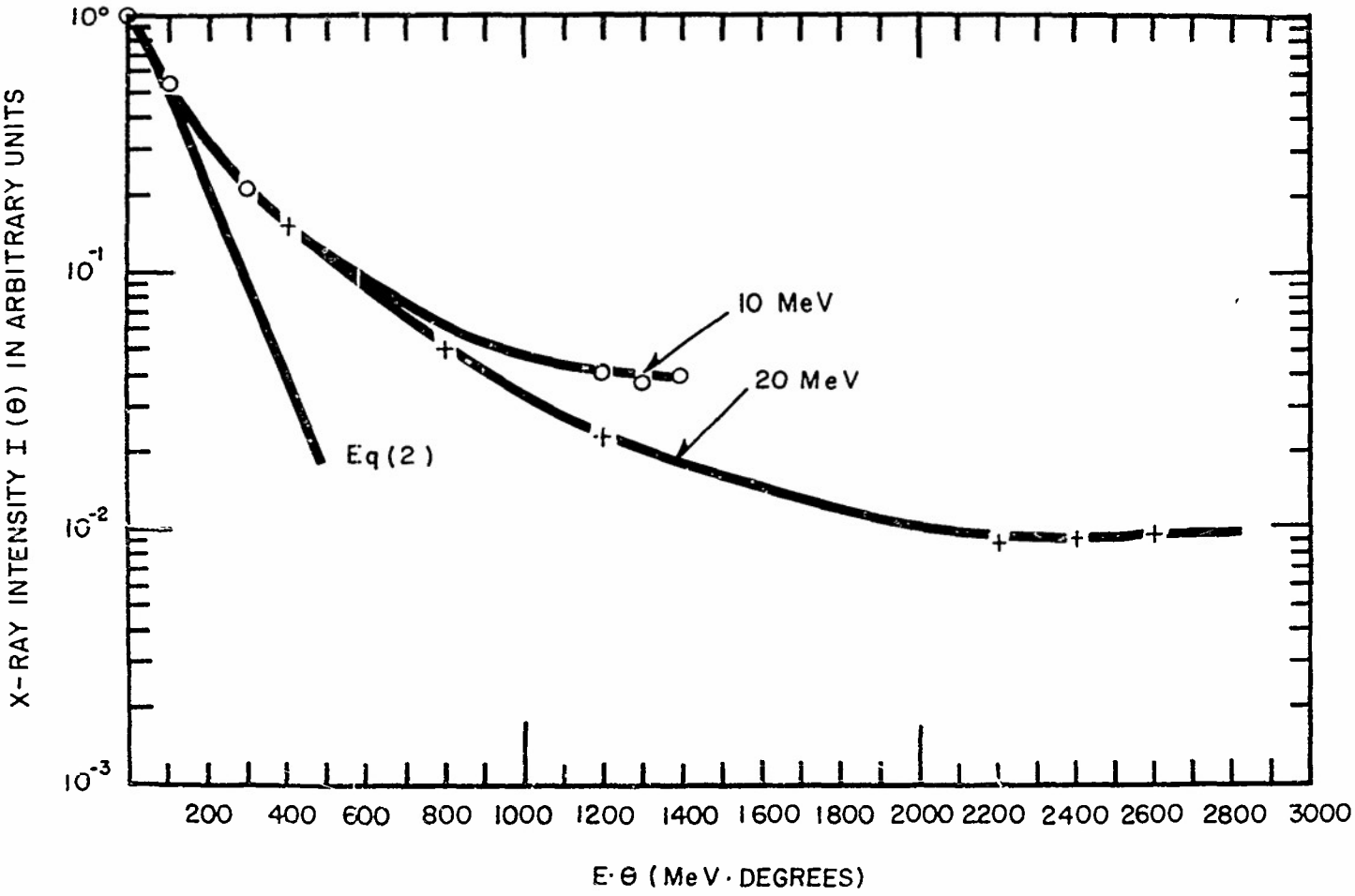

Figure II-3 - Relative X-ray intensity vs. angle θ from elec n beam. The abscissa shows the angle θ in degrees times the energ of the initial electron.

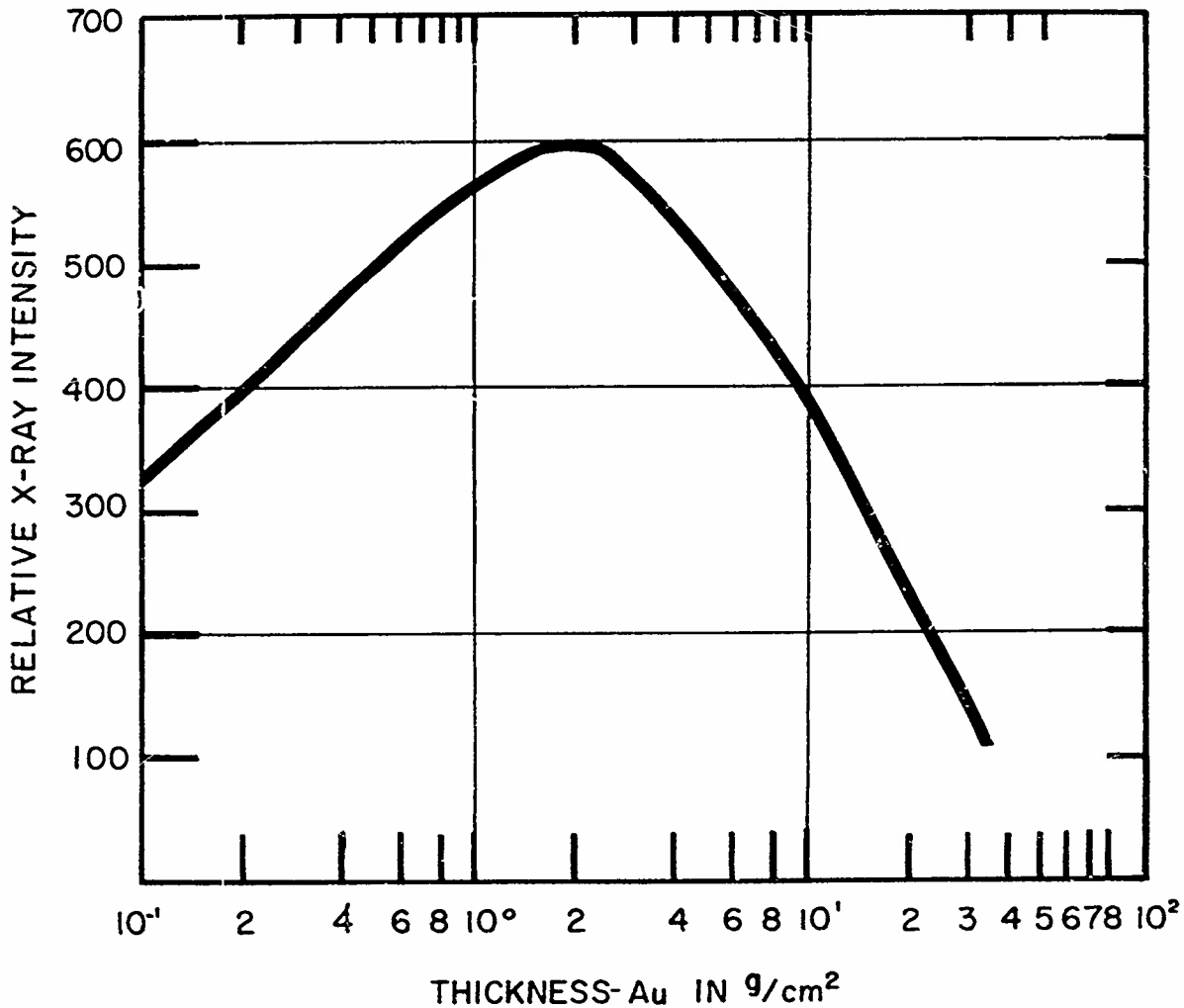

Figure II-4 Relative X-ray intensity vs. thickness of gold target at 16.93 MeV according to Lanzl and Hanson[4].

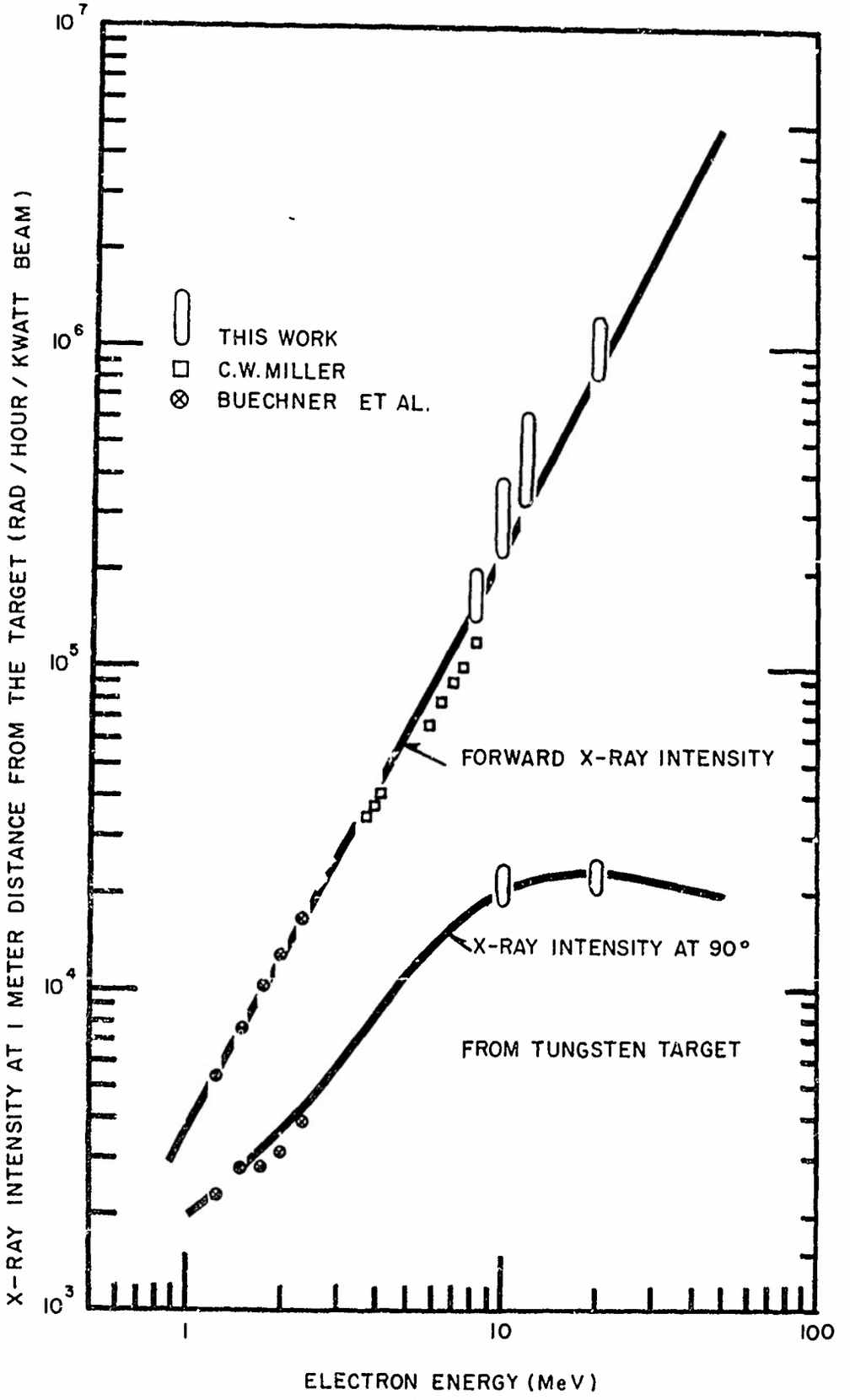

Figure II-5 X-ray intensity in rads per hour – kWatt at one meter from a tungsten target as a function of initial electron beam energy in MeV.

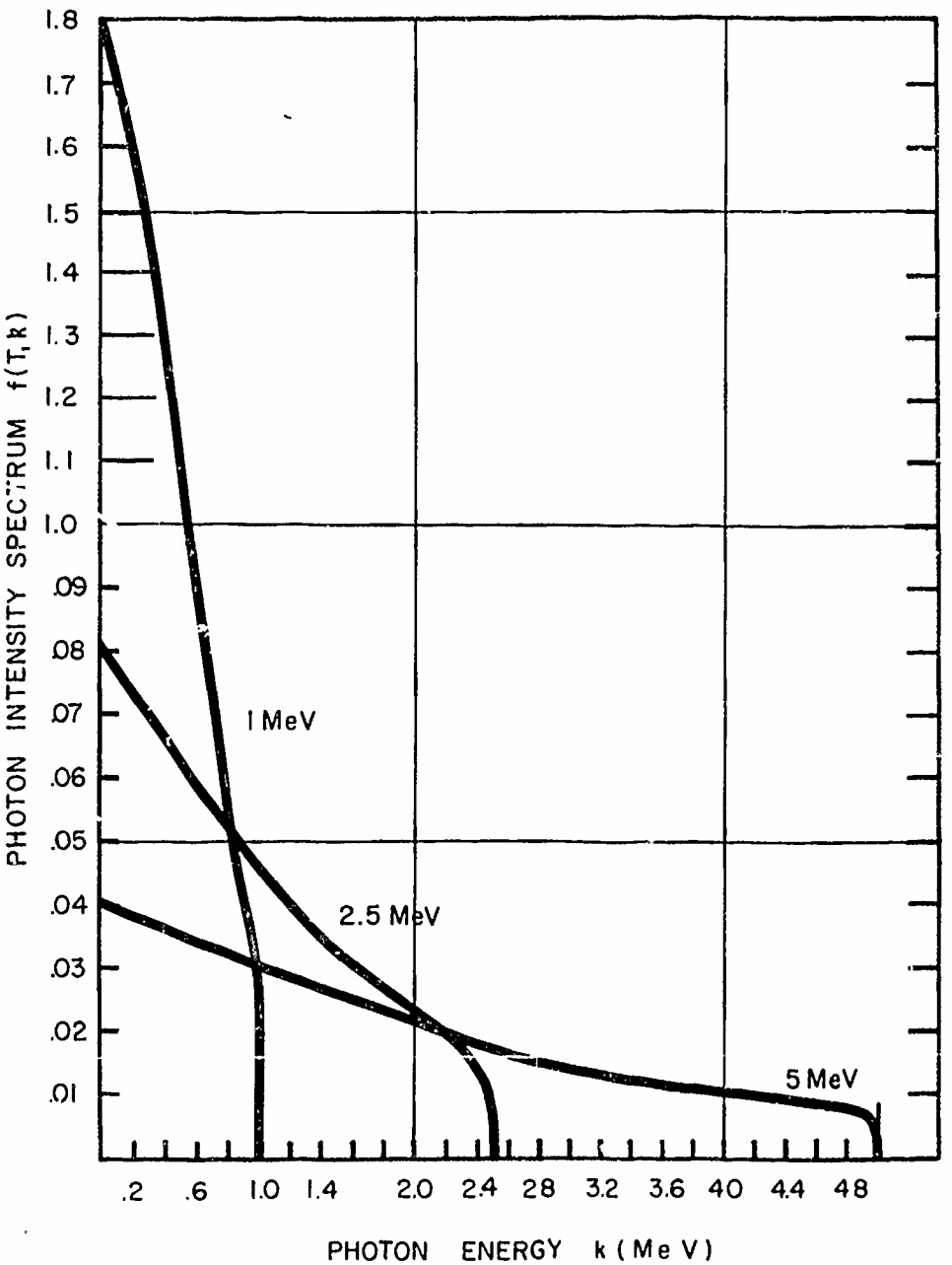

Figure II-6 - The normalized photon intensity spectrum, f(T,k) (i.e., the number of photons of energy k per energy interval (MeV) times the photon energy k) vs. photon energy k for electrons of 1.0, 2.5, and 5.0 MeV.

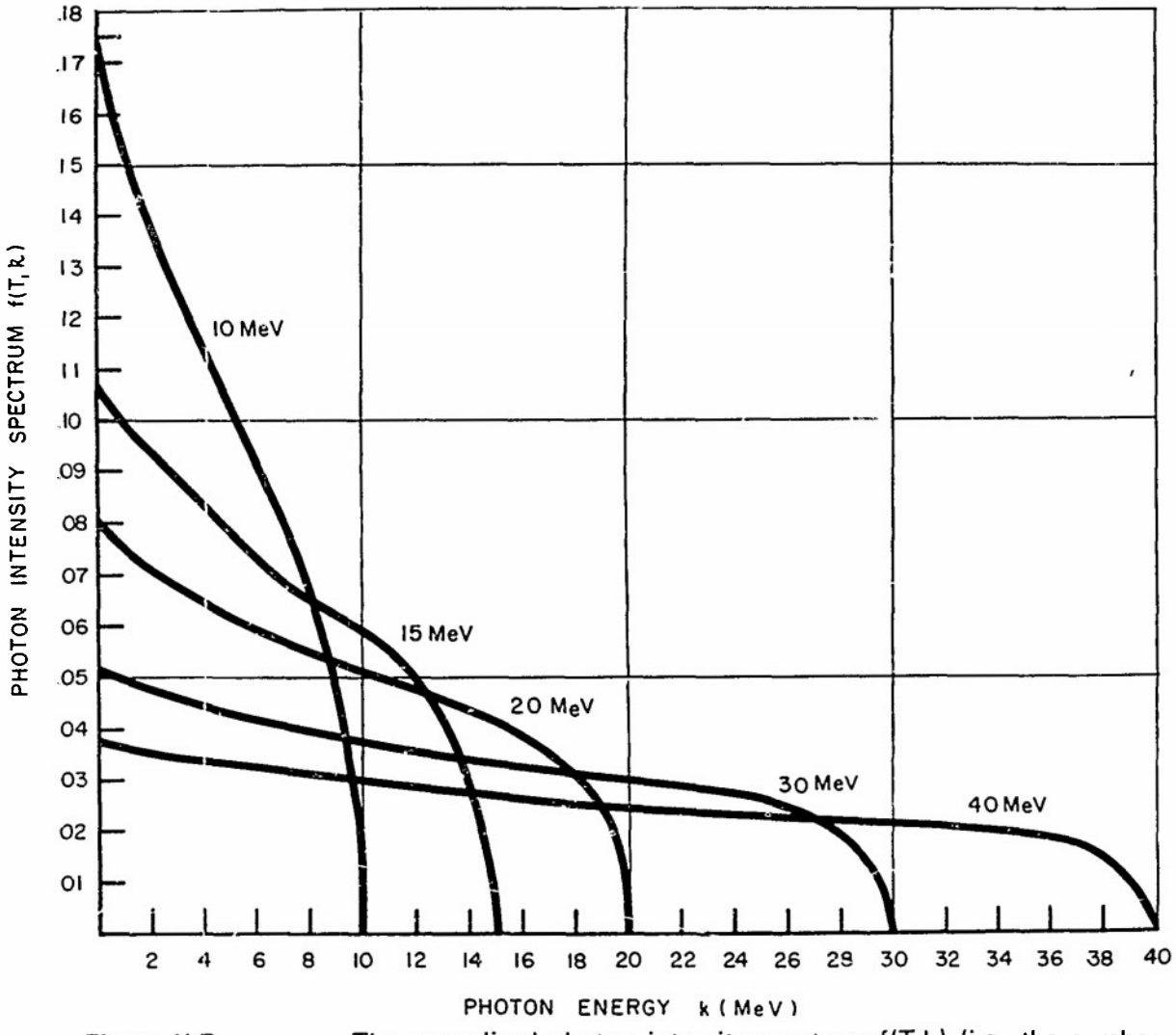

Figure II-7 - The normalized photon intensity spectrum f(T,k) (i.e. the number of photons of energy k per energy interval MeV) times the photon energy k) vs. photon energy k for electrons of 10, 15, 20, 30 and 40 MeV.

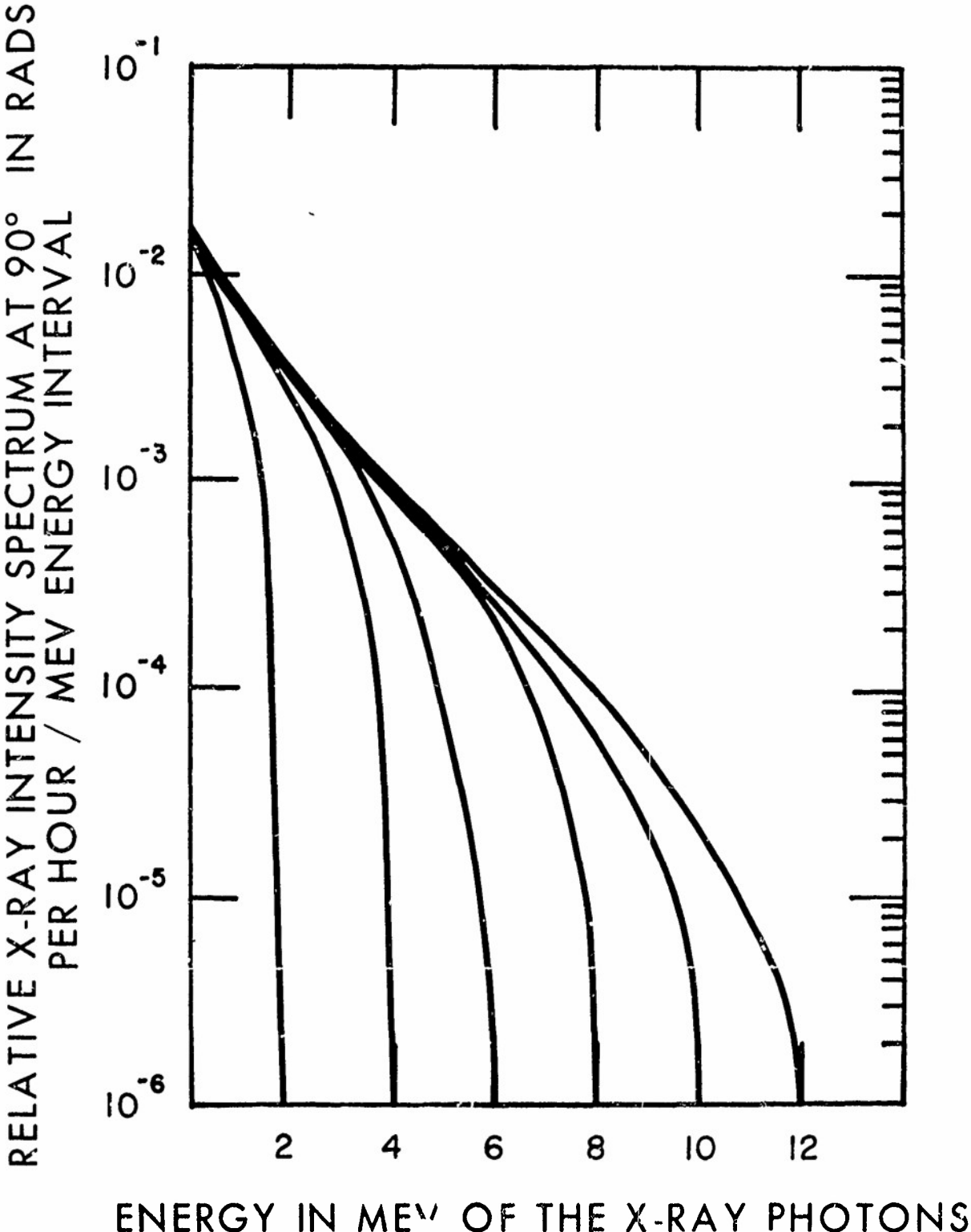

Figure II-8 - The relative X-ray intensity spectrum in rads/hr/MeV intervals at 90° from the electron beam axis vs. the initial electron beam energy for 2, 4, 6, 8, 10, and 12 MeV.

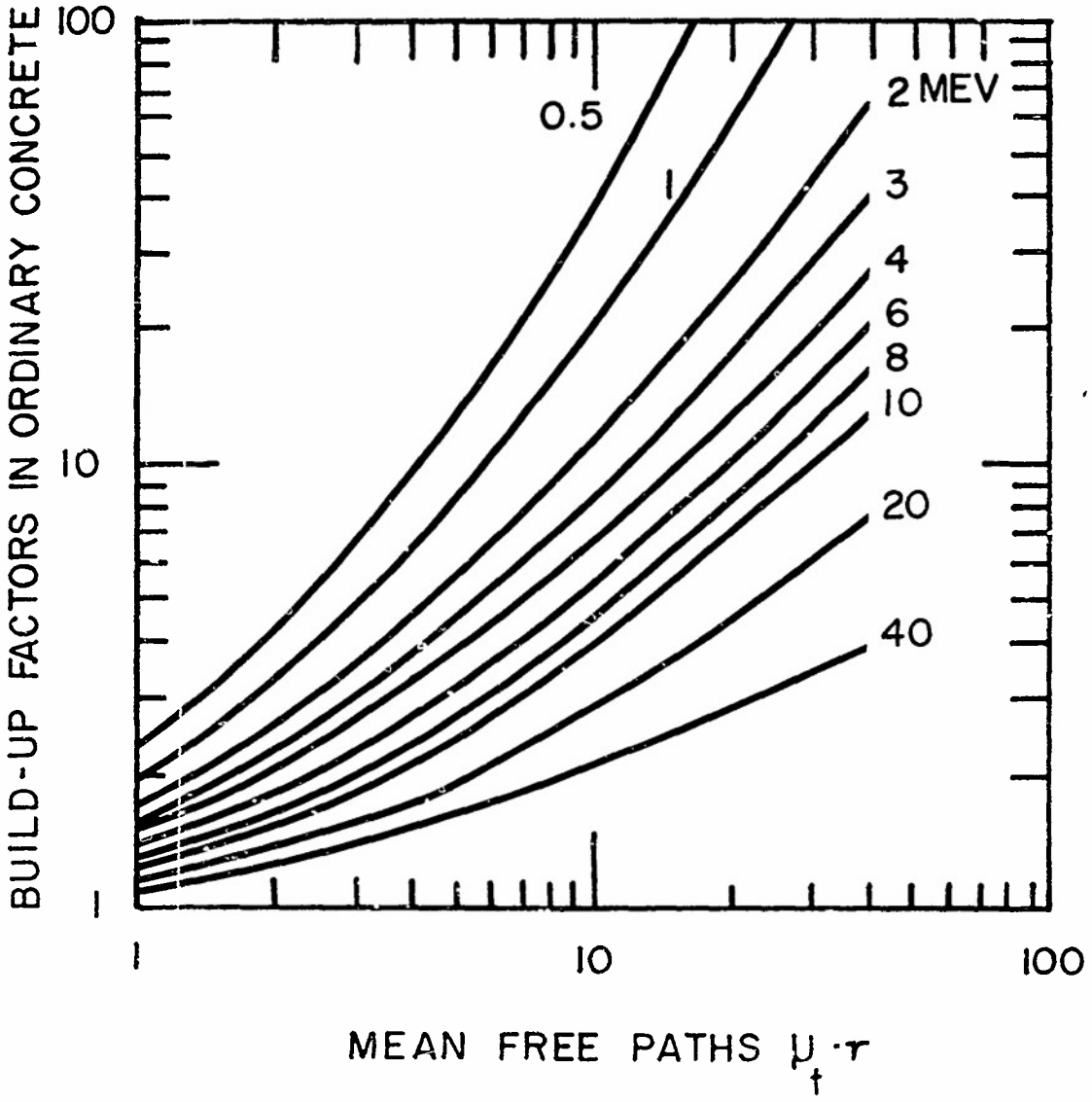

Figure II-9 Dose buildup factor B(k;x) in ordinary concrete as a function of mean-free path μ_f x for several energies from 0.5 to 40 MeV.

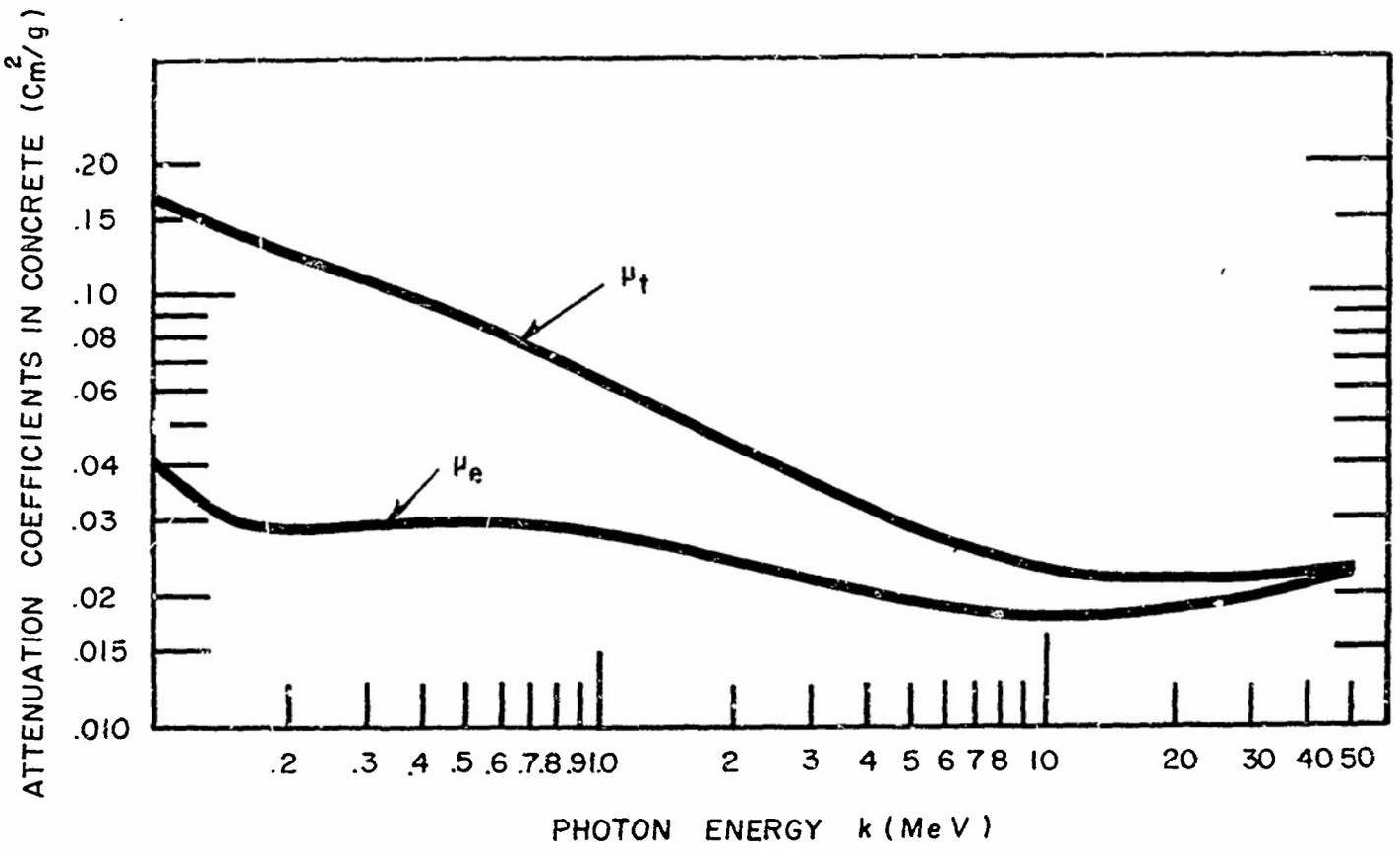

Figure II-10 Attenuation coefficients μ_t (total and μ_e(electron) in ordinary concrete as a function of photon energy in MeV.

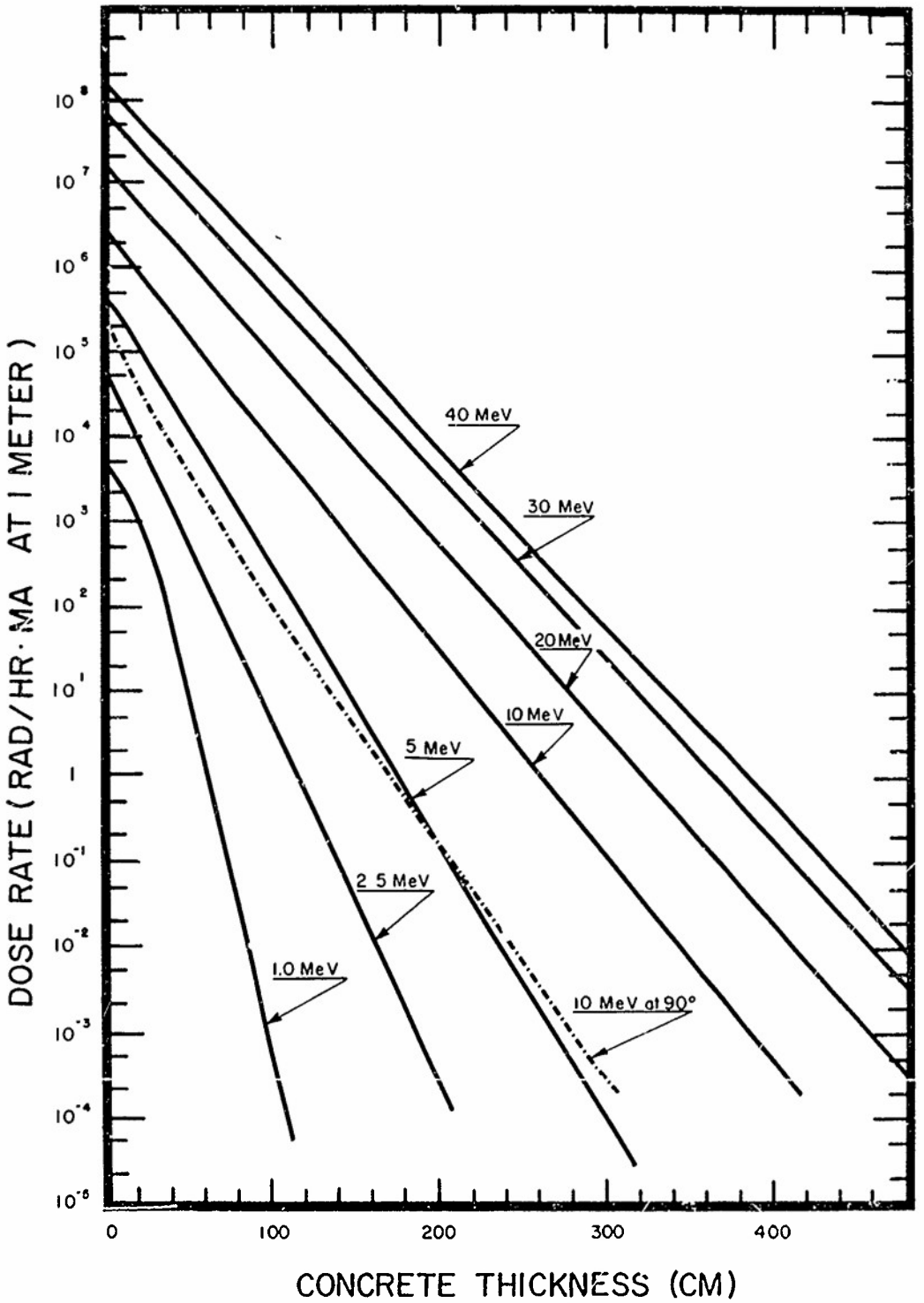

Figure II-11 - Dose rate rad/hr-ma at one meter for energies from 1.0 to 40 MeV, us. the concrete thickness in cm. Initial electron energy for each curve is indicated.

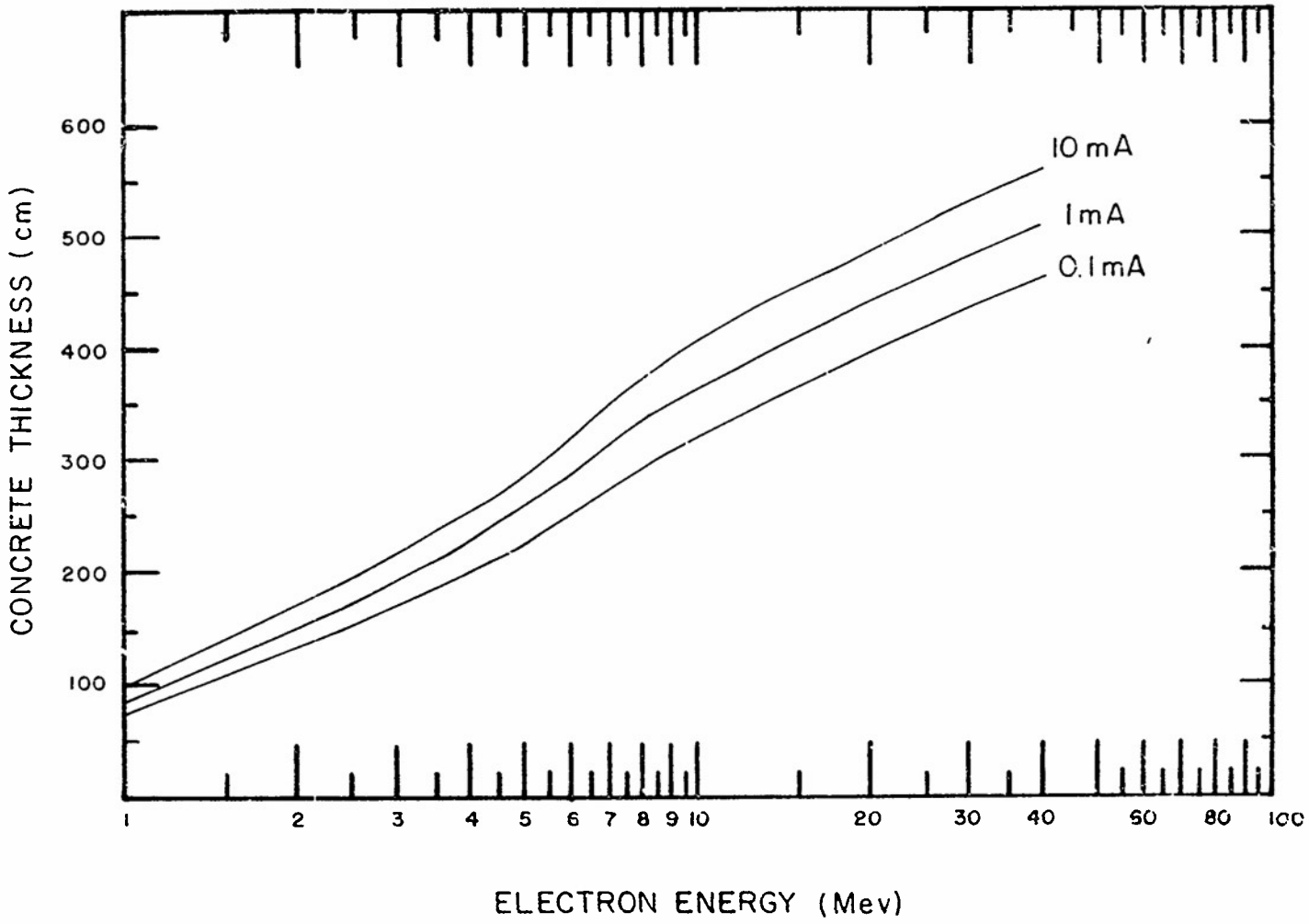

Figure II-12 - Concrete shielding thickness required in the forward direction for a terminal dose rate of 0.1 mrem/hr at 5 meters from its X-ray target as a function of electron energy (MeV) for beam currents of 0.1, 1.0, and 10 mA.

Chapter III

Neutron Production and Shielding

Francis J. Mahoney

Introduction

In addition to producing substantial photon radiation, charged particle beams from accelerators can produce neutrons via nuclear reactions if energy and cross sectional requirements are fulfilled. Because the primary purpose of this text is radiation protection for accelerators, emphasis will be placed on shielding of neutrons. In principle neutron shielding is not a particularly difficult calculational problem once the energy and spatial distributions of the source of neutrons are specified. This latter task however can be a formidable one. For this reason the presentation is split into a section on Neutron Production and a section on Neutron Shielding.

Very often ambiguities are encountered in the nomenclature regarding neutrons. To avoid these, Table III-1 presents the classification scheme for neutrons and target nuclei used throughout this discussion. This sceme may not be strictly adhered to in other texts so that one should take care. One should also note that designations employed in Table III-1 overlap in certain cases. This is an inevitable result of quantifying qualitative descriptions.

Neutron Production

In general, neutrons can be produced by the output of any type of accelerator which satisfies energy requirements. The most pertinent parameter is the binding energy of a neutron in the target nucleus. Its value can be determined experimentally from thresholds of (γ,n) (i.e., photoneutron) reactions. Table III-2 presents a sampling of these thresholds. A general though not universal trend is apparent, namely that the neutron binding energy decreases as the mass of the target nucleus increases. A decrease from about 18 MeV to about 7 MeV is seen. Observation of this trend suggests using low Z materials around accelerators which generate large amounts of X- and gamma radiation, in order to reduce neutron production from photodisintegration processes. This logic sounds fine but it presents some practical problems. First, hydrogenous materials with some deuterium contamination are exceptions to the trend, because of the anomalously low binding energy of the neutron in deuterium. Second, in deliberately generating high photon fluxes, such as bremsstrahlung from electron accelerators, one uses targets of high atomic number for maximum efficiency. Unfortunately such targets are also better for photoneutron production. Furthermore these targets are often cooled with water thus providing a significant amount of deuterium for interaction.

Table III-1

Classification Scheme of Neutrons

and Target Nuclei

Neutrons

Designation	Energy Range
Cold Neutrons *	$E<0.026$ eV
Thermal *	$0.001<E<0.1$ eV
Epithermal *	$0.1<E<10^2$ eV
Slow *	$0.1<E<10^3$ eV
Intermediate *	$1.0<E<500$ keV
Fast +	$0.5<E<10$ MeV
Very Fast †	$10<E<50$ MeV

* Low-energy neutrons.

\+ High energy neutrons.

† Very high energy neutrons.

Target Nuclei

Designation	Mass-Number Range
Light Nuclei	$1\leqslant A\leqslant 25$
Intermediate	$25<A\leqslant 80$
Heavy	$80<A\leqslant 240$

TABLE III-2

Threshold Energies for Photoneutron Processes

Reaction	Observed Threshold (MeV)
$H^2(\gamma,n)H^1$	2.23
$C^{12}(\gamma,n)C^{11}$	18.7
$N^{14}(\gamma,n)N^{13}$	10.65
$O^{16}(\gamma,n)O^{15}$	16.3
$Mg^{24}(\gamma,n)Mg^{23}$	16.2
$Al^{27}(\gamma,n)Al^{26}$	14.0
$Si^{28}(\gamma,n)Si^{27}$	16.8
$p^{31}(\gamma,n)P^{30}$	12.35
$S^{32}(\gamma,n)S^{31}$	14.8
$K^{39}(\gamma,n)K^{38}$	13.2
$Ca^{40}(\gamma,n)Ca^{39}$	15.9
$Fe^{54}(\gamma,n)Fe^{53}$	13.8
$Cu^{63}(\gamma,n)Cu^{62}$	10.9
$Cu^{65}(\gamma,n)Cu^{64}$	10.2
$Ag^{109}(\gamma,n)Ag^{108}$	9.3
$Sb^{121}(\gamma,n)Sb^{120}$	9.25
$Au^{197}(\gamma,n)Au^{196}$	8.0
$Hg^{201}(\gamma,n)Hg^{200}$	6.25
$Pb^{206}(\gamma,n)Pb^{205}$	8.25
$Pb^{207}(\gamma,n)Pb^{206}$	6.95
$Pb^{208}(\gamma,n)Pb^{207}$	7.44
$Bi^{209}(\gamma,n)Bi^{208}$	7.45

In producing neutrons from charged particle interactions, in addition to providing energy to overcome neutron binding, the incident particle must have sufficient energy to overcome a Coulomb potential barrier. Once this barrier is surmounted an energy bonus is obtained in the form of the binding energy of the incident particle in the nuclear potential well. The exception to this rule is electroneutron production where a Coulomb barrier is not involved. Electroneutron production can be looked upon as a special case of photoneutron production, by visualizing a fast electron as a flux of virtual photons.

Proton-Neutron Reactions: Energetics

Table III-3 presents a resume of proton reactions with intermediate and heavy nuclei. Reactions with light nuclei are not sufficiently generalizable to allow presentation in simple tabular form. The reactions in Table III-3 are presented in order of decreasing importance. Only those whose probability is at least 1% of the first reaction listed in the group have been presented. Elastic nuclear scattering has been omitted because of the difficulty in distinguishing it from non-nuclear (Coulomb) elastic scattering.

Because of the Coulomb barrier, proton cross sections for nuclear interaction are negligible below about 0.1 MeV. In light nuclei there are some exceptions which are of little interest here. Because of the mass difference between proton and neutron (0.78 MeV) the threshold for (p,n) reactions exceeds this value except for unstable target nuclei. For light and low-intermediate nuclei, (p,n) thresholds are of the order of an MeV. Neutron emission becomes the dominant reaction when the, incident particle energy exceeds the threshold by about 1 MeV. This is because an emitted charged particle faces a Coulomb barrier while an emitted neutron does not. Over about 10 MeV multiple particle emission becomes possible. As expected, because of the Coulomb barrier, (p,2n) is the dominant reaction.

Up to about 40 MeV most nuclear reactions procede via *compound nucleus* formation. A compound nucleus is a transition state in a nuclear reaction defined such that its mode of decay is independent of its mode of formation. In such a transition state, the incident particle interacts with the target nucleus as a whole rather then with individual nucleons and shares its energy among them.

For proper perspective it should be borne in mind that for energies of interest here, heavy charged particles still lose most of their energy via electromagnetic interactions with atomic electrons rather than through nuclear interactions. These electromagnetic interactions are primarily ionization and excitation with radiation losses of negligible importance.

Proton-Neutron Reactions: Probabilities

The existence of a Coulomb barrier to heavy charged particles means that reactions which are not forbidden by energy requirements may still have a very low probability (cross section) because they require tunneling through the barrier. When the probability

TABLE III-3

Proton Reactions with Intermediate and Heavy Nuclei

Proton Energy	Intermediate Nuclei ($25<A\leq80$)	Heavy Nuclei ($80>A$)
Low (0-1 keV)	--	--
Intermediate (1-500 keV)	n	--
	γ	
	α	
	(Resonance)	
High (0.5-10.0 MeV)	n	n
	p (inel)	p (inel)
	α	γ
	(Resonance for lower energies)	
Very high (10-50 MeV)	2n	2n
	n	n
	p (inel)	p (inel)
	np	np
	2p	2p
	α	α
	Three or more particles	Three or more particles

N.B. It should be noted that nuclear interactions do not constitute a relatively significant energy-loss mechanism in comparison with ionization losses for incident energies below about 100 MeV.

of barrier penetration becomes significant, the cross section increases rather sharply with increasing energy (Fig. III-1). This behavior is in contrast to certain incident neutron cross sections which exhibit a striking energy threshold phenomenon because neutrons face no Coulomb barrier (Fig. III-2). The resonance structure seen in the cross section for low energy neutrons may also exist for heavy charged particles but it is less marked. However the existence of a resonance structure means that nuclear reactions are highly individualistic as regards the incident particle, the target nucleus and the interaction energy. For this reason only a discussion of general cross sectional behavior is in order. Happily the resonance region is not of primary interest in neutron production or shielding.

For comparatively low energies, nuclear reactions can be described by a resonance theory. In this energy region compound nucleus formation is assumed to occur and the exited energy levels of this nucleus are discrete. For higher energies compound nucleus formation is still assumed to occur but exited levels now overlap, at least partially. For this reason, a continuum theory of cross sections is invoked which averages over many resonances. The region of applicability of resonance theory and continuum theory are characteristic of the target nucleus and the energy and type of the incident particle. Because the interest of this chapter is in energies well above the resonance region only continuum theory cross sections will be discussed.

The device of a compound nucleus is convenient precisely because it assumes that its production and decay are uncoupled events. This means that the probability of a reaction involving compound nucleus formation is the product of the probability of its formation and the probability of its decay. The probability of formation is the probability of absorption of the initiating particle. The probability of decay is quite analogous to that for radioactive decay, describable by a total probability which is the sum of all the probabilities for permitted decays. For a given state of the compound nucleus, decay by neutron emission generally is highly favored over decay by charged particle emission because of the Coulomb barrier. Furthermore it is generally favored over decay by gamma emission except when the excitation energy of the compound nucleus is small.

The cross section for formation of a compound nucleus by heavy charged particle absorption, for energies above threshold but well below the Coulomb barrier height, has a rather sharply rising front (Fig. III-3). This rise is indicative of the sharply increasing probability of Coulomb barrier penetration and continues to energies about half the barrier height. Eventually the rate of increase levels off, with the cross section ultimately approaching the geometrical cross section (πR^2) in an asymptotic fashion. For protons of energy equal to the barrier height (Ze^2/R), the cross section is of the order of one-half to one-fourth the geometrical area.

The assumption of validity of the compound nucleus model of interaction also allows semiquantitative inferences about the energy and angular distribution of neutrons from (p,n) reactions. So long as the model is valid the energy introduced into the nucleus by the incident particle is distributed fairly homogeneously throughout the nucleus. This is an alternative way of saying that the nucleus forgets how it was formed or equivalently

that the mode of decay is independent of the mode of formation. With a fairly homogeneous distribution of the incident particle among nucleons, the nucleus is "heated up" and therefore capable of "boiling off" nucleons. A further consequence of this boiling off phenomenon is that the emitted nucleons are spatially isotropic. This of course assumes that numerous modes of decay are available. Fission neutrons are an example of boiling off from a heated-up (fissioned) nucleus. For this reason neutrons from other reactions which proceed via compound nucleus formation have an energy and angular distribution similar to fission neutrons (Fig. III-4).

As the compound nucleus model breaks down (in the region 30-50 MeV) as interactions with individual nucleons become more important. Spatially this causes the isotropic component due to boiled off nucleons to be overlaid with an anisotropic component biased in the forward direction (relative to the incident beam). Energywise the spectrum becomes a fission spectrum skewed in the direction of high energy. In neutron shielding it is this forward-emitted, high energy component which imposes the major restrictions. While comprising a minority of the neutrons emitted, this component can dominate the shielding design for incident proton energies above 30 MeV. To quantify this discussion, Fig. III-5 presents the estimated total neuron yield per microampere of proton beam current onto targets of Be, Cu and U.

Deuteron – Neutron Reactions

Table III-4 presents a resume of deuteron reactions with intermediate and heavy nuclei. As in the proton case reactions with light nuclei are not simply generalizable.

One can obtain a valuable insight into the nuclear reactions of the deuteron from its anomalously low binding energy. From Table III-1 we see that the energy necessary to free a neutron (i.e., its binding energy) is 2.23 MeV as compared with more than ten MeV for most low atomic number nuclei. A second valuable insight is obtained from the recognition that the center of mass of a deuteron does not coincide with the center of charge. For these two reasons, two reaction schemes are available to deuterons in addition to those involving compound nucleus formation.

Compound nucleus reactions of deuterons are as expected if one ignores its loosely bound structure. Modes of deexcitation include proton and neutron emission.

The first new type of interaction for the deuteron involves decomposition into a neutron and a proton by the Coulomb field of the target nucleus. No nuclear interaction is involved. The result is a proton and a neutron being "emitted" from the interaction. This is in fact a dissociation reaction with the incident deuteron experiencing the time-varying electromagnetic field of the nucleus. Obviously, sufficient energy must be available; therefore this reaction appears for deuterons of the order of MeV. Its cross section may be comparable to that for competing processes and the angular distribution of the emitted neutrons will have a forward bias.

TABLE III-4

Deuteron Reactions with Intermediate and Heavy Nuclei

Deuteron Energy	Intermediate Nuclei ($25<A\leq80$)	Heavy Nuclei ($A>80$)
Low (0-1 keV)	--	--
Intermediate (1-500 keV)	p	--
	n	
High (0.5-10 MeV)	p	p
	n	n
	pn	pn
	2n	2n
	d (inel)	
Very high (10-50 MeV)	p	p
	2n	2n
	pn	pn
	3n	3n
	d (inel)	d (inel)
	Three or more particles	Three or more particles

The second new type of reaction involves absorption of only one component of the deuteron to form a compound nucleus, the other component being "emitted" from the reaction. This "emitted" component will obviously be spatially anisotropic. Such a reaction is understandably called a stripping reaction. Sometimes this designation is reserved for high energy reactions whose low energy counterpart is called the Oppenheimer Phillips process. In this low energy case, because of the Coulomb repulsion of the proton constituent of the deuteron, the neutron is absorbed while the proton is not. A stripping reaction should not be confused with a reaction in which the whole deuteron is absorbed to form a compound nucleus which subsequently decays by emitting a neutron or proton.

Neutrons which are produced by the deuteron stripping process have a continuous energy spectrum even for monoenergetic incident deuterons. This arises from the fact that in the interaction there are three components of deuteron energy which may be split in a continuous spectrum of ways.

Comparison of Tables III-3 and III-4 gives insight into the interplay of the various neutron generating processes involved in deuteron reactions. The Coulomb barrier faced by a deuteron is virtually the same as the for a proton when the deuteron energy is twice that of the proton. In this way the proton energy is about the same in both cases. Consequently barrier penetration becomes significant for both for energies of the order of an MeV. Below this in the deuteron case, stripping reactions prevail which emit protons. For the energy range considered here (<50 MeV), (d,p) reactions are the most probable, testifying to the importance of stripping even at high energies. The second most important reaction over this range is (d,n) with (d,2n) prevailing at higher energies. These neutrons come from both stripping reactions and compound nucleus reactions. A point to note here is that neutrons from the former have a forward bias and a higher average energy than those from the latter (Fig. III-6). To quantify this discussion Fig. III-7 presents the estimated total neutron yield per microampere of deuteron beam current onto targets of Be and Cu.

A discussion on deuteron-induced, neutron-generating reactions is of importance not only because deuterons themselves are of interest but also because their consideration provides insights into interactions of accelerated charged particles of higher atomic number. A study of alpha particles is less enlightening in this regard because of their atypically high binding energy. In fact deuterons and alpha particles represent extremes in binding energy per nucleon.

Alpha-Neutron Reactions

Table III 5 presents a resume of alpha reactions. Comparison with Table III-3 shows that the nuclear interactions of alphas and protons are remarkably similar energywise, when one matches proton energy with energy per nucleon of alphas. Because of its high binding energy (28 MeV) the alpha particle functions as a unit over the energy range of interest rather than a collection of nucleons as in the deuteron case. For this reason

TABLE III-5

Alpha Reactions with Intermediate and Heavy Nuclei

Incident Energy	Intermediate Nuclei ($25 \leq A \leq 80$)	Heavy Nuclei ($A > 80$)
Low (0-1 keV)	--	--
Intermediate (1-500 keV)	n	
	γ	
	p	
	(Resonance)	
High (0.5-10 MeV)	n	n
	p	p
	α (inel)	γ
	(Resonance for lower energies)	
Very high (10-50 MeV)	2n	2n
	n	n
	np	np
	2p	2p
	α (inel)	α (inel)
	Three or more particles	Three or more particles

the simplifications invoked for protons regarding cross sections for neutron production, and for angular and energy distribution of emitted neutrons, apply reasonably well for alpha particles. One must appreciate however that the Coulomb barrier is now ($2Ze^2/R$) because of the alpha double charge.

Figure III-8 presents the estimated total neutron yield per microampere of alpha beam current onto targets of C and Ta.

Photoneutron Reactions

Table III-2 presented a sampling of photoneutron thresholds. Such reactions also proceed via compound nucleus formation, just as the previously discussed cases. Therefore for sufficiently high energy the energy distribution is similar to the fission spectrum and the angular distribution is isotropic. For still higher energies the energy spectrum is similar to the fission spectrum skewed to higher energies (Fig. III-9) and angular distribution develops a forward bias.

Generally photodisintegration cross sections rise sharply from a threshold energy to a peak from 3 to 8 MeV higher (Fig. III-10). The curve is roughly bell-shaped and about 6 MeV wide. As the target mass number increases the integrated cross section generally increases while the peak value generally decreases.

Photoneutron production is associated with electron accelerators and therefore intermingled with electroneutron production. Yield curves will be presented in the next section.

Electroneutron Reactions

As mentioned earlier electroneutron production can be looked upon as a special case of photoneutron production by visualizing the fast electron as a flux of virtual photons. This is called the Weizsacker-Williams method. Essentially the electron undergoes inelastic scattering with the nuclear (as opposed to the Coulomb) field of the nucleus. The nucleus is left in an excited state from which it will decay as does any compound nucleus As regards neutron production, the intervention of a compound nucleus allows one to invoke the usual picture for energy and angular distribution. Furthermore it can be shown that the electronuclear cross section is less than the photonuclear cross section by a factor of approximately one hundred. Fig. III-11 presents total neutron yield per microampere of electron accelerator beam current for thick targets. The majority of these neutrons are from (γn) reactions arising from bremsstrahlung.

Neutron Shielding

Neutron shielding is a business of slowing down neutrons to thermal or near thermal energies where they can be captured with subsequent emission of a photon or series of photons. Table III-6 presents the hierarchy of neutron reactions with intermediate and

TABLE III-6

Neutron Reactions with Intermediate and Heavy Nuclei

Incident Energy	Intermediate Nuclei $25 \leq A \leq 80$	Heavy Nuclei $A \geq 80$
Low (0-1 keV)	n (elastic)	γ
	γ	n (elastic)
	Resonance	Resonance
Intermediate (1-500 keV)	n (elastic)	n (elastic)
	γ	γ
	Resonance	Resonance
High (0.5-10 MeV)	n (elastic)	n (elastic)
	n (inelastic)	n (inelastic)
	p	p
	α	γ
	Resonance for lower energies	
Very high (10-50 MeV)	2n	2n
	n (inelastic)	n (inelastic)
	n (elastic)	n (elastic)
	p	p
	np	np
	2p	2p
	α	α
	Three or more particles	Three or more particles

heavy nuclei for energies up to 50 MeV. For accelerators of energy less than 30 MeV the vast majority of neutrons produced have energy below 10 MeV (i.e., a modified fission spectrum.

In order to slow down neutrons to thermal energies one exploits the fact that the inelastic and elastic scattering cross sections are dominant in the 0.5 to 10 MeV range. By the former type of scattering, high energy neutrons are reduced to intermediate energies by losing energy to excited levels of target nuclei. By the latter type of scattering, neutron energies can be reduced to thermal values by increasing the kinetic energy of the target nucleus as a whole. At thermal energies elastic scattering is still the most favored reaction (at least in intermediate nuclei) however no net energy exchange occurs. Consequently neutrons eventually fall prey to neutron capture (n, γ) reactions. These gammas must be shielded against in turn.

Because slowing down is such an important part of neutron shielding the basic constituents of a shield are selected for their superior slowing down properties. From consideration of simple elastic collisions of billiard balls it is clear that more neutron energy is lost in elastic scattering by light nuclei than by heavy ones. Indeed hydrogen in water and carbon in graphite are the reasons why these materials are selected as neutron moderators (slowing down media) in thermal neutron reactors. Likewise for neutron shielding concrete, with its low A constituents, is far more effective than lead. Since accelerator facilities whose primary hazard is X- or gamma radiation are generally shielded with concrete, it is a fairly accurate rule of thumb that for energies of interest here, the facility generally contains adequate neutron shielding in the process. The more serious neutron shielding problem occurs when the X- and gamma ray hazard is exceeded by the neutron hazard. Proton and deuteron accelerators are cases in point.

Another type of problem arises from anisotropic neutrons in the high energy tail of the spectrum. It will be recalled that this spectral segment is explained by the breakdown of the compound nucleus model, and that its importance increases with increasing incident particle energy. Its existence necessitates additional shielding in objectionable directions. Because generally there are no severe restrictions on the amount of shielding permitted, it is customary to incorporate in design significant safety factors to compensate for possible effects of uncertainties in cross sections.

One should appreciate at the outset that neutron shielding is a complex topic from a theoretical point of view. Fortunately a reasonably effective empirical approach has been developed for neutron shielding of nuclear reactors. It is called the Removal Cross Section Method. This phenomenological technique describes penetration of fission neutrons through a shielding medium with a simple exponential function using an empirically selected "removal" cross section. It is obviously concerned primarily with the most penetrating component of the neutron flux. A simple exponential function suffices because these penetrating neutrons come from a narrow band in the fission spectrum whose specific energy depends on the thickness of the shield and on its detailed composition. For neutrons

in this energy band, elastic scattering with hydrogen or inelastic scattering of any type reduces their energy sufficiently to preclude the necessity of further consideration, at least as regards shield penetration. This effective absorption can be described by an appropriate, empirically-chosen, absorption (i.e., removal) cross section.

The reader will note the formal similarity between the removal cross section method for neutrons and the uncollided flux approximation for photons. In both cases, particles which undergo any type of interaction are assumed to be removed effectively from further consideration.

Experimental removal cross sections are roughly three-quarters of the total cross section for 8 MeV neutrons. For hydrogen this fraction is somewhat larger. Table III-7A presents experimentally determined values of the microscopic removal cross section for various materials. Figure III-2 presents the macroscopic removal cross section divided by density as a function of atomic weight. Table III-7B presents macroscopic removal cross sections for shielding materials.

In discussing the various methods of neutron production in accelerators of energy less than 30 MeV we concluded that the fission spectrum (skewed to the high energy end as needed) is a reasonably good approximation, at least for intermediate and heavy target nuclei and for energies an MeV or more above the neutron threshold. It is essential to appreciate that this conclusion is far from being universally true. Numerous exceptions to it can be found, for example for light nuclei, for incident particles just above threshold and above about 30-50 MeV (where the compound nucleus model begins to break down). Nevertheless because we are concerned with neutron shielding, some inaccuracy can be tolerated so long as it is in the safe direction. For a shielding point of view, high energy neutrons and their anisotropies are of concern as the primary shortcoming to the removal cross section approach. This shortcoming can be handled by reinforcing shield thicknesses based on removal cross section calculations in the appropriate directions.

One further shielding problem deserving of consideration is neutron skyshine. Just as in gamma skyshine, outside of the shielding wall a neutron flux might be found which is attributable to radiation passing over the shield via air scattering. This may be a significant problem when, for other reasons, little shielding is installed on the roof of the accelerator. Since the energy and spatial distribution of neutrons approximates the fission spectrum and since elastic scattering cross sections are well known for energies of interest, the problem can be formally treated in the same manner as gamma skyshine, discussed elsewhere in this text.

Shielding Calculations: Examples

Two examples will be considered to illustrate first approximation calculations for neutron shielding.

TABLE III-7A

Experimentally Determined Values of Microscopic Removal Cross Sections

Material	Cross Section (barns per atom or molecule) Fission Neutrons
Al	1.31
B	0.97
Be	1.07
Bi	3.49
C	0.81
Cl	1.2
Cu	2.04
F	1.29
Fe	1.98
Li	1.01
Ni	1.89
O	0.99
Pb	3.53
W	2.51
U	3.6
C_7F_{16}	26.3
C_2F_3Cl	6.66
CH_2	2.84
B_4C	47
B_2O_3	4.30
D_2O	2.76
H_2O	3.09

Table III-7B

Macroscopic Removal Cross Sections of

Some Shielding Materials

Materials	Cross Section (cm^{-1})
Iron	0.158
Graphite	0.785
Ordinary Concrete	0.0942
Barytes Concrete	0.0945

In the first example let us determine approximately how much neutron shielding is required for a proton accelerator operating at 20 Mev, with a Cu target optimized for neutron production. From Figure III-5 we see that about 6.5×10^{10} neutrons per second are produced for each microampere of proton current. Let us choose to locate the shield at 10^3 cm from the neutron-generating Cu target. The neutron flux onto the shield is therefore about 5×10^3 n/cm^2-sec for each μamp of protons, assuming that it is isotropic. To a good approximation this flux is normally incident onto the upstream side of the shield. Let us determine the shield thickness which will yield a downstream neutron flux of 5 n/cm^2-sec for a proton current of 1 mamp. This means the shield must reduce the fast neutron flux by six orders of magnitude. Therefore

$$e^{-\Sigma_r X} = 10^{-6}$$

For barytes concrete (i.e., $\Sigma_r = 0.0945\ cm^{-1}$, from Table III-7B):

$$X = 146 \text{ cm}$$

Therefore a shield of barytes concrete (or ordinary concrete for that matter) of about five feet is required. The assumption that neutron flux is normally incident onto the shield can be lifted by first correcting for the inverse square diminution over this additional five feet and then by repeating the calculation of the required shielding thickness. This yields a value of about 144 cm which indicates the "goodness" of the original assumption of a normally incident flux onto the shield.

The second example, to illustrate neutron skyshine, initially requires examination of the neutron cross sections for air for energies in the MeV range. Within a factor of about two the total neutron cross section for air is 1.5 barns. The major component of this is elastic scattering with inelastic scattering accounting for much less than 1% of

the total. The energy loss per elastic scattering can be assumed negligible since we are really dealing with averages over a broad spectrum and elastic scattering will effectively modify only the spectral shape. Finally the angular distribution of neutrons elastically scattered in air, although not isotropic, can be reasonably approximated by isotropic in this calculation. In fact the real angular distribution does not differ from an isotropic one by factors greater than about two.

To illustrate the central points of a skyshine calculation we shall treat the simplified problem indicated in Fig. III-13. We wish to calculate the neutron flux which traverses path "a" from a point source to a scatterer *and* path "b" from a scattering volume dV to a point detector. The source emits S neutrons per second. Of these, the number per cm^2 per second which reach the differential scattering volume along path a is $[S \exp(-\Sigma_r r_a)]/4\pi r_a^2$. The number which finally reach the point detector along paths a and b is $(S\Delta V\Sigma_s[\exp(-\Sigma_r r_a)]/4\pi r_a^2) \cdot [\exp(-\Sigma_r r_b)]/4\pi r_b^2$, where Σ_s is the elastic scattering cross section of air.

In order to account for all the skyshine reaching the detector we have to integrate over all possible air scattering paths between the source and the detector. In addition to single scattering, multiple scattering would have to be accounted for. Except in unusual cases, however, single scattering events would be the most important contributors to skyshine.

Calculation of shielding to protect against neutron skyshine proceeds substantially as in the first example of this section once the strength of skyshine has been determined.

References

1. Protection Against Betatron-Synchroton Radiations up to 100 Million Electron Volts, Handbook 55, National Bureau of Standards, (1954), Washington, D. C.

2. Protection Against Neutron Radiation Up to 30 Million Electron Volts, Handbook 63, National Bureau of Standards, Washington, D. C., 1957.

3. Shielding for High-Energy Electron Accelerator Installations, Handbook 97, National Bureau of Standards, Washington, D. C., 1964.

4. Hughes, D. J. and J. A. Harvey, Neutron Cross Sections, USAEC Report BNL-325, Brookhaven National Laboratory.

5. Etherington, H. (Ed.), Nuclear Engineering Handbook, McGraw-Hill Book Co., New York, 1958.

6. Price, B. T., C. C. Hortin and K. T. Spinney, Radiation Shielding, Permagon Press Ltd., Oxford, 1957.

7. Rockwell, Theodore, III, Reactor Shielding Design Manual, D. Van Nostrand Co., Inc., Princeton, N. J., 1956.

8. Livingston, M. S. and J. P. Blewett, Particle Accelerators, McGraw-Hill Book Co., New York, 1962.

9. Evans, R. D., The Atomic Nucleus, p 468, McGraw-Hill, N. Y., N. Y., (1955).

10. Moyer, B. J., unpublished data.

11. Kimel, L. R., Maschkovich, V. P., and Panchecko, A. M., Shielding from Radiations of Electron Accelerators with Maximum Energy of Accelerated Electrons up to 30 MeV., Instruments and Methods of Radiation Analysis FTD-MT-64-179 (1965).

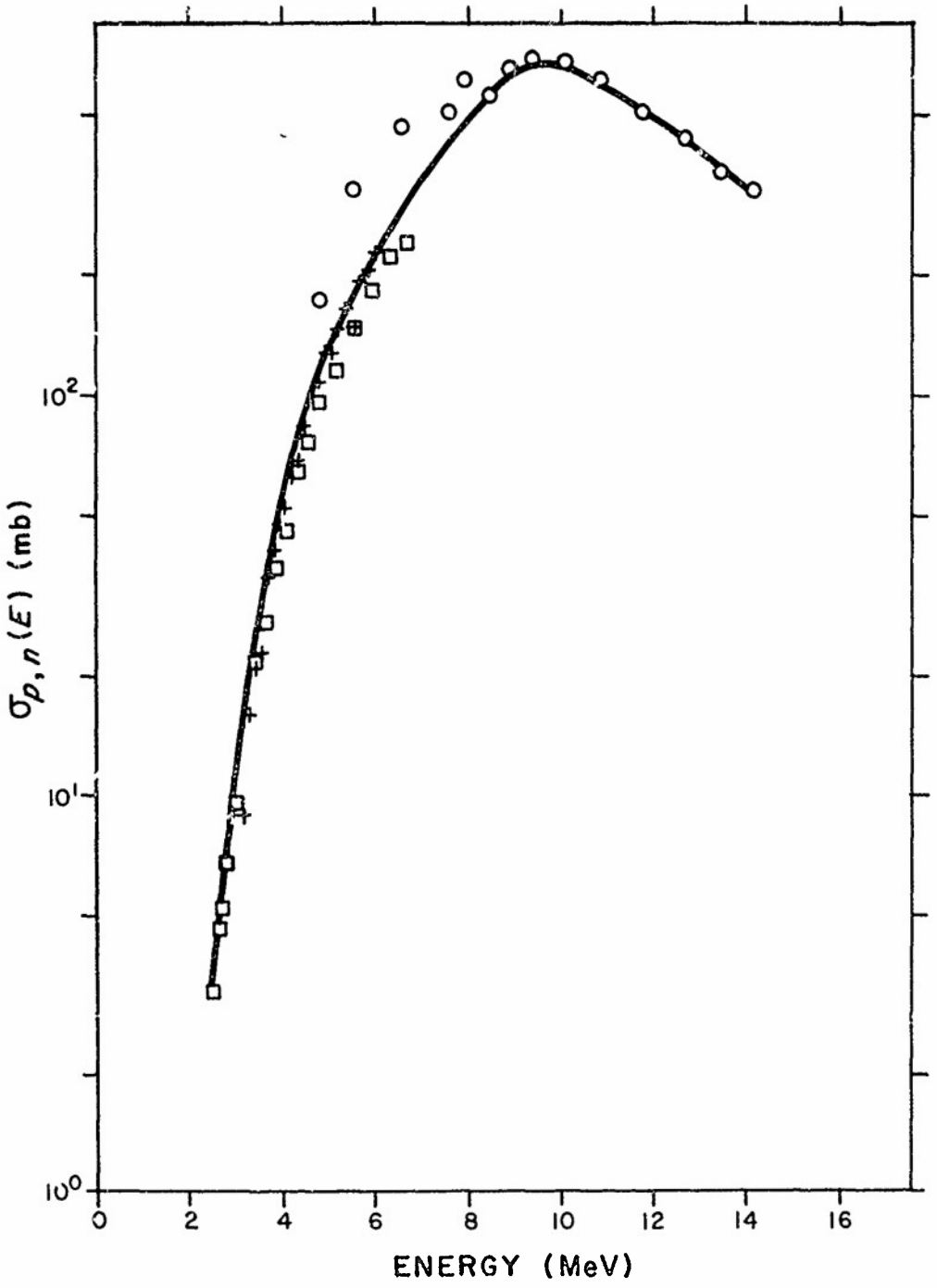

Figure III-1 – Cross section for the reaction (p,n) in Ni^{61}.[4]

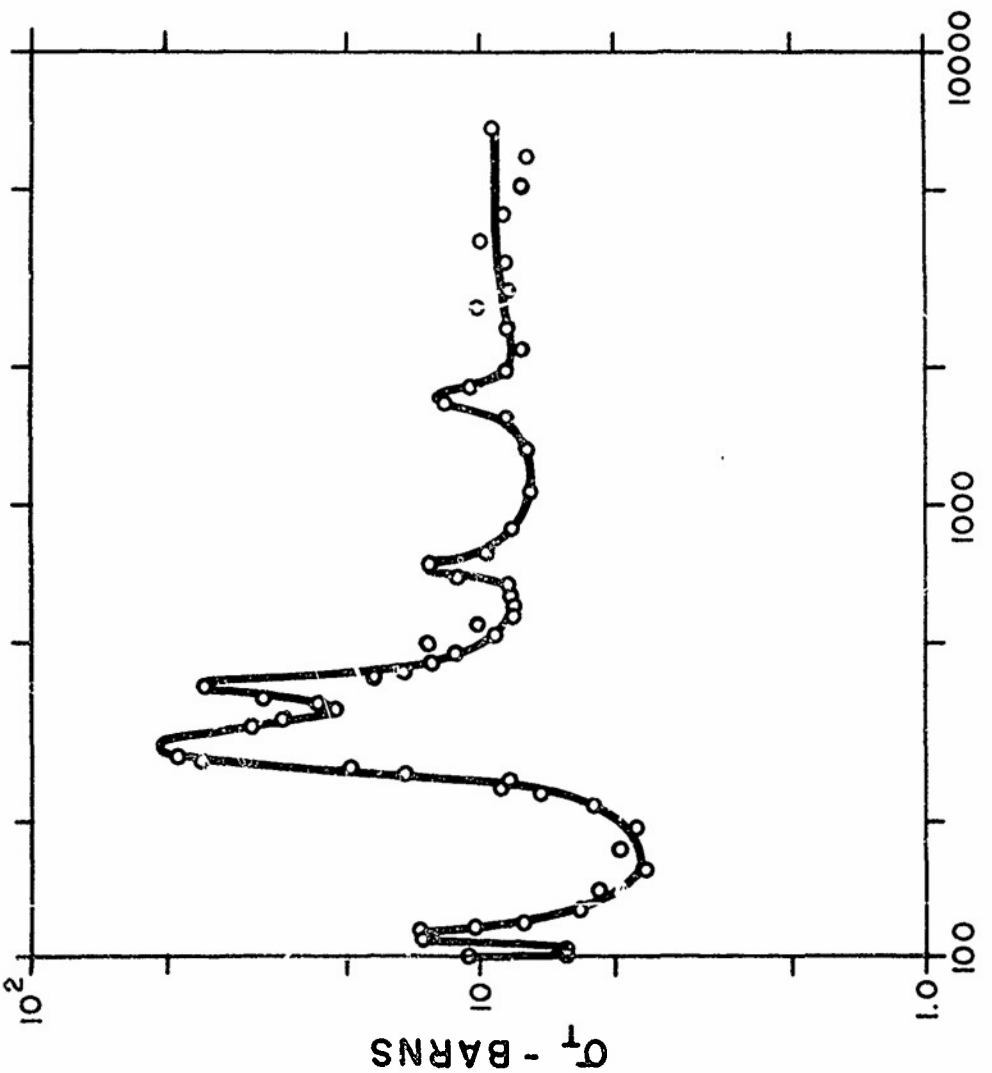

Figure III-2 — Total neutron cross section in the resonant region for Ga^{51} [4]

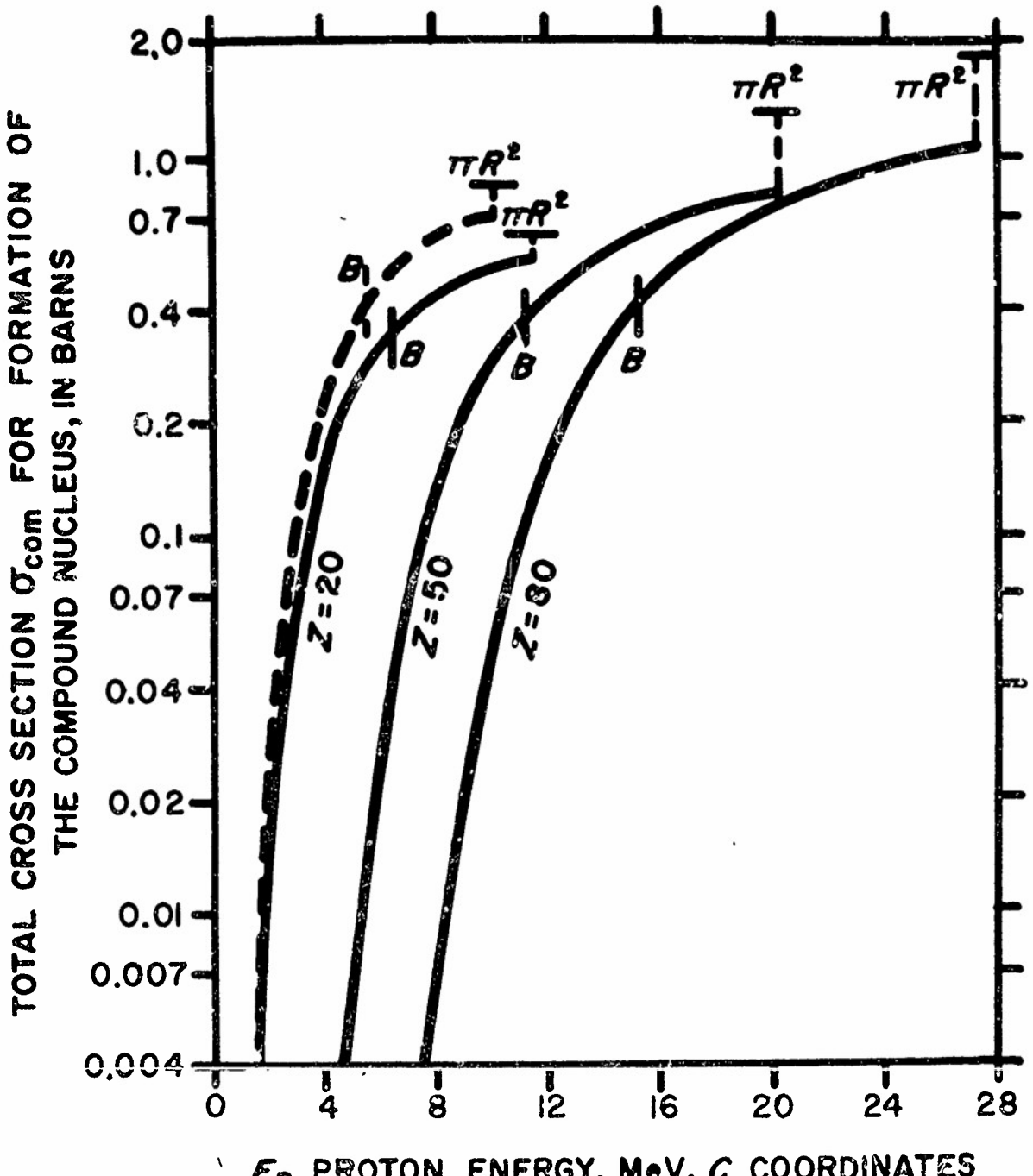

Figure III-3

Theoretical predictions of the total cross section for compound nucleus formation by protons for Z = 20, 50, and 80. Bars marked B indicate coulomb barrier height ($B = Ze^2/r$). The nuclear radius is assumed to be = $1.3 \times 10^{-13} A^{1/3}$ cm. The dotted curve is for Z = 20 if $r = 1.5 \times 10^{-13} A^{1/3}$ cm. For each curve the asymptotic limit πr^2, is indicated[9].

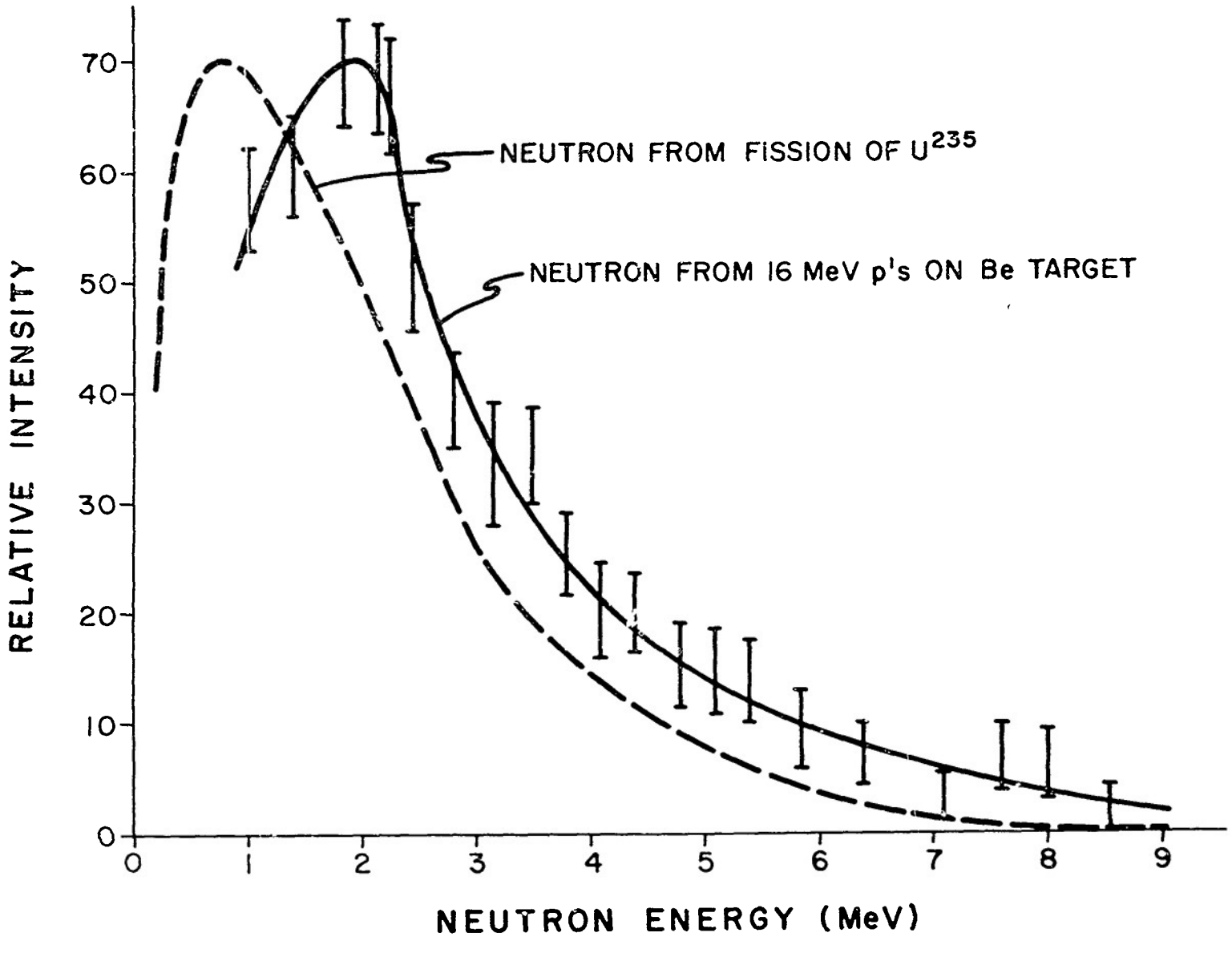

Figure III-4 — Neutron spectrum for 16 MeV protons on Be and from U^{235} fission[8].

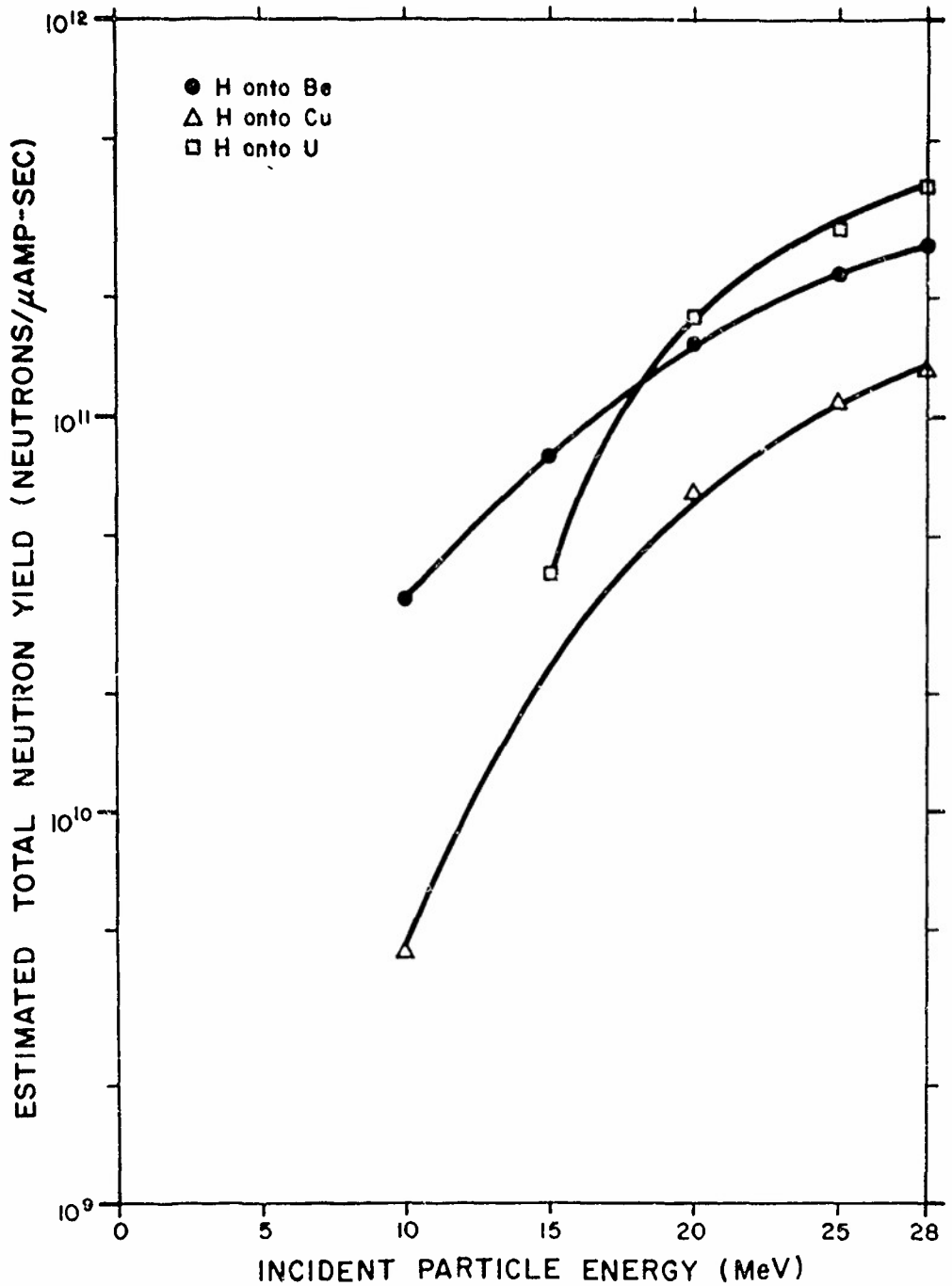

Figure III-5 — Estimated total neutron yield per microampere-second of proton beam on targets of Be, C , and U as a function of incident proton energy[10].

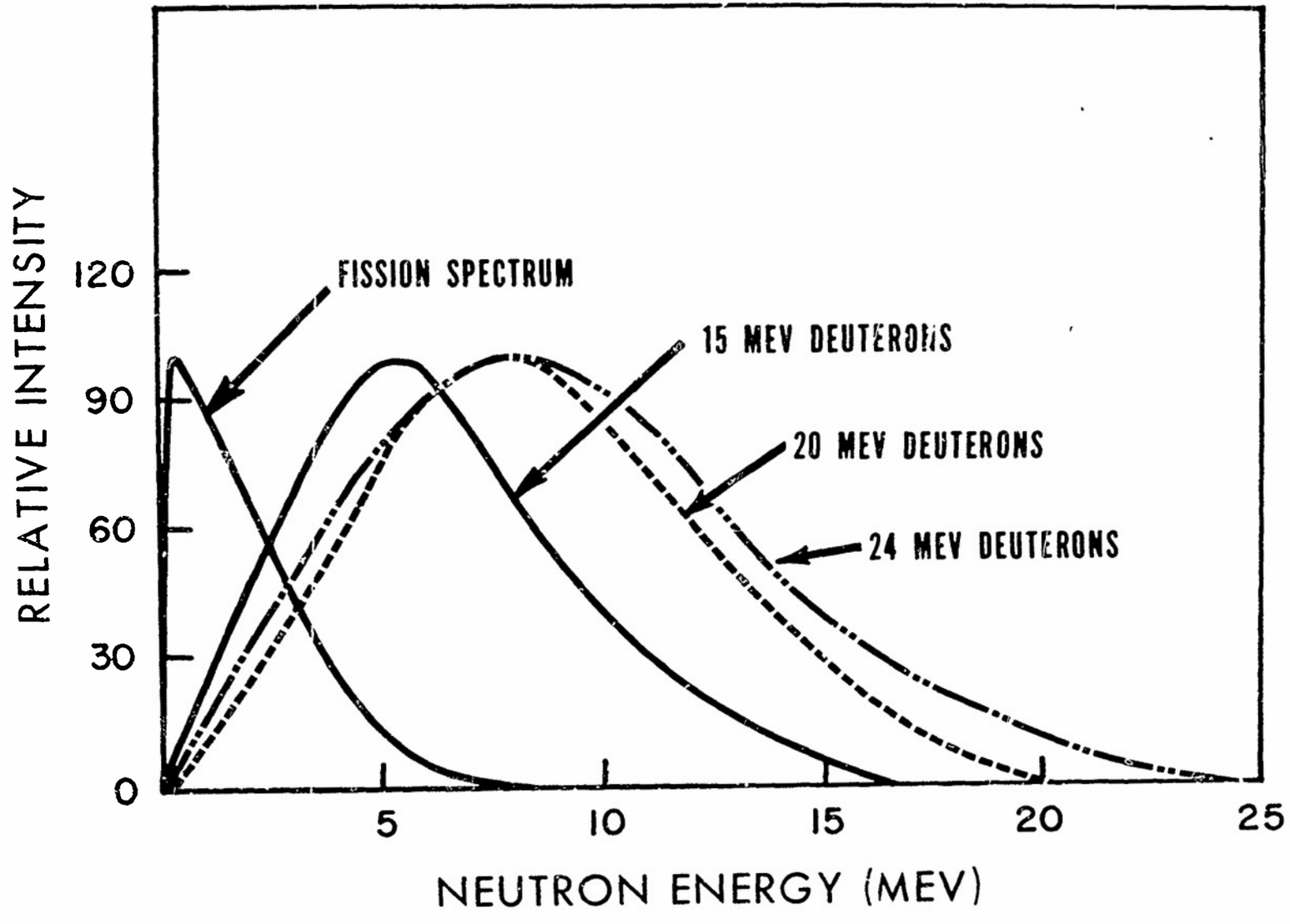

Figure III-6 — Neutron spectrum from (d,n) reactions on a thick Be target using 15, 20, and 24 MeV deuterons. The fission spectrum of U^{235} is included for comparison[11].

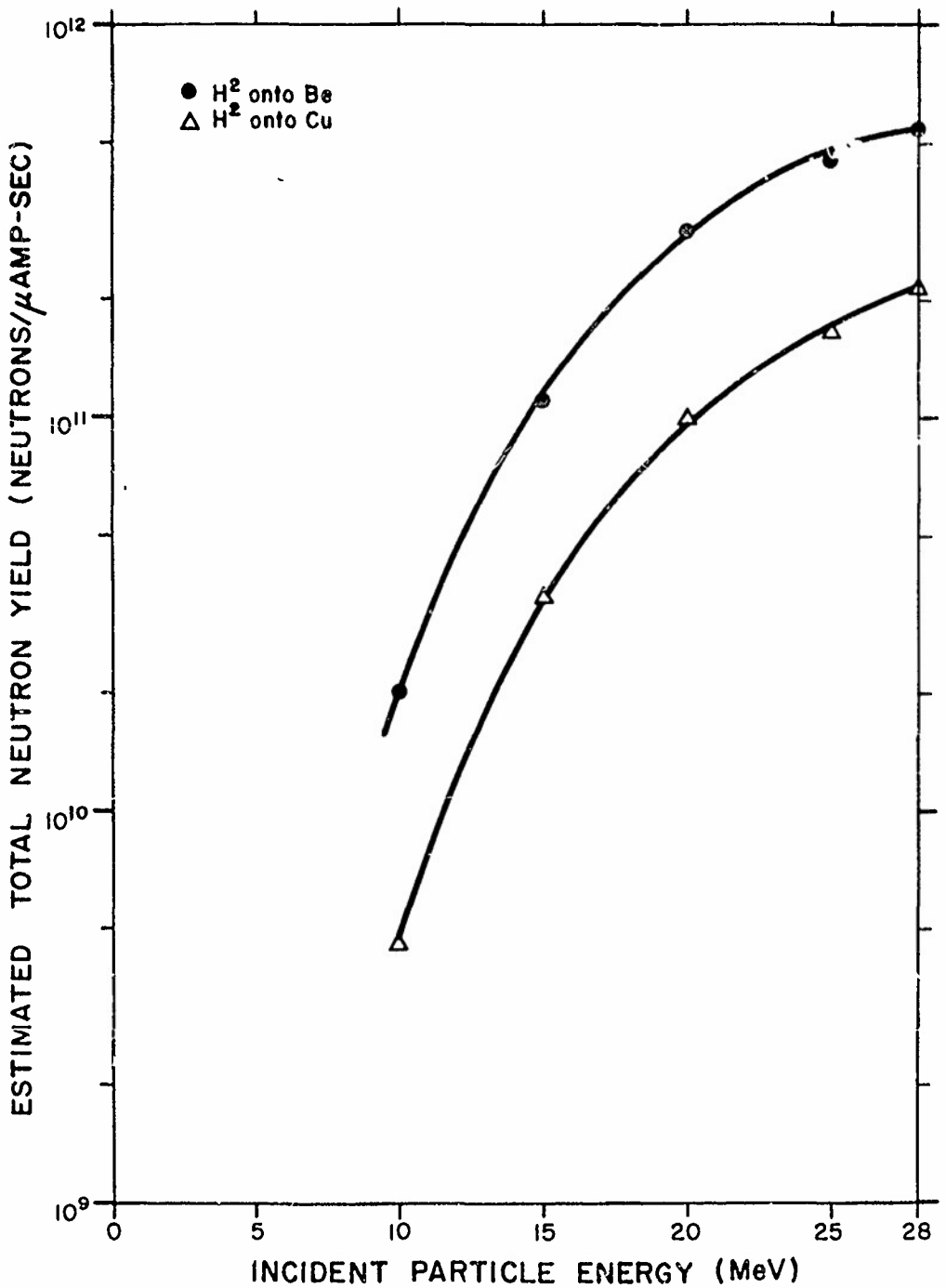

Figure III-7 – Estimated total neutron yield per microampere-second of deuteron beam on targets of Be and Cu as a function of incident deuteron energy[10].

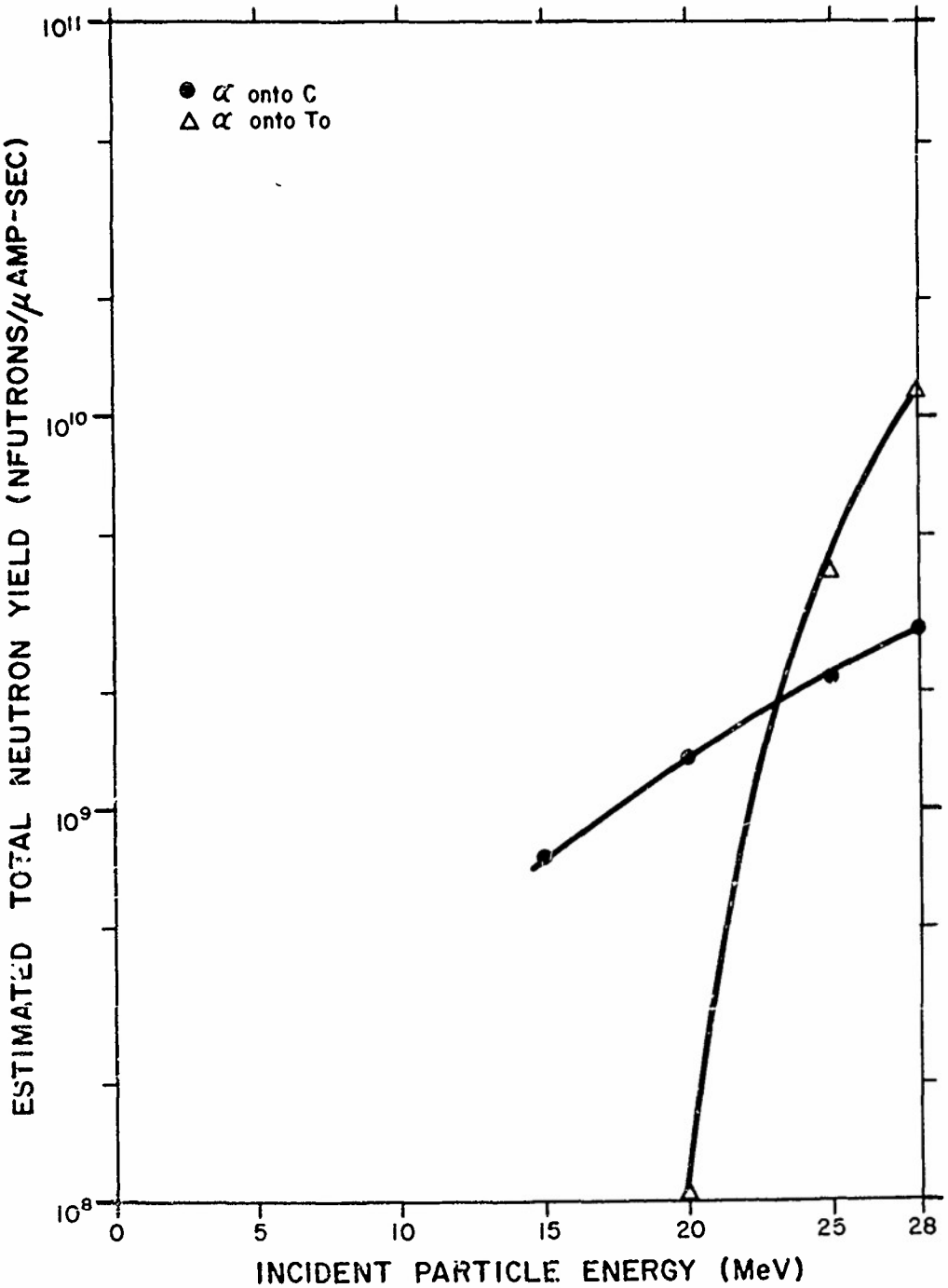

Figure III-8 – Estimated total neutron yield per microampere-second of alpha beam on targets of C and Ta as a function of incident alpha energy[10].

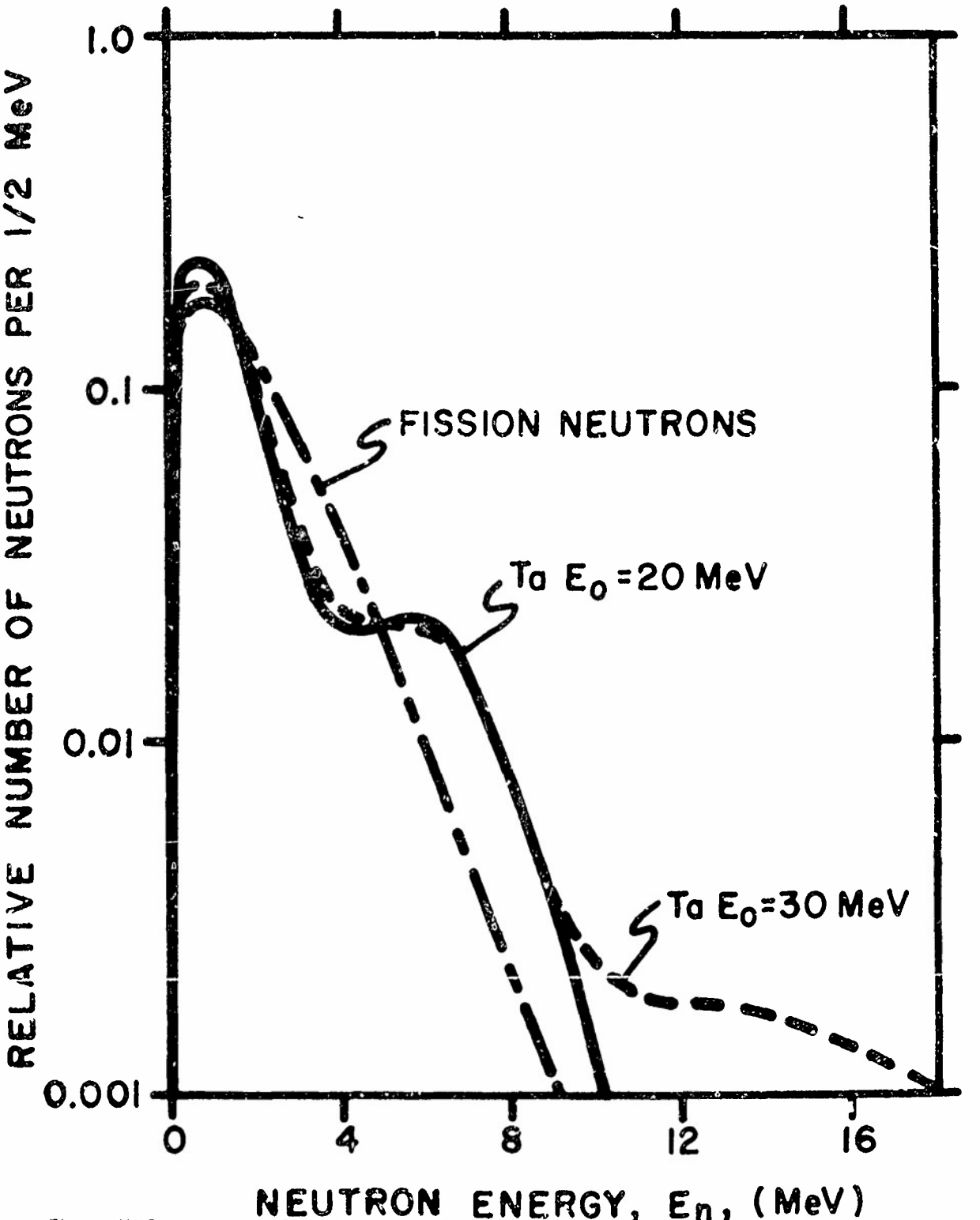

Figure III-9 – Photoneutron spectra for Ta with bremsstrahlung energies of 20 and 30 MeV. The fission spectrum for U^{235} is included for comparison[3].

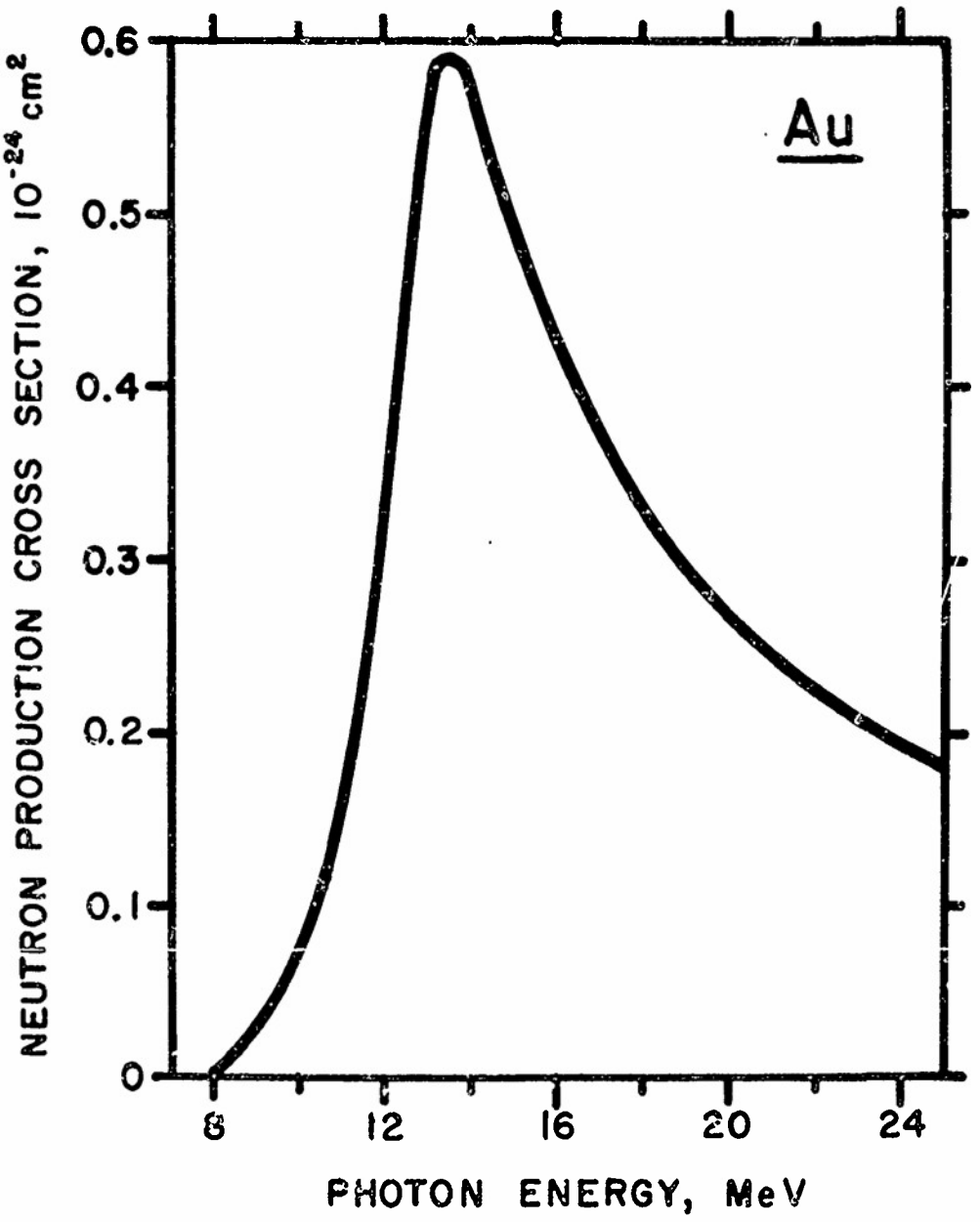

Figure III-10 – Photoneutron production cross section for Au^3.

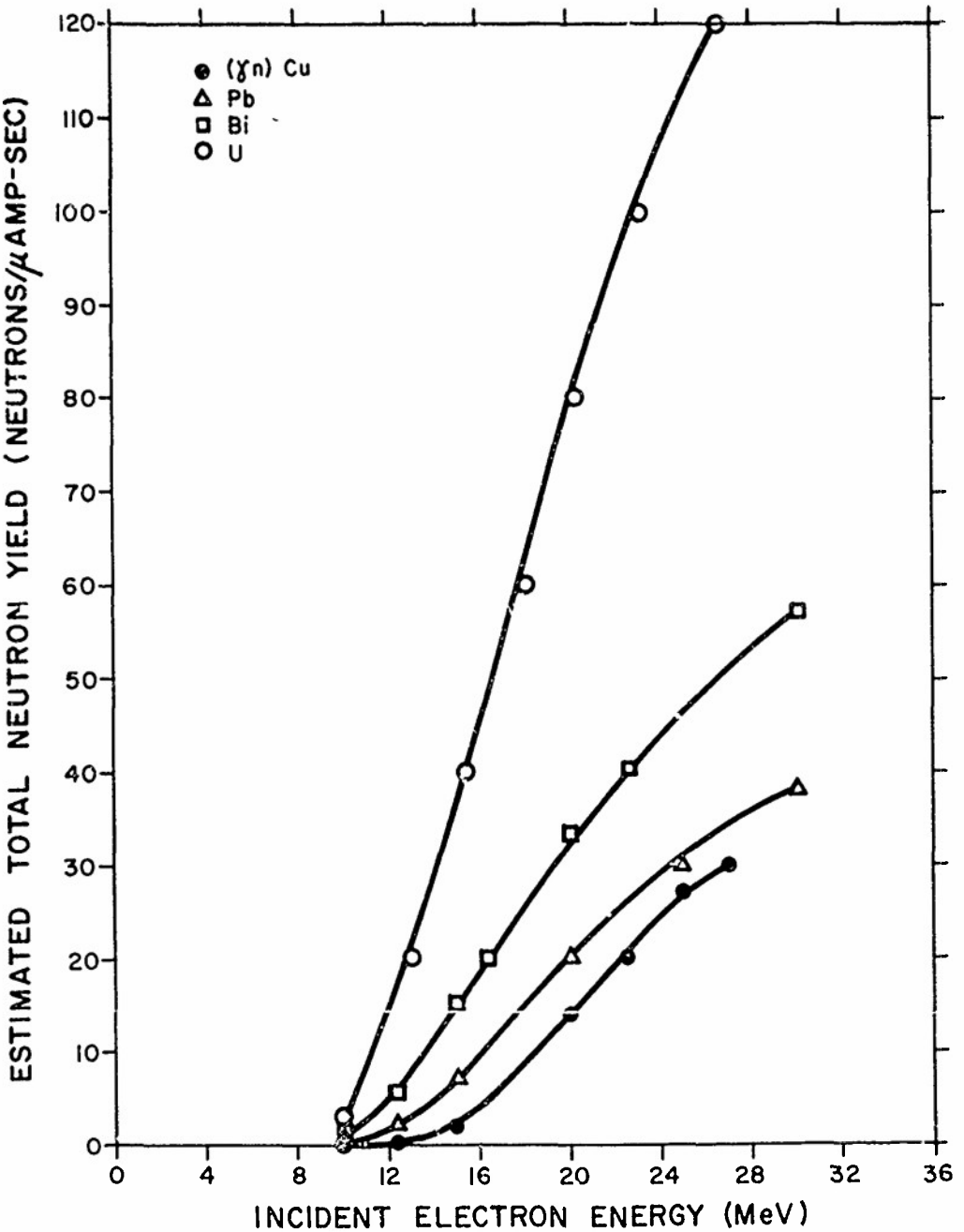

Figure III-11 – Estimated total yield per microampere-second of electron beam on targets of Cu, Pb, Bi, and U as a function of incident electron energy[11].

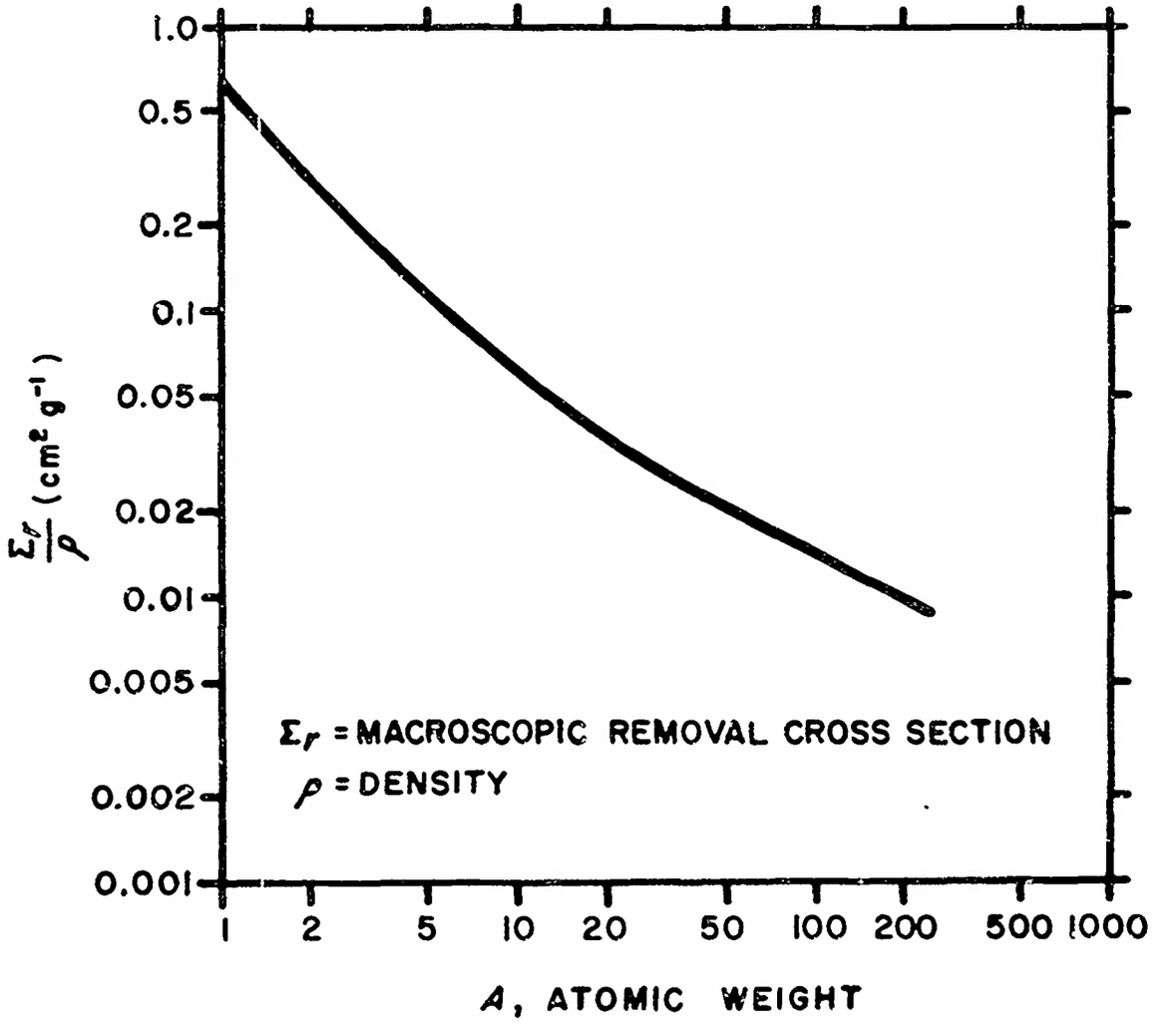

Figure III-12 – Neutron macroscopic removal cross section divided by density as a function of atomic mass number A^2.

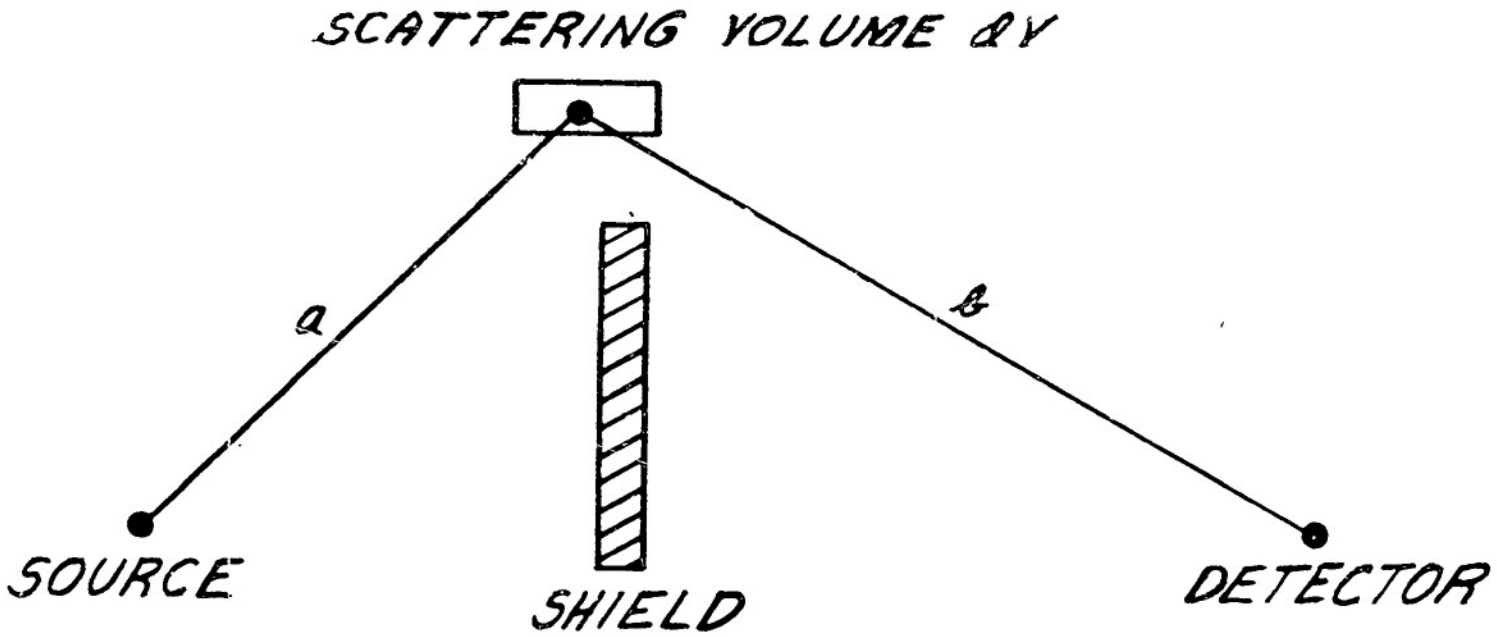

EXAMPLE OF NEUTRON SKYSHINE

Figure III-13

Chapter IV

Radioactivity Induced in Accelerator Installations

R. D. Cooper, T. G. Martin and A. Brynjolfsson

Introduction

The hazards presented by the primary and secondary beams from accelerators during the time that the machines are on have been discussed in Chapters II and III. Provided that the energy of the accelerated particle is sufficient there will exist certain hazards after the machine has been turned off. These hazards can be divided into short-term, lasting only a few minutes, and long-term build-up of radioactivity.

This discussion will consist first of a general description of the production and decay of accelerator induced activity. In the remainder of the chapter, emphasis will be placed on areas where the activity can be produced. This will allow concentration of attention on the few elements which occur in these particular areas.

The areas to be considered include the shielding, the target, the accelerator itself, auxiliary equipment in the area, and the circulating fluids such as air and water which enter the area on the accelerator beam and then leave again. Some of these are clearly short-term problems such as with the circulating fluids in which long-term activities may be removed by exhaust and filtration, and with targets that may be replaced. On the other hand, the shielding and the accelerator itself usually become only slowly radioactive but can build up to high levels over a long period of time.

Another difference which exists in these different areas is the particle or photon which can be effective in inducing the activity. The activity produced in the target is principally produced by the accelerated particle while the activity produced in the shielding and the accelerator itself is commonly produced by either neutrons or high energy bremsstrahlung.

Table IV-1 lists the major elements which occur in each of the areas to be considered. This will allow the determination of the radioisotopes which will be produced in the various areas and from this the amount of activity which will be present at different times and under different conditions.

A very complete discussion of the production of radioactivity by energetic particles and photons has been given by Barbier[1]. This chapter will deal only with the specific problems involved in the production and decay of radioactivity in and around accelerators which have energies less than about 50 MeV. Simplified methods and the necessary data will be given here to allow calculation of the approximate amounts of activity produced in these installations under a variety of practical conditions.

Production and Decay of Induced Activity

Except for the direct production of activity in targets which will be discussed later the induced activity around accelerators will be a two step process. First neutrons or high energy photons are created in the target by the primary beam. The neutrons and photons will then interact and induce radioactivity in the surrounding materials.

The discussion in this section will be divided initially into a discussion of the production reactions of neutrons, their angular and energy distributions followed by a description of the nuclear reactions by which the neutrons form radioactive products. Attention will then be focused on bremsstrahlung production and the activity which can subsequently be induced by these photons. The final part of this section will then be devoted to a description and a method of calculating the build up and decay of the activity as the accelerator is turned on and off.

TABLE IV-1 Important Elements Exposed to Radiation

Activated Unit	Important Constituents	Activating Radiation
Shielding	Oxygen Silicon Calcium Aluminum Sodium Barium Magnesium Iron	Neutrons and photons
Targets	Copper Tungsten Iron Carbon	positive ions electrons neutrons photons
Accelerator and Auxiliary Equipment	Copper Iron Aluminum Carbon	neutrons and photons
Circulating Fluids	Nitrogen Oxygen Hydrogen	neutrons and photons

When an energetic positive ion is incident upon a target, a compound nucleus is formed if the particle's energy is sufficient to overcome the Coulomb barrier. The compound nucleus has no memory of the channel by which it was formed, so its excess

energy will be removed by emitting either a particle which may or may not be like the incident particle or by radiating photons. The most likely particle to be thrown off is a neutron because there is no Coulomb barrier to inhibit it.

Figure IV-1 shows the energies both in the forward and backward direction of neutrons emitted in several reactions in light elements initiated by positive ions[2]. Two of these reactions, the $D(d,n)He^3$ reaction and the $T(d,n)He^4$ reaction are exoenergetic and can be initiated at very low energies. Thus these two reactions can be produced in small Cockcroft-Walton accelerators. The angular distribution in the laboratory reference system is connected to the energy of the primary positive ion with the higher energy neutron in the forward direction.

Most reactions are endoenergetic, that is require that more energy is put in than is carried away be the neutron. Figure IV-2 shows the cross sections for the production of neutrons by protons incident upon a number of different targets[3]. These cross sections are all seen to be similar, leveling off in the region of 0.5 to 0.7 barns. As has been pointed out, there are light elements with lower thresholds, but most neutron producing reactions will have cross sections similar to these.

Electron accelerators produce neutrons by (e,n) or (γ,n) reactions with the (γ,n) cross sections being larger by about two orders of magnitude. In this case the electron (or photon) must furnish at least the binding energy of the neutron before it can be removed. The thresholds for these reactions are usually in the neighborhood of ten MeV and the neutrons are emitted isotropically. The neutron yields per electron are dependent upon Z as is shown in Figure IV-3. This curve was made with 35 MeV electrons incident upon a one radiation length target[4]. For any other energy, it is necessary to know the yield as a function of energy which is dependent upon the shape of the giant resonance cross section. Figure IV-4 shows how this yield varies in copper of two different thicknesses[4]. Assuming that all yield curves have approximately the same shape, these two figures can be used to predict the order of magnitude of neutron output from any target at any energy up to about 40 MeV.

The process by which neutrons are absorbed into a nucleus is energy dependent with the highest cross sections at thermal energies. This is because the probability for interaction is proportional to the time spent in the neighborhood of the nucleus, i.e., inversely proportional to the speed of the neutron.

Most of the neutrons produced both by positive ions and by photonuclear reactions are produced with kinetic energies in the MeV region because the giant resonance rises to a peak several MeV above the threshold. In the slowing down process (see Chapter II) an insignificant amount of induced activity is produced as compared with the activity produced by thermal neutrons. Therefore the thermal cross section should be used for purposes of calculating the activity produced. Table IV-2 lists both microscopic and macroscopic activation cross sections for thermal neutrons for a number of elements likely to be found in an accelerator installation[5].

Table IV-2 Macroscopic Thermal Neutron Activation Cross Sections

Atomic No.	Element	Isotopic %	Activation Cross* Barns	Macroscopic C.S. (cm^2/g)
11	Na	100	0.53 ± 0.02	1.39×10^{-2}
12	Mg	11.3	0.026 ± 0.002	7.28×10^{-5}
13	A1	100	0.21 ± 0.02	4.69×10^{-3}
14	Si	3.12	0.11 ± 0.01	7.36×10^{-5}
19	K	6.91	1.15 ± 0.11	1.22×10^{-3}
20	Ca	0.0033	0.25 ± 0.10	1.24×10^{-1}
20	Ca	0.185	1.1 ± 0.1	3.06×10^{-5}
24	Cr	4.31	13.5 ± 1.4	6.74×10^{-3}
25	Mn	100	12.4 ± 0.3	1.47×10^{-1}
26	Fe	0.31	0.9 ± 0.2	3.01×10^{-5}
27	Co	100	20 ± 3	2.04×10^{-1}
28	Ni	1.16	1.6 ± 0.2	1.90×10^{-4}
29	Cu	69	3.9 ± 0.2	2.55×10^{-2}
29	Cu	31	1.8 ± 0.4	5.29×10^{-3}
30	Zn	48.9	0.5 ± 0.1	2.25×10^{-3}
48	Cd	28.86	1.1 ± 0.5	1.92×10^{-3}
50	Sn	5.98	0.2 ± 0.1	6.07×10^{-5}
74	W	28.4	34 ±7	3.16×10^{-2}
79	Au	100	96 ± 10	2.93×10^{-1}
82	Pb	52.3	0.5 ± 0.01	7.60×10^{-4}

*From Reactor Physics Constants ANL-5800 2nd Edit. (1963).

Activation by high energy bremsstrahlung is a two step process just as is neutron activation. Since bremsstrahlung radiation is produced when an electron is slowed down by the Coulomb field of a nucleus, the energy distribution is continuous from the electron's energy down to zero. The relative amount of radiation produced depends upon the energy of the electrons and upon the charge of the target nucleus (see Chapter II).

The cross sections for the (γ,n) and (γ,p) photonuclear reactions are generally of the form of large resonances as has been mentioned before. These resonances are usually six to ten MeV wide with thresholds between 6 and 18 MeV. The yield of a particular reaction is given by the following integral:

$$Y = N\phi \left| \int \frac{dI(E,E_o)}{dE} \sigma(E) \, dE \right| (1-e^{-\lambda t_r}) \quad e^{-\lambda t_c} \qquad \text{(IV-1)}$$

where

Y	=	activity produced with radiation time t_r and cooling time t_c
N	=	number of atoms in the beam
ϕ	=	flux (photons/cm sec)
$\frac{dI(E,E_o)}{dE}$	=	bremsstrahlung spectrum for electrons of energy E.
$\sigma(E)$	=	cross section
λ	=	decay constant (sec^{-1}) = $.693/T_{1/2}$
$T_{1/2}$	=	Half life (sec)
t_r	=	irradiation time
t_c	=	cooling time

In order to make it possible to estimate the bremsstrahlung activity produced under various circumstances, calculations have been made of the yields per gram element using a numerical approximation of the previous formula under the following specific conditions.

a) Monoenergetic electrons of energy shown
b) Beam power of 10 kilowatts
c) Optimum tungsten target (maximum photon production)
d) Sample on axis 10 cm down stream of target
e) Total irradiation of one hour.

Table IV 3 lists a number of elements which might be activated by the high energy photons present in an electron accelerator target room[6]. To make use of this table, it is necessary to scale the various factors which determine the activity. For example, the beam power and the amount of element present scale directly while the distance scales as the inverse square.

For thin targets, the angular distribution of the bremsstrahlung is very strongly peaked in the forward direction (see Chapter II, Fig. 11-2). The angle θ at which the bremsstrahlung intensity is one half the central value is given by

$$\theta E_e = 100 \text{ MeV degrees} \qquad \text{(IV-2)}$$

See discussion in Chapter II. For thick targets the angular distribution is much more isotropic.

To a first approximation, the irradiation time T_r scales directly when T_r is small compared to the half-life. If T_r is large compared to the half-life, the activity will have reached saturation and further irradiation will not increase the amount present.

As an example of this scaling procedure, consider a piece of equipment containing 50 gms of iron which is on the beam axis at a distance of two meters in front of an optimum target. If 3 kilowatts of 22 MeV electrons bombard the target for 6 hours, the results of Table IV-3 scale as follows:

$$\text{Yield} = \frac{0.3 \times [2.7 \text{ mCi} + (2/5)1.6 \text{ mCi}] \times 50}{20^2} = .125 \text{ mCi}$$

In this case, the half-life of Fe^{53} is much shorter than an hour, so the activity shown in the table is the saturation activity. Thus the irradiation beyond an hour does not increase the amount of Fe^{53} activity produced. The 2/5 factor is the interpolation between 20 and 25 MeV values on Table IV-3.

All activity produced by accelerators either by neutron interactions or by photonuclear reactions grows while the accelerator is on and decays when it is off. Thus the final activity is the result of a series of periods of growth followed by periods during which the activity is decaying. This final activity can be calculated and expressed as a series of terms, one for each time during which the accelerator is on.

$$A = A_{oo}(1-e^{-\lambda t_{r1}})e^{-\lambda t_{c1}} + A_{oo}(1-e^{-\lambda t_{r2}})e^{-\lambda t_{c2}} + \ldots \qquad \text{(IV-3)}$$

Table IV-3 Photonuclear Reaction Yields per Gram Element[6]

At. No.	Element	Reaction	Half-Life	Yields at Energy Shown 12	15	20	25
6	Carbon	$C^{12}(\gamma,n)C^{11}$	20.5 m	—	—	3.5 mc	30 mc
8	Oxygen	$O^{16}(\gamma,n)O^{15}$	2.1 m	—	—	36 μc	11 mc
11	Sodium	$Na^{23}(\gamma,n)Na^{22}$	2.6 y	—	0.2 μc	1.8 μc	2.4 μc
12	Magnesium	$Mg^{25}(\gamma,p)Na^{24}$	15 h	—	2.7 μc	69 μc	210 μc
14	Silicon	$Si^{39}(\gamma,p)Al^{38}$	2.3 m	—	0.6 mc	4.5 mc	8.2 mc
19	Potassium	$K^{39}(\gamma,n)K^{38m}$	7.7 m	—	—	13 mc	26 mc
24	Chromium	$Cr^{50}(\gamma,n)Cr^{49}$	42 m	—	53 μc	3.5 mc	4.8 mc
		$Cr^{52}(\gamma,n)Cr^{51}$	28 d	—	17 μc	140 μc	160 μc
25	Manganese	$Mn^{55}(\gamma,n)Mn^{54}$	300 d	0.2 μc	2.4 μc	13 μc	17 μc
26	Iron	$Fe^{54}(\gamma,n)Fe^{53}$	8.9 m	—	.35 mc	2.7 mc	4.3 mc
27	Cobalt	$Co^{59}(\gamma,n)Co^{58}$	71.3 d	0.8 μc	10 μc	49 μc	58 μc
28	Nickel	$Ni^{58}(\gamma,n)Ni^{57}$	36 h	—	43 μc	.41 mc	.59 mc
29	Copper	$Cu^{63}(\gamma,n)Cu^{62}$	10 m	1 mc	17 mc	92 mc	100 mc
		$Cu^{65}(\gamma,n)Cu^{64}$	12.8 h	30 μc	0.5 mc	2.3 mc	2.5 mc
30	Zinc	$Zn^{64}(\gamma,n)Zn^{63}$	38.3 m	1 mc	8 mc	28 mc	33 mc
48	Cadmium	$Cd^{114}(\gamma,p)Ag^{113}$	5.3 h	—	—	34 μc	110 μc
50	Tin	$Sn^{124}(\gamma,n)Sn^{123}$	39.5 m	.54 mc	4.7 mc	12 mc	12 mc
74	Tungsten	$W^{186}(\gamma,n)W^{185}$	75.8 d	.06 μc	.26 μc	.37 μc	.37 μc
		$W^{186}(\gamma,p)Ta^{185}$	50 m	1.0 μc	10 μc	130 μc	390 μc
		$W^{184}(\gamma,p)Ta^{183}$	5.2 d	0.3 μc	1.4 μc	4.2 μc	5.0 μc
82	Lead	$Pb^{204}(\gamma,n)Pb^{203}$	52.1 h	12 μc	55 μc	92 μc	93 μc

In this equation A_{∞} is the saturation activity, assuming the X-ray intensity and spectrum to be the same each time. t_{r1}, t_{r2}, etc. are the times during which the accelerator is on and the activity is growing, and t_{c1}, t_{c2}, etc. are the times between the end of each irradiation and the time of measurement. Clearly this calculation can be done for any particular situation.

Another way in which this problem can be attacked is by making use of a graphical method. Figure IV-5 shows a plot of the percentage saturation activity versus time in units of half-lives. Both a growth curve and a decay curve are shown. To use this method, the growth curve is followed for the time t_{r1} which is the first accelerator irradiation period. From this point on the growth curve, a decay line is drawn parallel to the one shown and extending for a time t_{c1} half-lives. A horizontal line from the end of this decay line cuts the growth curve at the activity present at this time. If the accelerator irradiation is resumed at this time, the growth curve can be followed up again from this point. This can be repeated as many times as the accelerator is turned on to obtain the final activity.

Radioactivity Produced in Shielding

Accelerator shielding is commonly made of cement and steel, of earth, or of lead. The most commonly used material is cement or loaded cement. Table IV-4 shows the elemental make up of cement together with the radioisotopes which could be important problems and their half-lives.

Fortunately most of the elements which are found in high concentrations in shielding material do not have isotopes with long half-lives which can be produced by neutrons and high energy photons. The elements which turn out to be important in the activation of shielding are principally sodium and potassium due to their half-lives.

The production of a radioactive species depends upon the cross section, the flux of neutrons or photons, the amount of target material, and the time during which the exposure occurred. The radioactivity produced by neutrons in time t_1 is given by an equation similar to Eq. IV-1 where we replace the bremsstrahlung spectrum dI/dE by the neutron flu. ϕ. For ϕ constant during irradiation we have for the amount A_0 of the radioactivity formed

$$A_0 = M\phi\sigma(1-e^{-\lambda t_r}) \qquad (IV-4)$$

Here the amount of the initial element present is given by M and its cross section is σ and the irradiation time is T_r. This equation shows that the radioactivity of an isotope produced relative to another depends not only upon the amount of each parent present but also upon the size of the cross sections and relative saturation of each. Even though an element may have a large cross section, if its half-life is measured in years, its build-up will be so slow that it will rarely ever become a hazard unless the cross section is very high. The activity A of the radioactive element formed is given by

$$A = A_0 \cdot e^{-\lambda t_c} \qquad \text{(IV-5)}$$

where t is the time after end of irradiation.

The geometrical distribution of the activity in the shielding depends upon the geometry of the room and whether it was neutrons or photons responsible for the particular isotopes. Both neutron and photon fluxes fall off with the inverse square of the distance, so those shields closest to the radiation source will become most active. In general, the neutrons produced will be emitted isotropically, so the neutron induced activity can easily be calculated. As we have seen, high energy bremsstrahlung is strongly peaked in the forward direction especially when thin targets are used. Therefore, most of the photon produced activity will be found in the shielding within a few degrees of the beam axis.

Because of the rapid attenuation of both neutrons and photons by shielding materials, most of the induced activity occurs near the surface. Thermal neutrons are attenuated to about one-third of their initial flux by the first 10 cm of ordinary concrete. Therefore 2/3 of the activity produced by the neutrons would occur in this region. This makes it possible to design shielding with a row of concrete blocks on the inside. If these become too active to tolerate, they can be removed, disposed of and new blocks installed.

The high energy gamma photons are attentuated to about one third of their initial flux by the first 30-40 cm of ordinary concrete. Those photons which are below the threshold cause no activity. Therefore, approximately 2/3 of gamma produced activity will be found within the first 30-40 cm of the surface.

The major isotopes produced in concrete shielding are listed in Table IV-4. The percentages shown in column 4 and 5 indicate the naturally occurring amount of the stable isotope from which the radioisotope is formed.

In ordinary concrete most of the neutron produced isotopes can be eliminated from serious consideration either because of short lifetime or low concentration. Because of its long lifetime Ca^{41} could never build up to amounts which would be a problem. Only Na^{24} and perhaps K^{42} could present any kind of hazard. Because of the half-lives of these two isotopes, a shut down of three to five days will allow decay to very low levels.

The barium in barytes concrete occurs in large concentration and results when irradiated with neutrons in a fairly short-lived isotope. This can build up to high levels during the day, but will decay by a factor of several thousand overnight.

When high energy bremsstrahlung is incident for long periods of time on shielding concrete, two long-lived isotopes Fe^{55} and Na^{22} are produced. Fortunately, Fe^{55} has no gamma ray, so only sodium-22 will result in a hazard. If large quantities of this isotope build up, it will be necessary to physically remove the activated shielding, so plans for this contingency should be made in the design of the walls.

Table IV-4 Possible Activity in Shielding Material

Ordinary concrete

Element	Atomic Wt.	Density (gm/cm^3)	Neutron Prod. Isotope	γ Prod. Isotope
O	16.0	1.103	--	100% O^{15} 2 m
Si	28.06	0.282	3% Si^{31}-2.6 h	--
Al	26.97	.033	100% Al^{28}-2.3 m	--
Fe	55.85	.018	3% Fe^{59}-45 d	97% Fe^{55}-2.4 y
Ca	40.08	.771	97% Ca^{41}-7×10^4 y	--
C	12.01	.076	--	99% C^{11} 20.5 m
Na	23.00	.012	100% Na^{24}-15 h	100% Na^{22} 2.6 y
K	39.10	.008	7% K^{42}-12.4 h	93% K^{38} 7.7 m
H	1.0	.025	--	--
Mg	24.32	.043	11% Mg^{27}-9.5 m	--
Total		2.37		

Barytes Concrete

This includes the elements above plus the following ·

Ba	137.36	1.470	71% Ba^{139}-83 m	2% Ba^{133}-7.2 y
S	32.07	.348	4% S^{35}-86.4 d	--
Mn	54.93	.003	Mn^{56}-2.6 h	Mn^{54}-312 d
Total		3.49		

As an example of the activity which might be found in a concrete shield, consider the Na^{24} which would be produced under the following conditions:

Electron Linear Accelerator
Electron Energy – 25 MeV
Average Current – 200 μamps
Target – 1 Radiation Length Tungsten
Irradiation Time – 8 hours
Target to Shield Distance – 3 meters
Ordinary Concrete as shown in Table IV-4

Making use of Figures IV-3 and IV-4 there is seen to be about 10^{-3} neutrons produced per electron. For the 200 μamp current, the total neutron output per second is then 1.24×10^{12}. Since the neutrons would come off essentially isotropically, they would be spread over an area of 1.13×10^{6} cm^2 at a distance of 3 meters. Thus the neutron flux in the region of the concrete shielding is approximately 10^{6} neutrons per cm^2 second.

Since sodium makes up only 0.5% of the concrete, and the macroscopic cross section from Table IV-2 is 0.0139 cm^2/g, the saturation activity is 167 d.p.s. per cm^3. From Figure IV-5 the percent saturation activity reached in .53 half-lives is 31%. Thus the activity produced in eight hours at the surface of the concrete is 0.0019 $\mu Ci/cm^3$. Although this is not a lot of activity per cm^3, there will clearly be much activity in an exposed wall.

Radioactivity Produced in Targets

The targets to be discussed here differ from the other areas because activity is produced by being bombarded by the primary accelerated particles. Besides those devices normally considered as targets, the definition will be broadened here to include beam dumps and any parts of the accelerator and beam handling system such as collimators which come in direct contact with the beam. Thus the targets are the only places where activity can be found produced by particles other than neutrons or gamma ray photons.

One of the most important discoveries in nuclear chemistry involved a target from Lawrence's cyclotron laboratory in Berkeley. While visiting the laboratory, Emilio Segre noticed that the vacuum chamber from the 27 inch cyclotron had been discarded and was lying in a corner with some shielding around it because of its activity. He asked for and received quick assent from Lawrence to take the chamber back to his own lab to try to determine what isotopes were present. In a molybdenum lip against which the deuteron beam had scraped, Segre was able to find element 43, Technetium which had never been observed before. The name was taken from the Greek technetos meaning artificial in recognition of the fact that this was the first artificially produced element.

Table IV-5 lists the most common elements to be found in usual targets and beam bumps together with the important radioisotopes of each element. In general, materials

Table IV-5 Major Elements in Targets

Aluminum Alloy	Element Percentage	Neutron Prod.	P-N Reaction	γ-N Reaction
Aluminum	99%	--	--	--
Manganese	0.5%	Mn^{56}-2.5 h	Fe^{55}-2.4 y	Mn^{54}-312 d
Sodium	0.1%	Na^{24}-15 h	--	Na^{22}-2.6 y
Zinc	0.2%	49% Zn^{65}-243 d 18% Zn^{69}-14 h	Ga^{67}-78h	--
Stainless Steel				
Iron	68%	6% Fe^{55}-2.4 y	92% Co^{56}-77 d 2% Co^{57}-272 d	--
Manganese	2%	Mn^{56}-2.5 h	Fe^{55}-2.4 y	Mn^{54}-312 d
Cobalt	1%	Co^{60}-5.3 y	--	Co^{58}-71 d
Chromium	18%	--	84% Mn^{52}-5.7 d	84% Cr^{51}-28 d
Nickel	11%	--	--	68% Ni^{57}-36 h
Target Materials				
Tungsten		28% W^{187}-24 h	28% Re^{186}-90 h	26% W^{181}-130 d
Copper		69% Cu^{64}-12.9 h	31% Zn^{65}-243 d Bi^{206}-	--
Gold		Au^{198}-64.8 h	Hg^{197}-65 h	Au^{196}-62 d
Lead		Very little induced activity.		
Beryllium		--	--	--

which are subjected to the direct accelerator beam must be cooled by some fluid, usually water. The activity produced in these fluids will be discussed in a later section.

The targets themselves can be divided into heavy materials such as tungsten and lead used principally to convert electrons to bremsstrahlung and a light group used to produce neutrons at low energies. In addition, the target holders, beam dumps, collimators and such things are usually made of either aluminum or stainless steel.

Among the heavy targets lead usually results in the lowest amount of induced activity although six day Bi^{206} can be produced by a (p-n) reaction. Because of its low melting point, lead cannot be used in a highly concentrated beam, so only small amounts of induced activity are expected in this material. Tungsten on the other hand can become radioactive either by the capture of a neutron, a p-n reaction, or the loss of a neutron. In addition, where high fluxes of neutrons are present, 2.5 hour manganese-56 will often be found as a contaminant and a short-term hazard.

Most light elements including beryllium do not result in induced activity hazards because the isotopes which are formed are generally either stable or extremely short-lived. Thus only the target holders might be expected to present problems in this case.

When protons are used on a target, the most probable isotopes resulting from the p-n reactions are those shown in the table. An estimate of the amount of each isotope produced requires a knowledge of the cross section at the particular proton energy. The activity build-up can easily be calculated using Eq. IV-4. Thus very long-lived isotopes such as Fe^{55} will build up only very slowly.

Figures IV-6, IV-7, and IV-8 show the expected radiation dose rates from several thick targets which have been irradiated with 50 MeV protons for periods of time between one and 10,000 hours[7]. Dose rates after cooling for one day, one week, and one month are shown[7].

Radioactivity in Accelerator and Auxiliary Equipment

The most important determinant of the activity produced in the accelerator itself is the type and energy of the accelerated particle. Activity will be produced only by neutrons and high energy gammas since we have defined anything which intercepts the beam itself as a target. The rate of production of neutrons and photons depends strongly on the energy of the primary beam. The activity which these neutrons and photons induce then depends upon the geometry and composition of the accelerator. For example, the activity induced in a cyclotron where the neutrons are actually produced within the dees differs considerably from the activity induced in a linac where the neutron source is beyond the end of the machine.

Accelerators and the equipment found around them are very complex devices made out of a variety of elements. The most likely materials used in accelerators and the equipment around them are stainless steel, aluminum, copper and iron in magnets, and insulating material. The elements which are included in these materials are listed in Table IV-6.

Most of these elements have been discussed in previous sections with the exception of components of insulating material. Again, as has been pointed out earlier, the principal contribution to the activity is often a component which occurs only in trace or very small amounts. An example of this is shown in Figure IV-9. This shows the activity of a stainless steel sample which has been irradiated for a very long time by a flux of neutrons. Even though cobalt represents only a small percentage of the metal, it has a large cross section and a long half-life, so after several weeks of decay, it becomes the dominant activity.

Radioactivity Produced in Circulating Fluids and Gases

The hazards due to the production of activity in air and water are essentially limited to high energy electron accelerators since thermal neutrons do not produce radioactive isotopes in the elements involved. Above 10.6 MeV nitrogen-13 is produced by the reaction $N^{14}(\gamma n)N^{13}$ and radioactive O^{15} is produced by $O^{16}(\gamma,n)O^{15}$ above its threshold of 15.7 MeV. The production rate of these gases in air is given by

$$a_o = \frac{a_r E\ i\ d}{V} \qquad \text{(IV-6)}$$

where

a_o = production rate in μCi/sec m^3 air

a_r = rate constant in μCi/sec MeV Amp m (See Table IV-7)[6]

E = electron energy in MeV

i = beam current in Amps

d = path length of X-rays in air in m

V = cell volume in m^3.

The concentration build-up of the activity during operation of the accelerator is then given by

$$A_o = \frac{a_o}{v/V + 1/\beta}\,[1 - \exp-(v/V + 1/\beta)t] \qquad \text{(IV-7)}$$

Table IV-6 Major Activity Produced in

Accelerators and Auxiliary Equipment

Material	Element Percentage	Neutron Produced Isotopes	Gamma Produced isotopes
Structural Steel			
Iron	99%	–	2% Mn^{56}-2.6 h
Carbon	1%	–	C^{11}-20 m
Polyethylene			
Carbon	86%	–	C^{11}-20 m
Fluorine	0.1%	––	F^{18}-110 m
Glass			
Sodium	11%	Na^{24}-15 h	––
Rubber			
Sodium	<1%	Na^{24}-15 h	
Potassium	<2%	7% K^{42}-12 h	
Aluminum Alloy		(See Table IV-5)	
Stainless Steel		(See Table IV-5)	

where

A_o = activity of the isotope in $\mu Ci/m^3$

a_o = production rate

β = lifetime of the isotope (sec.)

v = velocity of exhaust in m^3/sec.

This equation is seen to be very similar to an ordinary build-up equation except that the activity not only decays but also is removed by the exhaust.

After the accelerator is shut off, the activity at time t_1 is

$$A_1 = A_o \exp-(v/V + 1/\beta)t_1 \qquad (IV\text{-}8)$$

If A_1 is set equal to 2 $\mu Ci/m^3$ which is the occupational maximum permissible concentration (MPC), we get

$$t_1 = (v/V+1/\beta)^{-1} \ln \frac{0.5\, a_r\, T\, i\, d}{v + V/\beta} (1-\exp-(v/V+1/\beta)t) \qquad (IV\text{-}9)$$

It is clear from the discussion above that the primary problem in the activation of gases in air is the production of nitrogen-13. This isotope has the lowest threshold, the longest life, and of course, nitrogen makes up the largest percentage of the atmosphere. Both N^{13} and O^{15} are positron emitters, so the hazard is due to the 0.51 MeV annihilation gammas.

To try to minimize the activity produced in air by the accelerator, the place to start is to reduce d, the path length of the gammas. This should be an inherent consideration in the design of any experiment with a high energy electron accelerator. The only other design parameter which should be chosen carefully because of its effect on the waiting time is the exhaust velocity. Since the exhausted air can be a hazard outside of the irradiation chamber as well as in, its proper disposal will be discussed in Chapter VIII.

As an example of the calculation of the waiting time for an electron accelerator operating at 18 MeV, assume the following conditions:

v = 4 m^3/sec

V = 560 m^3

i = 10^{-3} amps

d = 5 m

Although 18 MeV is above the threshold for the production of O^{15}, the major activity produced in air will be the nitrogen isotope. If the time that the accelerator has been operated, t is much greater than $(v/V + 1/\beta)^{-1}$, then the amount of N^{13} would reach saturation.

The lifetime of nitrogen-13 in seconds is about 862, so substituting into the equation for t_1 we find

$$t_1 = 120.4 \ln \frac{57.60}{4.49} = 303 \text{ seconds}$$

A similar calculation made for O^{15} results in a waiting time of only about 82 seconds. Thus N^{13} is the limiting hazard in air under these conditions as is expected.

Oxygen-13 can be produced in water as well as in air. Thus the circulating water used to cool the accelerator, targets, and other equipment can be a hazard under certain conditions. To calculate the production rate of O^{15} in a water target, the equation for a_o described above can be used with certain modifications. The primary difference is that the density of oxygen in water is about 3865 times as great as in air. Thus using the same definitions as before, the production rate of oxygen-15 in water is

$$a_W = \frac{3865\, a_r T\, i\, d}{V} \qquad \text{(IV-10)}$$

If the water is in a closed system as often is the case, the concentration build-up is given by

$$A_W = a_W \beta\, [1\text{-}\exp\text{-}t/\beta] \qquad \text{(IV-11)}$$

and the rate of decay after the accelerator is turned off is just the final activity times $\exp(-t_1/\beta)$.

Table IV-7 Production Rate of Activity in Air by

X-Rays from a Tungsten Target[7]

Electron Energy T(MeV)	Production Rate Constant a_r (μCi/sec m Amp Mev) averaged over 4π solid angle	
	N^{13}	O^{15}
12	81	
14	460	
16	920	
18	1280	450
20	2440	1850
22	4100	5160
24	6150	14500
26	8820	28200
28	11100	42700
30	11700	54800
32	12200	57300

References

1. M. Barbier, **Induced Radioactivity**, North Holland Publishing Co. (1969).

2. A. C. Graves, R. L. Walker, R. F. Taschek, A. O. Hanson, J. W. Williams, and H. M. Agnew, Neutron Sources in **Miscellaneous Physical and Chemical Techniques of the Los Alamos Project** edited by Graves & Froman, McGraw Hill (1952).

3. F. K. McGowan, W. T. Milner, and H. J. Kim, Nuclear Cross Sections for Charged-Particle Induced Reactions, ORNL-CPX-1 and ORNL-CPX-2 (1964).

4. W. C. Barber and W. D. George, Neutron Yields from Targets Bombarded by Electrons, Phys. Rev. **116**. pp. 1551-59 (1959).

5. Argonne National Laboratory, Reactor Physics Constants, U. S. Atomic Energy Commission, ANL-5800, 2nd Edition, pp. 637-45 (July 1963).

6. R. D. Cooper, Sensitivities for Photon Activation Analysis, unpublished.

7. C. B. Fulmer, I. R. Williams, and J. B. Ball, Residual Radiation Studies for Medium Energy Proton Accelerators, IEEE Trans. Nucl. Sci., pp. 977-79 (June 1967).

8. A. Brynjolfsson and T. G. Martin, Bremsstrahlung Production and Shielding of Static and Linear Electron Accelerators Below 50 MeV. Toxic Gas Production, Required Exhaust Rates, and Radiation Protection Instrumentation. Int. J. Appl. Rad and Iso. **22** pp. 29-40 (1971).

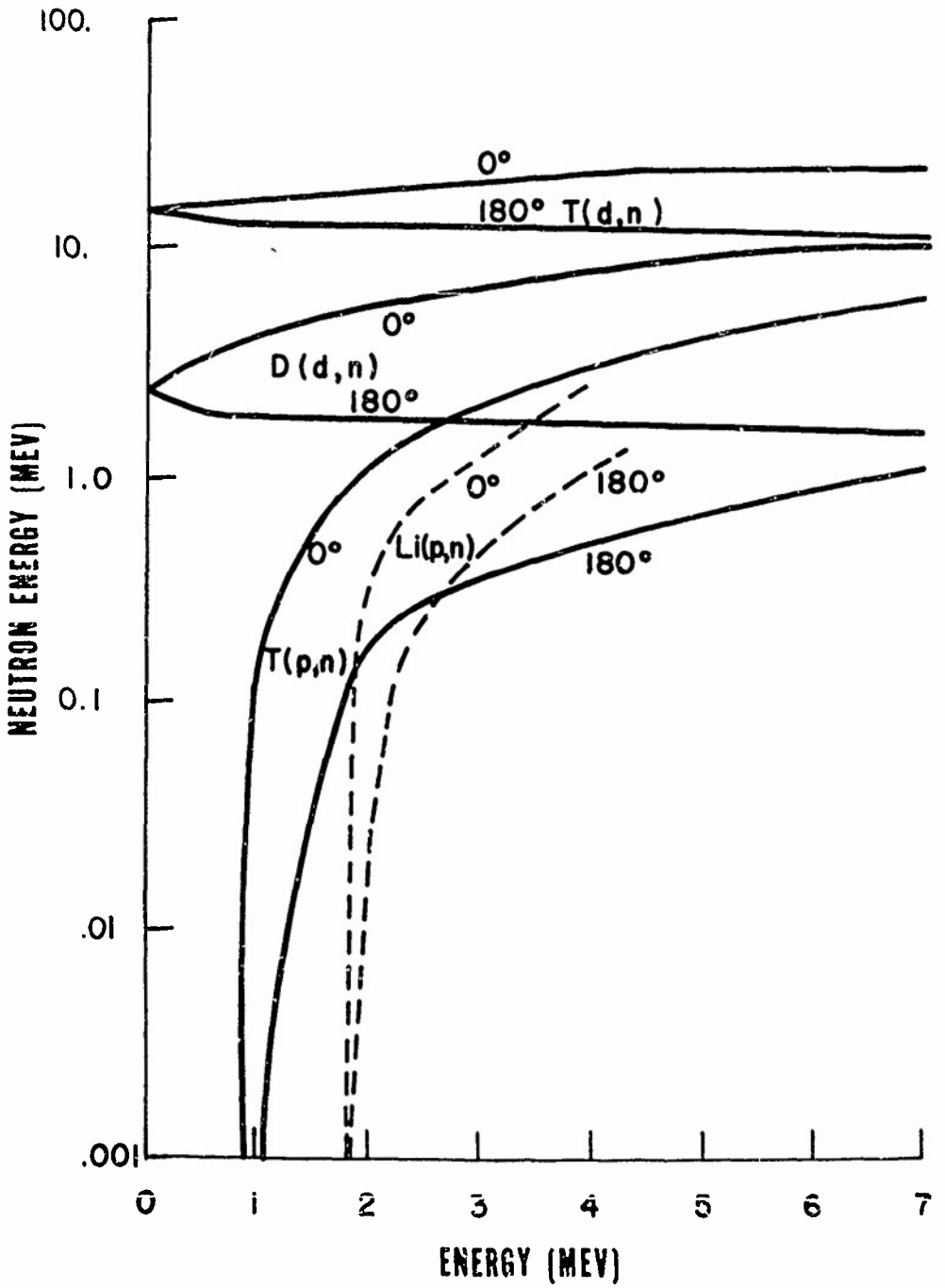

ENERGIES OF NEUTRONS PRODUCED BY POSITIVE IONS

Figure IV-1

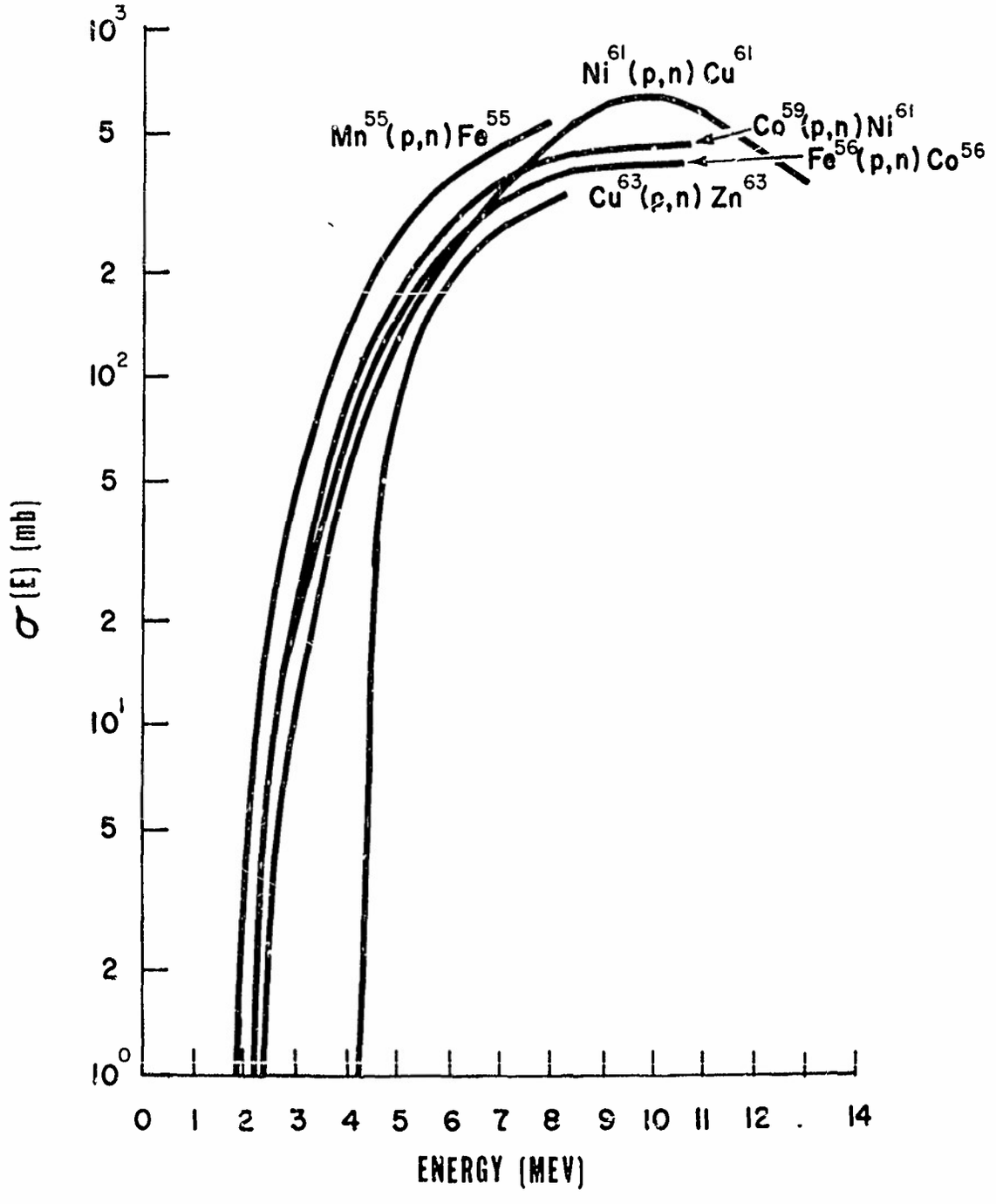

CROSS SECTIONS FOR P-N REACTIONS

Figure IV-2

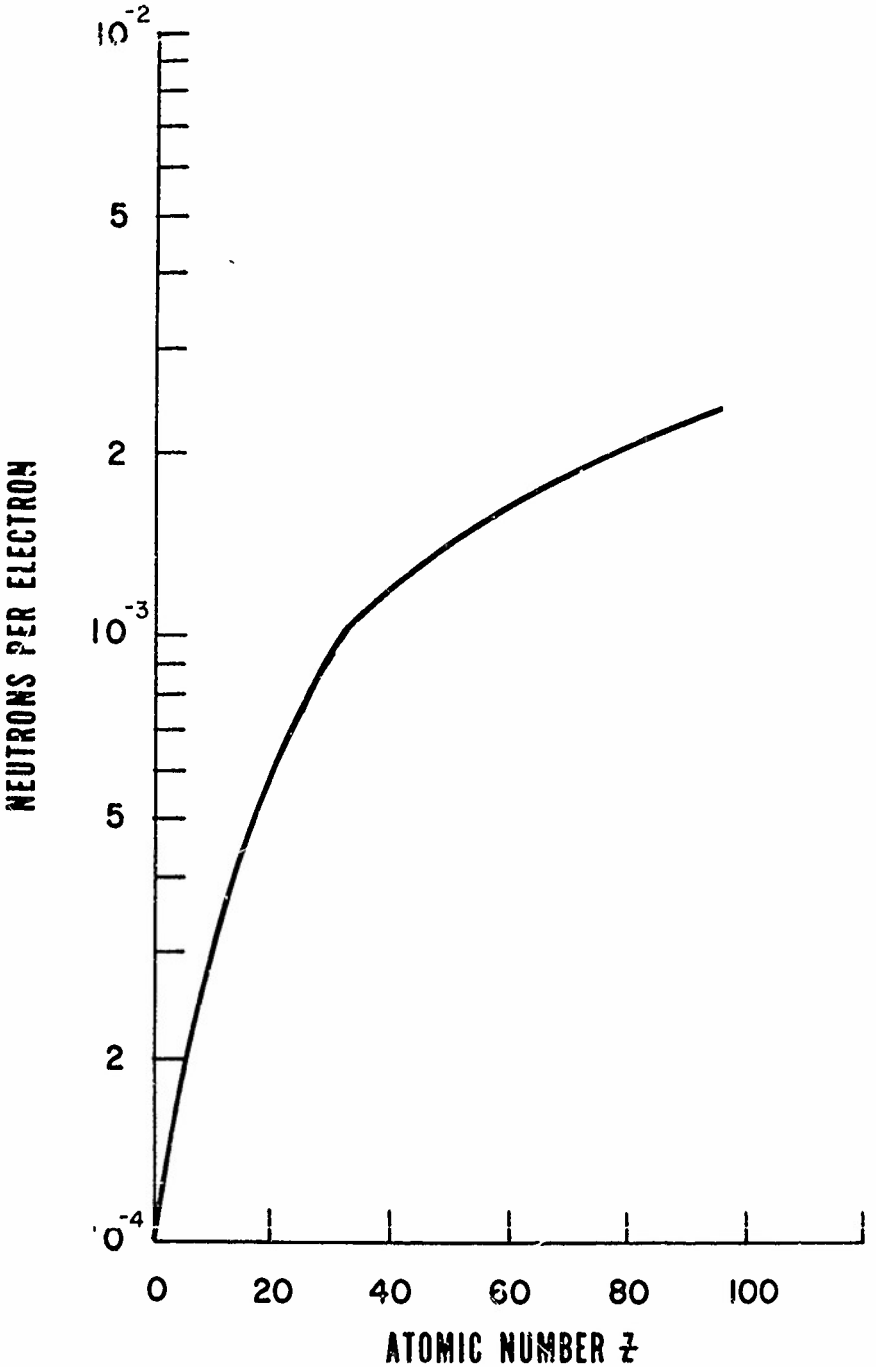

NEUTRON YIELDS FROM 35 MEV ELECTRONS

Figure IV-3

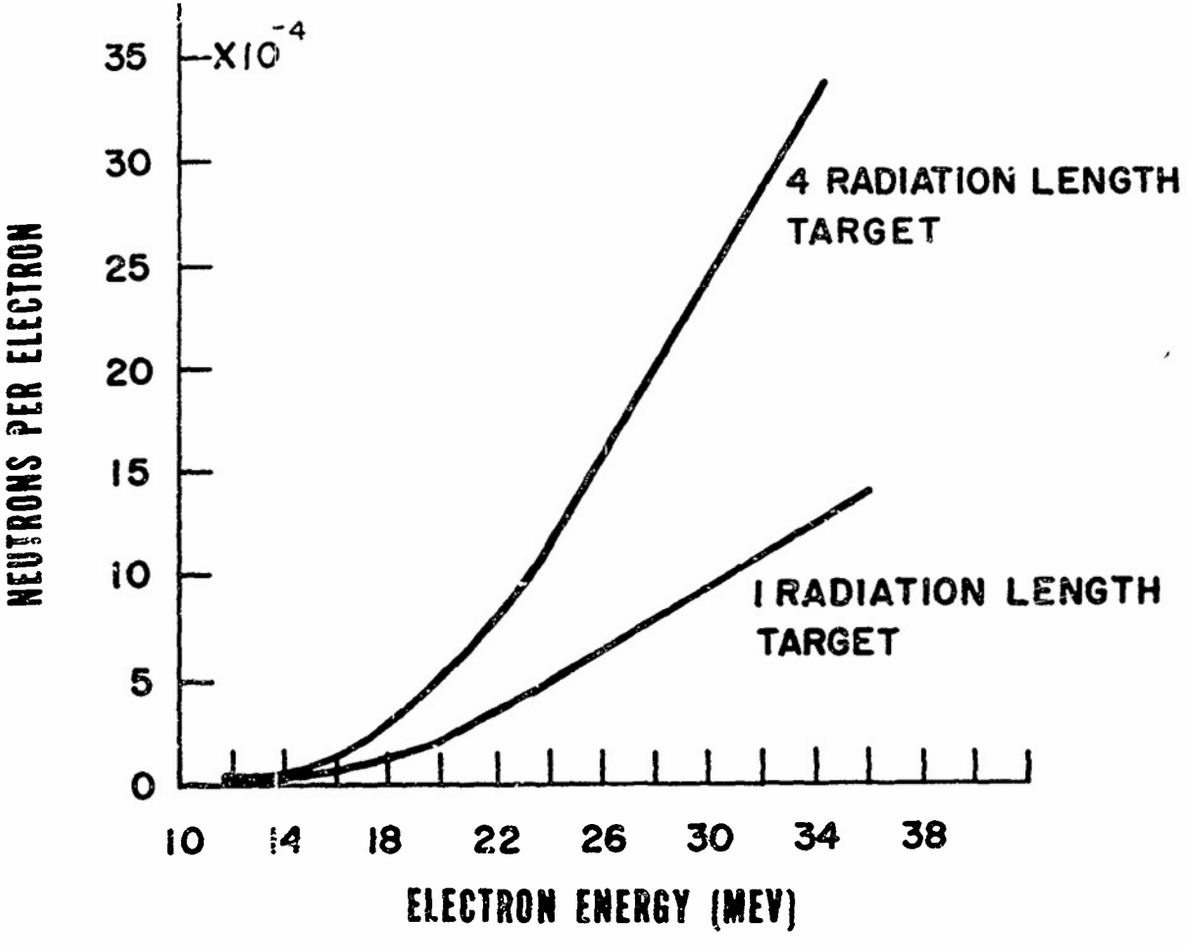

NEUTRON YIELDS IN COPPER TARGETS

Figure IV-4

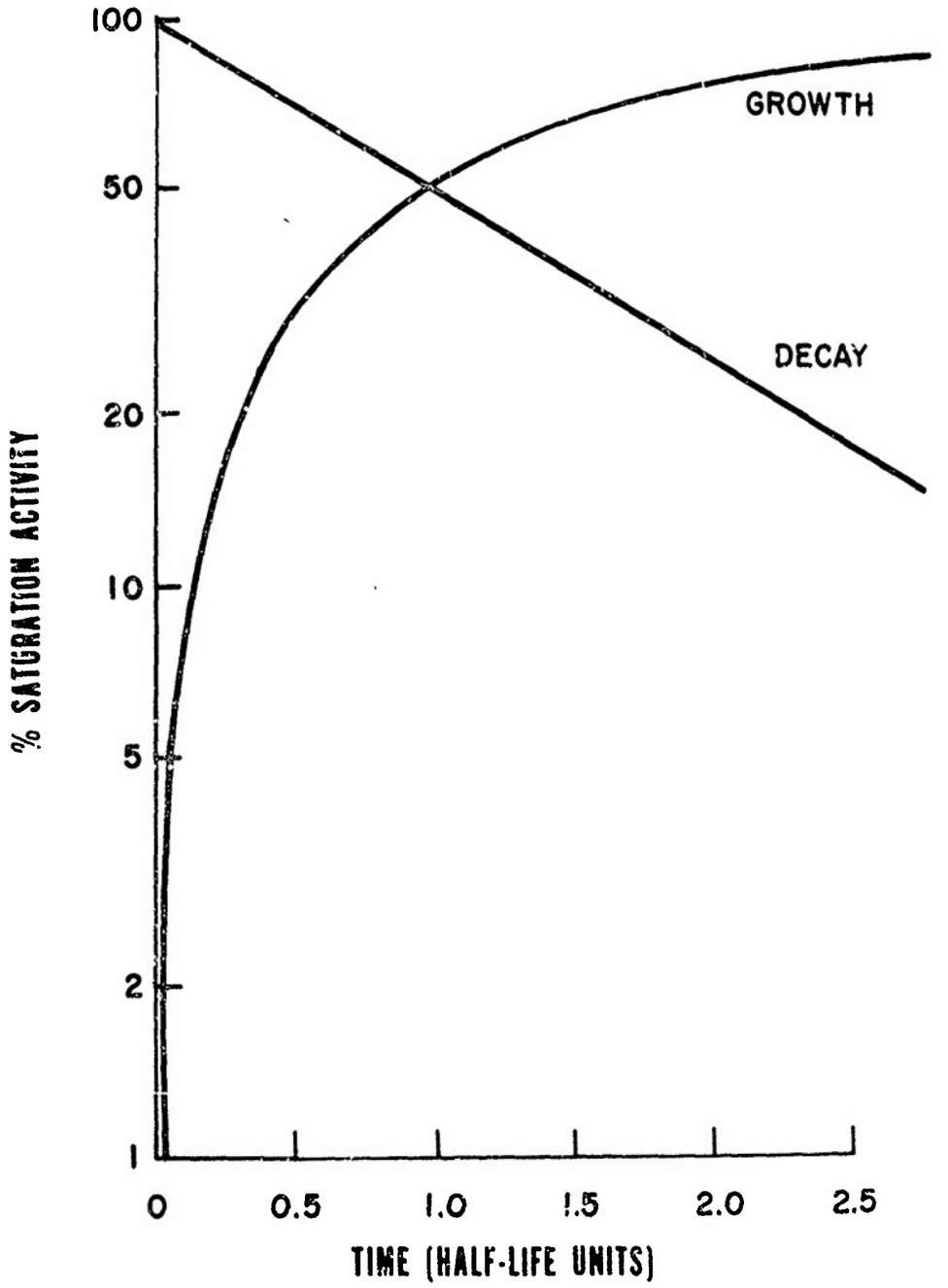

ISOTOPE GROWTH AND DECAY CURVES

Figure IV-5

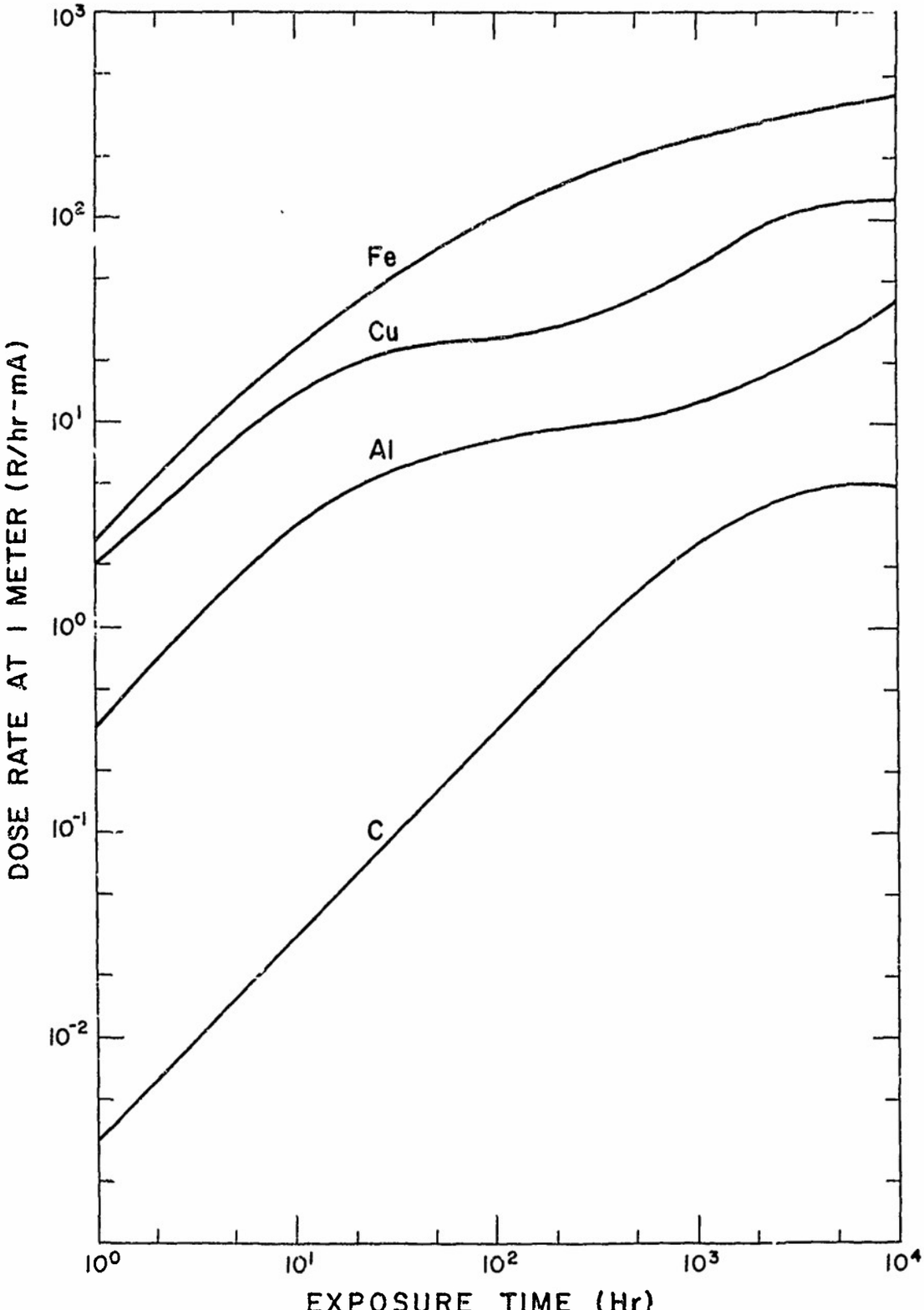

Figure IV-6 – Expected Dose Rates from Several Thick Targets Irradiated with 50 MeV Protons (one day cooling)[7]

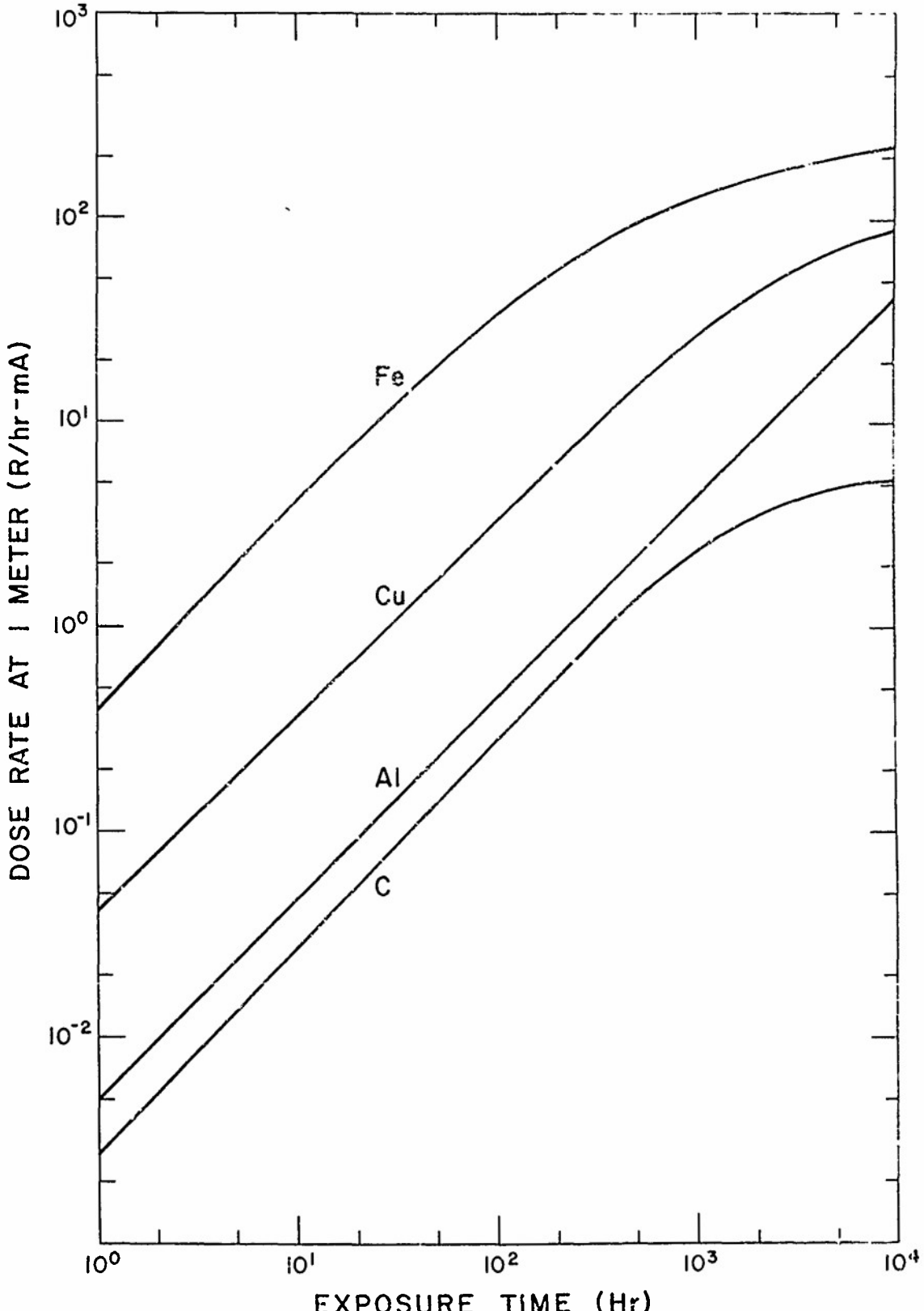

Figure IV-7 – Expected Dose Rates from Several Thick Targets Irradiated with 50 MeV Protons (one week cooling)[7]

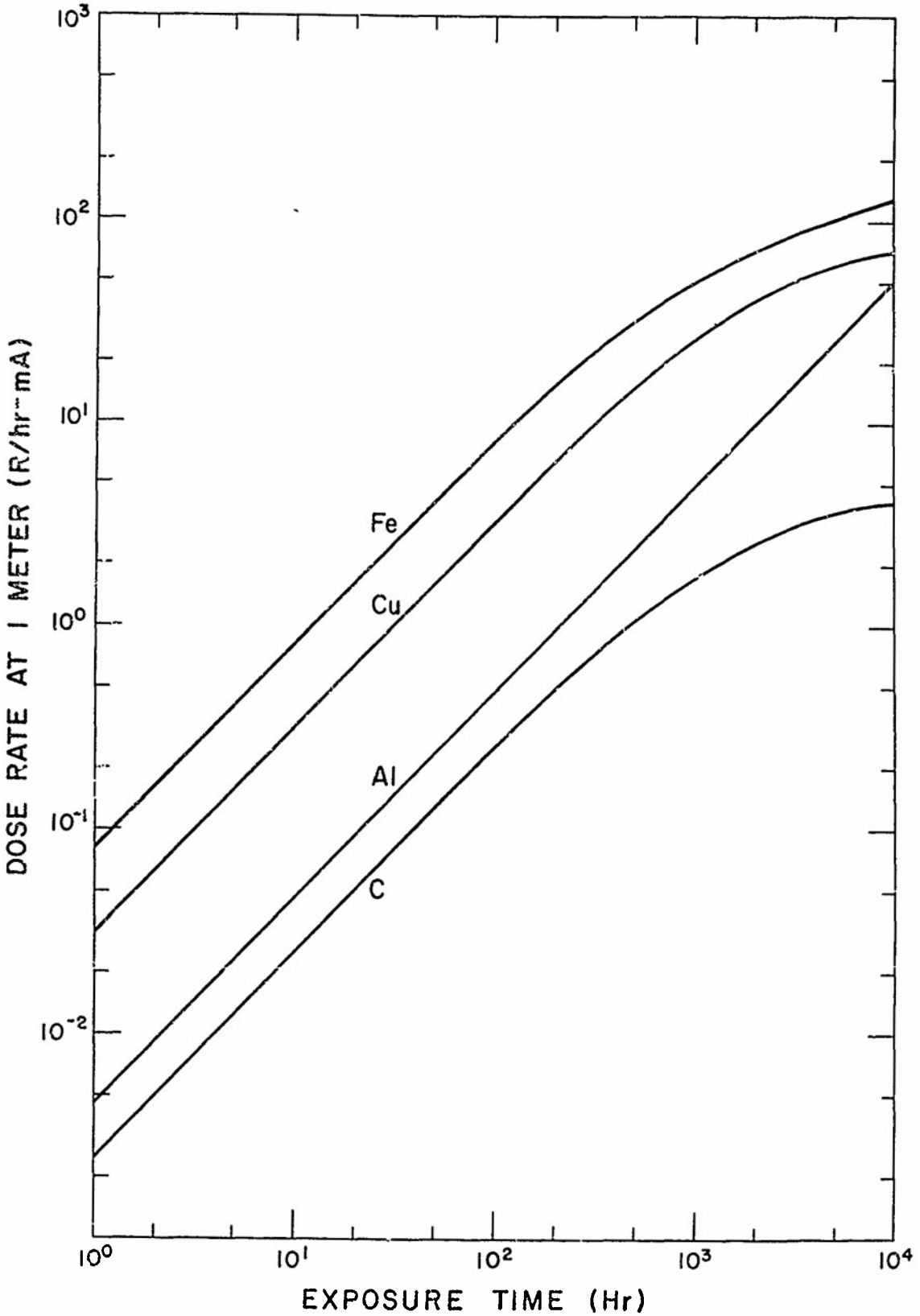

Figure IV-8 — Expected Dose Rates from Several Thick Targets Irradiated with 50 MeV Protons (one month cooling)[7]

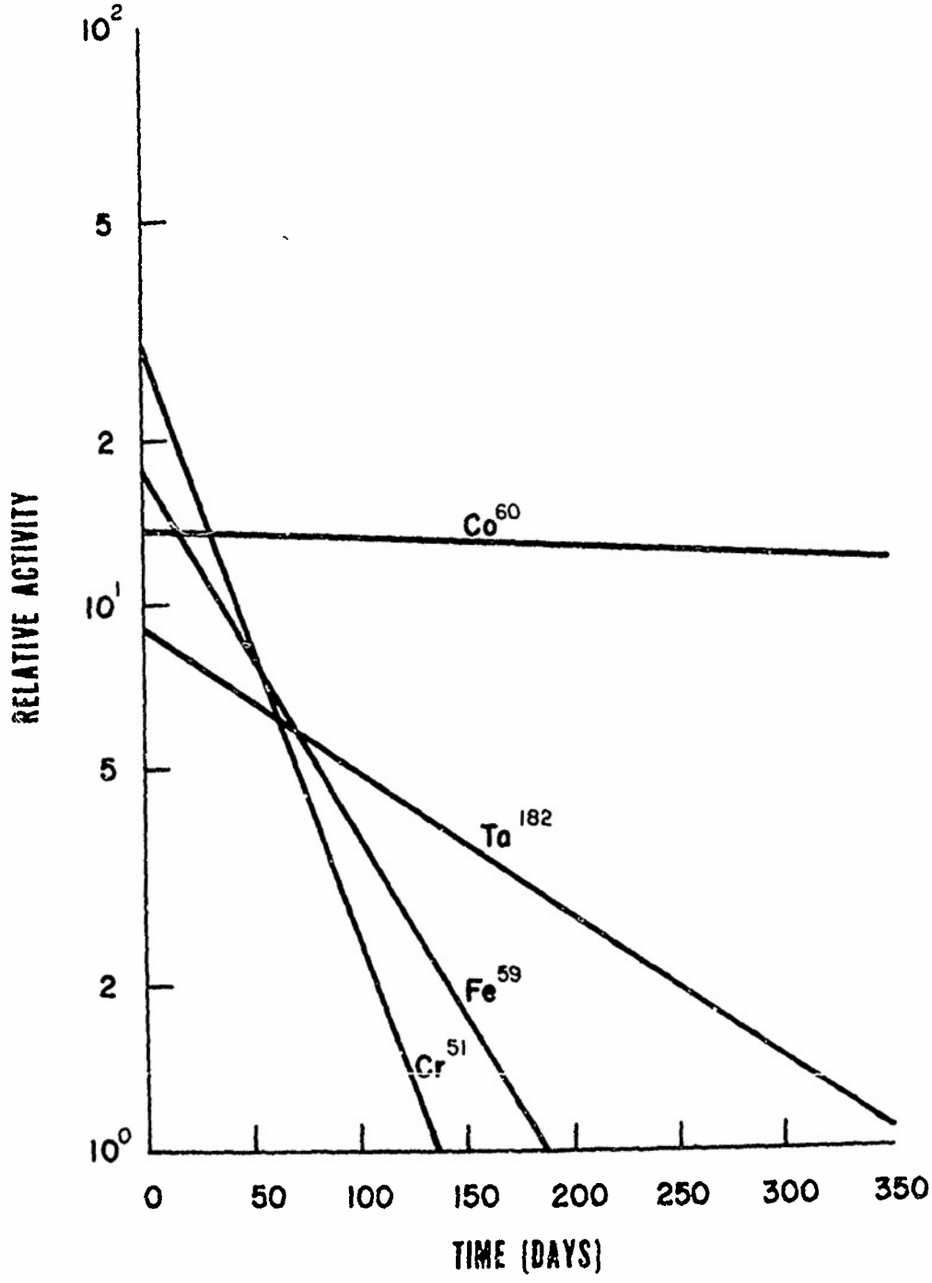

RELATIVE ACTIVITY IN NEUTRON ACTIVATED STAINLESS STEEL

Figure IV-9

Chapter V

Radiological Physics and Radiation Exposure Limits

F. J. Mahoney, T. G. Martin and R. D. Cooper

Introduction

This chapter concerns itself basically with radiological physics, i. e., the study of the interaction of ionizing radiation with matter in general and biological matter in particular. With accelerators of energy up to about 50 MeV the radiations of concern include photons, neutrons, and electrons in addition to heavy charged particles. The types of interactions experienced by these radiations vary considerably in nature. However it can readily be shown for all of them that energy is generally deposited on the local level either by means of heavy charged particles or electrons. If the primary radiations are heavy charged particles or electrons, this is obvious. For primary neutrons or photons some further explanation is necessary.

For nonthermal neutrons the primary interactions are either elastic scattering or inelastic scattering on the nucleii. These lead to either energetic heavy charged particles (nuclei) or photons or both. Thermal neutrons are generally absorbed by nuclei in (n,γ) reactions. In this case interest then continues to follow the gamma ray photons and the electrons they produce.

The predominant reactions of photons in the energy range of interest are photoelectric absorption, Compton scattering and pair production. In all of these cases energetic electrons (and perhaps positrons) are produced. A fourth mode, that of photonuclear reactions (e.g. (γ,n) and (γ,p)) which frequently results in radioactive products is discussed in Chapter IV.

1. The Photoelectric Effect:

Interaction by photoelectric effect results when a photon suffers a collision with an atomic electron and transfers all of its energy to that electron. The result is an electron with energy equal to the energy of the incident photon minus the energy necessary to remove the electron from its orbit. The photon is completely lost. The energy of the electron is given as:

$$\text{Kinetic Energy} = h\mu - W$$

where W is the amount of energy necessary to remove the electron from its orbit.

The photoelectric effect is primarily a low energy interaction and as the energy increases, the probability of interaction by photoelectric effect decreases. Figure V 1 indicates a typical curve showing this characteristic.

2. The Compton Effect:

It is possible that in the collision with the electron, the photon may not give up all of its energy, but may be deflected and lose only a part of its total energy. This process is called the Compton Effect or Compton Scattering.

Since the inciddent photon is deviated from its original direction by some angle (θ), the resulting change in photon energy is a function of the energy needed to cause this deflection. The change in wavelength of the photon is then given by:

$$\Delta\lambda = \frac{h}{m_o c} (1 - \cos\theta)$$

where h is Planck's constant and m_o is the rest mass of the electron. Note that the change in wavelength is independent of the incident wavelength.

The probability of interaction by Compton Scattering decreases with increasing photon energies to a somewhat lesser degree than photoelectric interactions. Figure V-1 gives a typical curve.

Compton Scattering is independent of the atomic number of the interacting matter.

3. Pair Production:

When a high energy photon passes close to a nucleus, it may be transformed into a positron and an electron. The process is a conversion of photon energy into mass with two opposite charges. The law of conservation of mass and energy ($E = mc^2$) applies and we see that the incident photon must have an energy equal to:

$$(2)\ (0.00055)\ (931) = 1.02\ \text{MeV}$$

in order to produce a pair. Excess energy above 1.02 MeV is given to the positron and electron as kinetic energy. Figure V-1 shows how the probability of interaction increases with increasing energies. The positron will generally come to rest before annihilation which occurs when it comes in contact with an electron. This is the reverse process of pair production and results in the emission of two 0.51 MeV photons in opposite directions.

Figure V-1 is a composite graphical illustration of the gamma interaction processes. The total probability curve has a minimum point. Such a graph can be drawn for all materials and will differ in scale, but the minimum in the total probability will always exist. This point, a characteristic of the material is sometimes called the gamma window. The position of this gamma window is about 3 MeV for lead, 7 MeV for iron, and about 20 MeV for aluminum. The significance of the gamma window can be seen by noting that at the corresponding energy, maximum penetration exists.

The deposition of energy on the local level by charged particles affords a great simplification because the interactions underlying these depositions are generally electromagnetic in nature involving mainly the atomic electrons. The primary difference between electrons and heavy charged particles is the density of ionizations (and excitations) along the particle trajectory in the irradiated medium.

By invoking this basic simplification one can more readily acquire a working knowledge of radiation dosimetry.

Dose Units

The basic unit of (absorbed) radiation dose is the rad which corresponds to the deposition of one hundred ergs per gram of absorbing material or 1 rad = 100 erg/g = $\frac{1}{100}$ J/kg. The rad is intended to describe the difference between the sum of the energies of all the directly and indirectly ionizing particles which have entered a volume of matter and the sum of the energies that have left the volume minus the energy equivalent of any changes in rest mass which may have taken place in the volume.[1]

No further specification of the absorbing material is made in this definition of the rad. Therefore it applies equally well for all absorbers. If we employ the approximate figure of 34 eV to produce one ion pair than one rad corresponds to about 1.8×10^{12} ion pairs per gram. This means that in water exposed to one rad about one molecule is ionized out of every 2×10^{10}.

Since the ionization potential for water is about one-half of the 34 eV per ion pair, considerable excitation occurs along with ionization.

Of the energy absorbed from ionizing radiation only a small amount, typically of the order of a few percent, ultimately goes into enduring radiation damage. The remainder eventually appears as heat. In fact this heat may be used for calorimetric estimation of absorbed dose. Since during the degradation of the incident energy it will diffuse and the distribution of the heat produced may differ from the distribution of the imparted energy, the energy imparted cannot always be equated with the heat produced. The first law of thermodynamics describes the energy balance.

$$dQ_T = E_r + W \qquad \text{(V-1)}$$

$$= E_r + \Sigma dQ_{ix} - \sum_j dE_{jn} \qquad \text{(V-2)}$$

where

dQ_T = the total heat generated

E_r = the incident radiant energy

dQ_{ix} = the net energy generated in the i-th exothermic chemical reaction

dE_{jn} = the net energy used up in the j-th endothermic chemical reaction

Radiation-promoted chemical reactions are accounted for such that the heat out equals the radiant energy in less the net energy involved in chemical reactions.

From the quantum nature of both radiation and matter it can be appreciated that the physical quantities of radiation dosimetry such as dose actually represent averages of quantities which are spatially and temporally discontinuous. Such averages become inadequate only when sufficiently small volumes are considered. A subdiscipline called "microdosimetry" concerns itself with the significance of actual fluctuations around these average quantities which are of importance, for example, at the cellular level where effects may be attributable to only a few particles or even a single one. For conventional radiation dosimetry it is adequate to deal with averages and to assume that such averaged quantities are continuously variable. This approach defines a radiation field in the classical sense.

Stopping Power and LET

Ionizations and excitations produced by ionizing radiation are not spatially homogeneous over the irradiated volume. Rather they cluster along the trajectories of the inducing charged particles. The primary difference between electrons and heavy charged particles is the density of ionization along the trajectory. This density of ionization is described by a quantity called specific ionization, the number of ion pairs produced per unit path length. The specific ionization is, in turn, related to a more basic quantity called stopping power, the energy deposited per unit path length. Clearly the specific ionization is deducible from the stopping power by utilizing the rule of thumb that the deposition of about 34 eV results in the generation of one ion pair.

Closely related to the concept of stopping power is linear energy transfer (LET). It should be noted for thoroughness, however that these two quantities are not precisely equivalent.

The basic expression for the stopping power for heavy charged particles with spin 1/2 is due to Bethe's quantum mechanical generalization of Bohr's classical formula:[2]

$$S = \frac{dT}{dx} = \frac{4\pi z^2 e^4}{m_o v^2} \cdot \frac{N_o \rho}{A} \cdot Z \ln\left[\frac{2m_o v^2}{I(1-\beta^2)}\right] - \beta^2 \qquad \text{(V-3)}$$

where

T = charged particle kinetic energy

ze = the charge of the incident particle

Z = the atomic number of the absorbing material

v = the velocity of the heavy charged particles

β = v/c

$N_0\rho/A$ = number of atoms for cm^3 of the absorbing material

m_0 = the electron mass

Γ = the average ionization potential of the absorbing material atoms, averaged over all its electrons

It should be noted that this equation depends directly upon the heavy charged particle's velocity but not on its mass. Figure V-2 presents the stopping powers for various heavy charged particles in air. The electron stopping power curve is included for comparison. The expression for the stopping power for electrons is:

$$\frac{dT}{dx} = \frac{2\pi e^4}{m_0 v^2} \cdot \frac{N_0\rho}{A} \cdot Z \left\{ \ln \left[\frac{m_0 v^2 T}{I^2 (1-\beta^2)} \right] - \ln 2 + 1 - \frac{m_0 c^2 (2T+m_0c^2}{(T+m_0c^2)} \ln 2 + \frac{1}{8} \frac{T^2}{(T+m_0c^2)^2} - \beta^2 \right\} \quad \text{(V-4)}$$

This expression applies to electrons which satisfy the condition $(2Z/137 << \beta)$. Physically this means that the incident electron velocity is well above atomic electron velocities. Thus it applies to relativistic electrons in addition to non-relativistic ones. Figure V-3 presents the electron stopping power in air from this expression with extension from more sophisticated theory down to 100 eV. It can be seen that the sharp increase in stopping power with decreasing energy levels off and reverses itself at about 100-500 eV when the incident electron velocity begins to approach the lowest velocity of atomic electrons. Alternatively stated the incident electron energy is approaching the minimum energy necessary to produce an ionization. From this energy down to thermal values the physics of electron slowing down in condensed media is complicated and rather poorly understood.

Studies of energy deposition patterns have shown that along the electron trajectory there is not really a continuous deposition of energy. Rather it is deposited inhomogeneously and the stopping power is an average of these events. Further it has been shown that an "event" may be composed of a number of closely spaced ionizations presumably with associated excitations. The most likely number of ionizations per event is about three which corresponds to about 100 eV deposited. Therefore the electron trajectory is composed of clusters of ionizations separated by variable distances whose average can be deduced from the stopping power. For example in air for 20 keV electrons, 100 ev clusters would have an average spacing of about 10^6 Å. Considering that three

closely spaced ionizations may all be within a radius of perhaps 10 Å we see that energy deposition along the trajectory is indeed discontinuous. Even for a condensed medium such as water with a density about one thousand times that of air, event spacings are generally far greater than event sizes. It is pertinent to repeat in this context that the concepts generally used in dosimetry represent the result of a spatial averaging process which is adequate for sufficiently small volumes such as clusters of ionizations.

A further important point can be made by applying the same approach to heavy charged particles. Let us consider protons in Figure V 2. Twenty keV electrons have about the same velocity as 40 MeV protons and therefore about the same stopping power. Assuming the slope of the stopping power curves are about the same down to negligible velocities then the range of 20 keV electrons is approximately the same as that of 40 MeV protons. Yet the protons deposit 2×10^3 times more energy. Consequently the spatial density of "events" along the particle trajectory is about two thousand times higher. This means that individual events are not nearly so isolated from another and in fact they may overlap in condensed systems. This higher spatial density of events has profound effect in radiation chemistry and radiation physics because of recombination of appropriate ions or free radicals from different, overlapping events.

LET and Dose Weighting Factors

It can now be appreciated that an absorbed dose quotation does not adequately specify a radiation field because of the different possible spatial distribution patterns of the dose. Quantities such as Quality Factor (QF) and Relative Biological Effectiveness (RBE) have been defined as weighting factors to compensate for the inadequacies of a simple dose description of a radiation exposure of a biological system. Quality Factor and RBE are quite close in meaning, the former being applied to radiation protection and the latter to radiation biology. Both are LET-dependent factors, QF is a defined quantity and RBE is a measured quantity.

In its earliest definition RBE was devised to compare biological effects caused by different types of radiation. In effect it was the ratio of absorbed doses of different types of radiation or different energies of the same radiation to produce the same biological effect. The problem with this definition is that RBE values vary from one biological effect to another. This difficulty simply illustrates the fact that more than two variables (rad dose and RBE) are required to uniquely specify the conditions of irradiation. Nevertheless factors such as RBE which endeavor to describe the QUALITY of radiation represent an improvement over simple rad dose which only describes the QUANTITY of energy. In radiation protection work the product of QF, rad dose and other modifying factors such as the dose distribution factor (DF) has been defined as Dose Equivalent in units of rem. In radiation biology the product of RBE and rad dose serves the same purpose for a particular biological end point.

For certain types of biological effects, there is a correlation between RBE and LET which indicates that for these effects the spatial distribution of the radiation dose is important. Alternatively stated, certain biological effects are most efficiently produced by a characteristic linear energy transfer (i.e., ion density) such that, for example, electrons and protons of the same LET, delivering the same absorbed dose, produce the same biological effect. Variation of LET while keeping absorbed dose constant, may then cause a difference in biological effect.

While calling attention to the overriding facts that QF's may vary considerably with biological effect and that the dependence of QF or RBE on LET may likewise vary, we present Tables V-1 and V-2 respectively, the QF as a function of radiation type and as a function of LET.

In employing data from these tables it is obvious that they are at best semi-quantitative. Only a small number of biological effects were taken into consideration. These include skin cancer, leukemia, impairment of fertility and induction of cataracts. It should be noted that QF increases monotonically with increasing LET. There are obviously exceptions to this in which a characteristic LET is optimum for biological damage (e.g., scission of a chromosome). It is clear that absorbed dose in the form of neutrons will have a different effect on human tissue than the same absorbed dose of gamma rays. The effective dose called the "Dose Equivalent" in units of rem is given by

$$DE = D \cdot QF \cdot DF \ldots \qquad (V\text{-}5)$$

where

D = the measured dose

QF = the quality factor of the radiation

DF = the distribution factor (a means of accounting for a non-uniform distribution of internally deposited nuclides)

... = other modifying factors which may be required

The quality factors proposed by the RBE Committee to the ICRP[3] can be approximated in tissue by the equation

$$QF = 0.8 + 0.16\ \overline{LET} \qquad (V\text{-}6)$$

where $\overline{LET}$ is in keV/μ. Table V-2 gives the relationship between LET and QF together with the approximate number of ion pairs produced per micron.

In any case, if a knowledge exists of the flux density and the spectrum of the radiation, the quality factors above can be used to calculate the dose equivalent. Table V-3 gives data which can be useful if such knowledge is available in determining neutron dose equivalent.

An alternative which is sometimes used when the flux density and spectrum are not known is to determine the Kerma for uncharged primaries such as gamma rays and neutrons. This can be done experimentally by using a tissue equivalent ionization chamber as long as charged particle equilibrium exists.

TABLE V-1

Practical Quality Factors

Radiation Type	QF
X-rays, gamma rays, electrons or positrons	1
Neutrons, Energy $<$ 10 KeV	3
Neutrons, Energy $>$ 10 KeV	10
Protons	1 - 10
Alpha particles	1 - 20
Fission fragments, recoil nuclei	20

TABLE V-2 QF as a Function of LET

(for X-rays, electrons and positrons: QF = 1)

Avg. LET (keV/μ of H_2O	QF	Avg. Specific Ionization (ion pairs/μ of H_2O)
3.5 or less	1	100 or less
3.5 to 7.0	1 to 2	100 to 200
7.0 to 23	2 to 5	200 to 650
23 to 53	5-10	650 to 1,500
53-175	10-20	1,500 to 5,000
560	30	16,000
1,000	35	29,000

TABLE V-3

Mean QF's and neutron flux densities which result in maximum Dose Equivalent of 100 mrem/40 hrs

Neutron Energy (MeV)	QF	Neutron Flux Density ($cm^{-2} s^{-1}$)
2.5×10^{-8} (thermal)	2	680
1×10^{-7}	2	680
1×10^{-6}	2	560
1×10^{-5}	2	560
1×10^{-4}	2	580
1×10^{-3}	2	680
1×10^{-2}	2.5	700
1×10^{-1}	7.5	115
5×10^{-1}	11	27
1	11	19
2.5	9	20
5	8	16
7	7	17
10	6.5	17
14	7.5	12
20	8	11
40	7	10
60	5.5	11

Charged particle equilibrium is usually defined by the following conditions:[4]

a) the energy distribution and intensity of all primary radiation are uniform over a volume extending in all directions from the point of measurement to a distance equal to the maximum range of a secondary.

b) the properties of the medium such as the energy absorption coefficient and the stopping power for secondaries are uniform over the volume described above.

Since for every secondary which leaves the volume there will be an equivalent one entering, the energy dissipated is equal to the total energy of all secondaries produced within the volume.

Charged particle equilibrium does not usually exist near interfaces where there is a considerable change in density or near point sources of radiation. Of most importance with high energy accelerators, electron equilibrium does not exist where the primary radiation is attenuated by a large amount over a distance equal to the range of the secondaries. Under these conditions it is possible to define a region of transient equilibrium at a depth where the ratio of primaries to secondaries is constant.

Kerma is defined essentially as the sum of initial kinetic energies of all charged particles produced by uncharged primaries per unit mass of a particular material.[2] So long as none of the charged secondaries escape or radiate from the mass in which radiation effects are being determined, kerma is equivalent to the dose. However, when an instrument is used which is not in charged particle equilibrium, the kerma cannot be determined but only some sort of average dose within the chamber.

The kerma, K, per neutron or per photon per square centimeter at an energy E is given by

$$K(E) = \sum_i \sum_j N_i \, \sigma_{ij} \, (E) \, \epsilon_{ij} \qquad \text{(V-7)}$$

where

N_i = number of atoms per unit mass of material which can react with incident radiation

σ_{ij} = cross section for reaction of type i

ϵ_{ij} = average kinetic energy of the outgoing charged particle

Calculations have been made[5] of the neutron Kerma for a standard man consisting of 10%H, 18%C, 3%N, 65%O, and 4% other elements. Table V-4 lists the neutron kerma per n/cm^2 (fluence) which has been calculated for bone and for the standard man. The calculations were made considering only elastic collisions of the neutrons and neglecting

both inelastic scattering and neutron produced charged particle reactions. Later calculations[6] have been made which include these other factors and result in slightly higher values of the kerma.

Biological Effects of Radiation

Ionizing radiation, in general, has a deleterious effect on biological systems. This comes as no surprise since a cell is a finely tuned device and radiation introduces energy into it indiscriminately. The kind and degree of effect depends upon the type and amount of radiation and the kind of cell irradiated. The dose required for lethality varies from hundreds of rads for humans to millions of rads for bacteria. In general the higher the organism the greater the radiosensitivity. As a general rule cellular radiosensitivity is well described by the very old law of Bergonic and Tribondeau (1906): cellular radiosensitivity is directly proportional to the time rate of reproduction and to the length of the period of mitosis and inversely proportional to the degree of differentiation. Within the cell, the most radiosensitive materials are the chromosomes, the carriers of genetic information encoded in DNA (deoxyribonucleic acid) molecules. Cellular sensitivity varies over cell lifetime, which is characteristic of the cell type. Higher sensitivity may be related to mitosis, to DNA functioning in making RNA (transcription) and to DNA duplication (replication).

TABLE V-4 Kerma per Neutron per cm^2 (erg/gm)/(n/cm^2)

Neutron Energy (MeV)	Kerma Bone (erg/gm)	Kerma in Standard Man (erg/gm)
1	1.0×10^{-7}	2.3×10^{-7}
2	1.2×10^{-7}	3.0×10^{-7}
3	1.5×10^{-7}	3.6×10^{-7}
4	1.8×10^{-7}	4.0×10^{-7}
5	1.9×10^{-7}	4.3×10^{-7}
6	1.9×10^{-7}	4.5×10^{-7}
7	2.0×10^{-7}	4.7×10^{-7}
8	2.0×10^{-7}	4.8×10^{-7}
9	2.0×10^{-7}	4.9×10^{-7}
10	2.1×10^{-7}	4.9×10^{-7}

Higher cells often exhibit radiation recovery so that effects vary with the dose delivery pattern. For example time fractionation of a dose may mean a higher total dose is necessary to produce a particlular effect.

In humans a total body dose of about 450 rad will have a fifty percent chance of causing death within 30 days. Higher doses have correspondingly shorter survival times and higher probabilities of death. Human tissues vary widely in radiosensitivity with blood cells (lymphocytes, erythocytes) and germinal cells (ova and sperm) among the most sensitive and muscle and nerve cells among the least. With increasing total dose three different fatality syndrones can be recognized. Low doses cause death through blood cell damage; medium doses through gastrointestinal cell damage and high doses through central nervous system damage. The dose span for the onset of these syndrones goes respectively from about 100 rad to tens of thousands of rads. Higher dose damage has a correspondingly shorter time to death reaching virtually immediate central nervous system death at sufficiently high doses.

Permissible Radiation Limits

The risk of potential damage by ionizing radiation necessitates balancing the risk against potential benefits accruing from its use. Such an approach leads to the maximum permissible dose concept for radiation. Such maximum permissible doses must be used as guidelines only since no dose can be inflexibly assigned below which absolutely no damage results.

Great controversy periodically arises over the proper balance of risks and benefits primarily because definitive evidence about effects of chronic, low dose exposures has been unavailable. This necessitates extrapolations from higher dose data with consequent disagreement about slopes and zero crossing points. Slopes are important since they allow translation of each increment of radiation into additional leukemia deaths, for example. Zero crossing points are important because they predict the presence or absence of a threshold and therefore a true tolerance dose for the radiation if such a threshold exists.

In establishing a permissible dose level it is necessary to factor in various important pieces of information. Perhaps the foremost fact is that we are all continually in a radiation environment called background radiation, therefore a zero maximum permissible dose is absurd. Since background radiation varies considerably over the earth (approximately 50-175 mrad/year with isolated areas over 1000 mrad/year) a zero increment above background may be also unrealizable.

A distinction must also be made in regard to somatic and genetic radiation effects. Somatic effects concern the individual himself while genetic effects concern man as a member of the genetic pool of mankind. Genetic effects as regards an isolated individual and his offspring are not believed to be restrictive. The reason for this is that majority

of genetic mutations (radiation induced or otherwise) are believed to be recessive in nature and therefore require combination with another recessive to yield its effect. Mutations in isolated individuals therefore should not represent the most restrictive factor in establishing maximum permissible dose (MPD) involving genetic damage. As a matter of fact it can be shown that in establishing a maximum permissible dose for individuals occupationally involved with radiation the restrictions imposed by somatic effects are far more serious than those imposed by genetic effects. This leads to a value dictated by somatic effects.

When the whole body is exposed to relatively non-penetrating radiation it may be assumed that the skin is the "critical organ" which determines the maximum permissible dose and that skin cancer is the deleterious effect of primary interest.

When the whole body is exposed to penetrating radiation the blood-forming tissue is assumed to be the critical organ and leukemia one of the deleterious effects of primary interest. It is believed that other organs are sufficiently radioresistant that the maximum permissible dose dictated by the choice of blood-forming tissue as the critical organ will be adequately conservative.

At the present time the maximum permissible dose for external exposure to critical organs is obtained from the following prescription:

For the whole body, head and trunk, active blood-forming organs or gonads, the maximum permissible dose to the most critical organs, accumulated at any age, shall not exceed 5 rems multiplied by the number of years beyond 18. The dose in per calendar quarter shall not exceed 3 rems.

For external exposure to organs other than critical ones the prescription is:

(a) (For the skin of the whole body) the maximum permissible dose shall not exceed 15 rems per year.

(b) (For the hands, forearms, feet and ankles) the maximum permissible dose shall be 75 rems in any one year and the dose in per calendar quarter shall not exceed 25 rems.

As stated earlier these values apply only to persons occupationally involved with radiation. Obviously different criteria are required for the general population. The most obvious difference is that for the general population genetic effects assume a far more important role, in fact, they occupy the central role. In addition, latent in the prescription for MPD is the assumption that occupational exposure may not commence until the age of eighteen. For the general population this restriction is absent so that one must make allowance for eighteen additional years for deleterious effects of radiation to become apparent. With these factors taken into consideration it has been decided that the maximum permissible dose to an individual member of the general population is lower by a factor of ten than that for occupationally exposed personnel and that for the general population should not exceed 0.17 rem/yr.

References

1. Radiation Quantities and Units, International Commission on Radiological Units and Measurements Report 10a NBS Handbook 84. (1962).

2. Recommendations of National Council on Radiation Protection and Measurements, Basic Radiation Protection Criteria, NCRP Report No. 39, (Jan 15, 1971).

3. Fitzgerald, J. J., Brownell, G. L. and Mahoney, F. J. Mathematical Theory of Radiation Dosimetry Gordon and Breach Science Publishers, Inc., New York (1967).

4. Halliday, D., Introductory Nuclear Physics p 156, John Wiley & Sons, New York (1955).

5. Report of Subcommittee M 4 (Relative Biological Effectiveness). Dose-Effect Modifying Factors in Radiation Protection BNL 50073 (T-471) (Aug 1967).

6. Williamson, F. S., and Mitacek, P. Jr., Calculations of Kerma due to Fast Neutrons in Tissue-Like Materials, Neutron Monitoring p 17 (1967).

7. Bach, R. L., and Coswell, R. S., Energy Transfer to Matter by Neutrons, Rad. Res. 35, 1 (1968).

8. White, G. R. N.B.S. Report No. 1003 (1952)

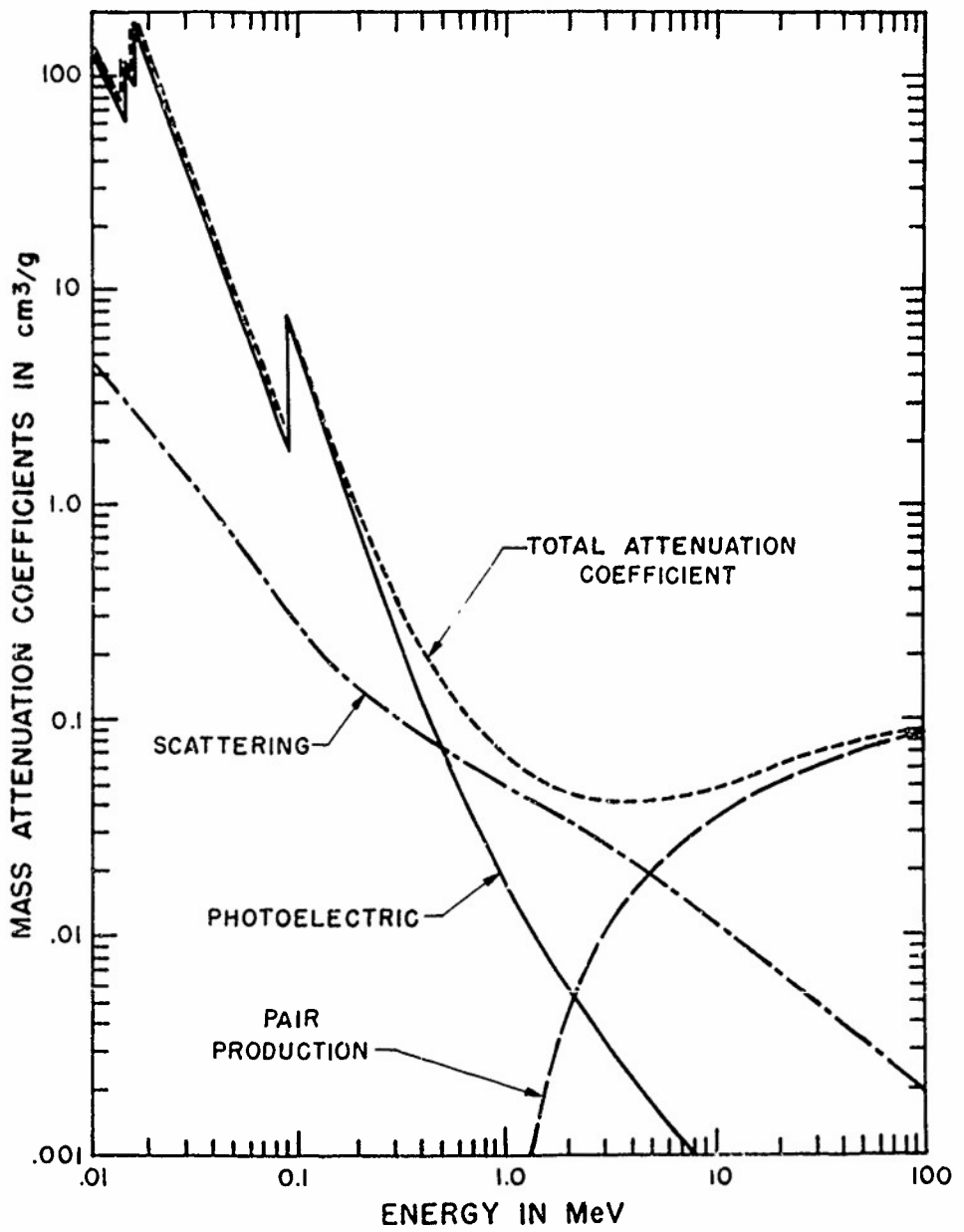

Figure V-1 — Probability of Photon Interaction vs Incident Photon Energy[8]

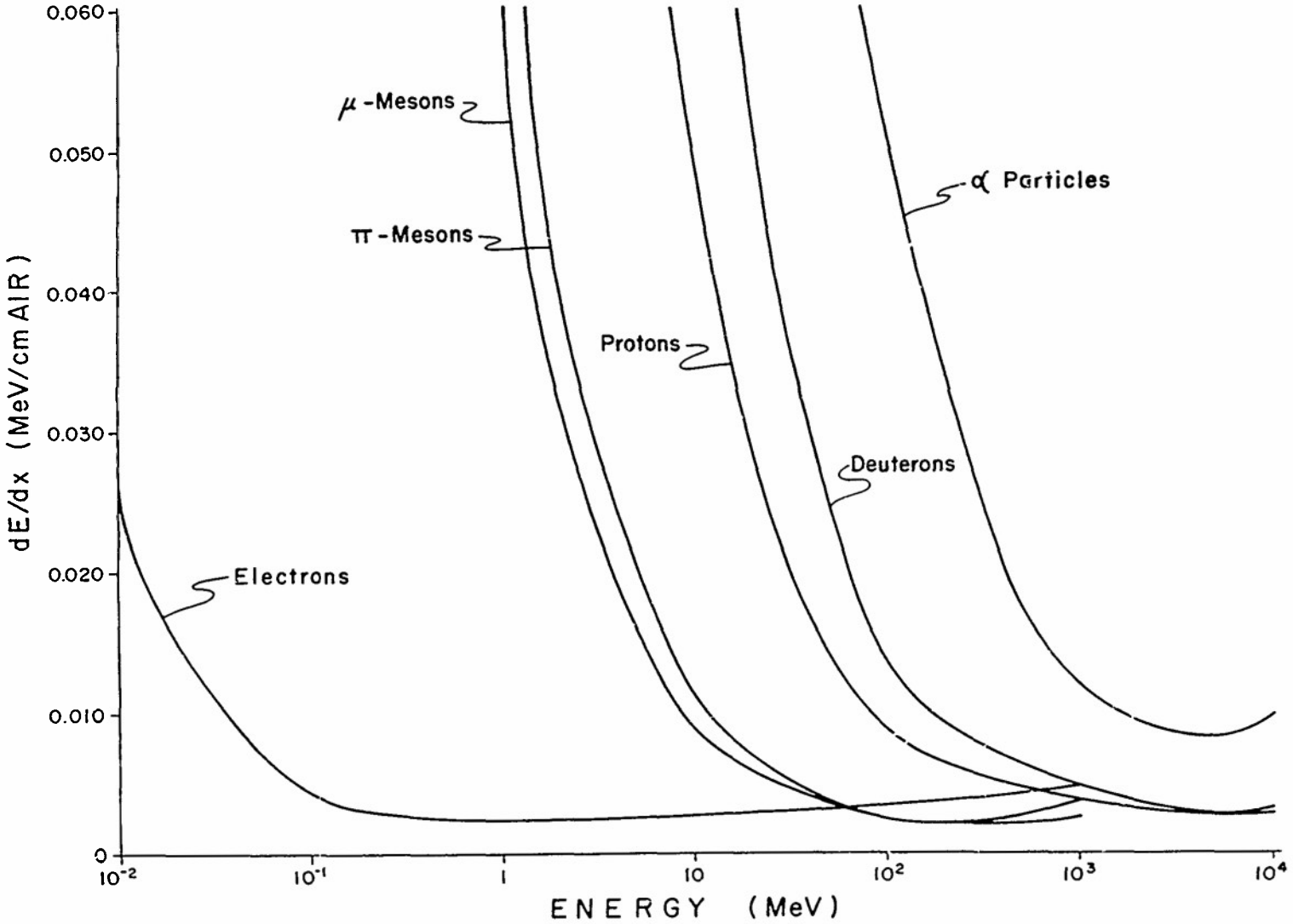

Figure V-2 — Stopping Power for Various Charged Particles in Air

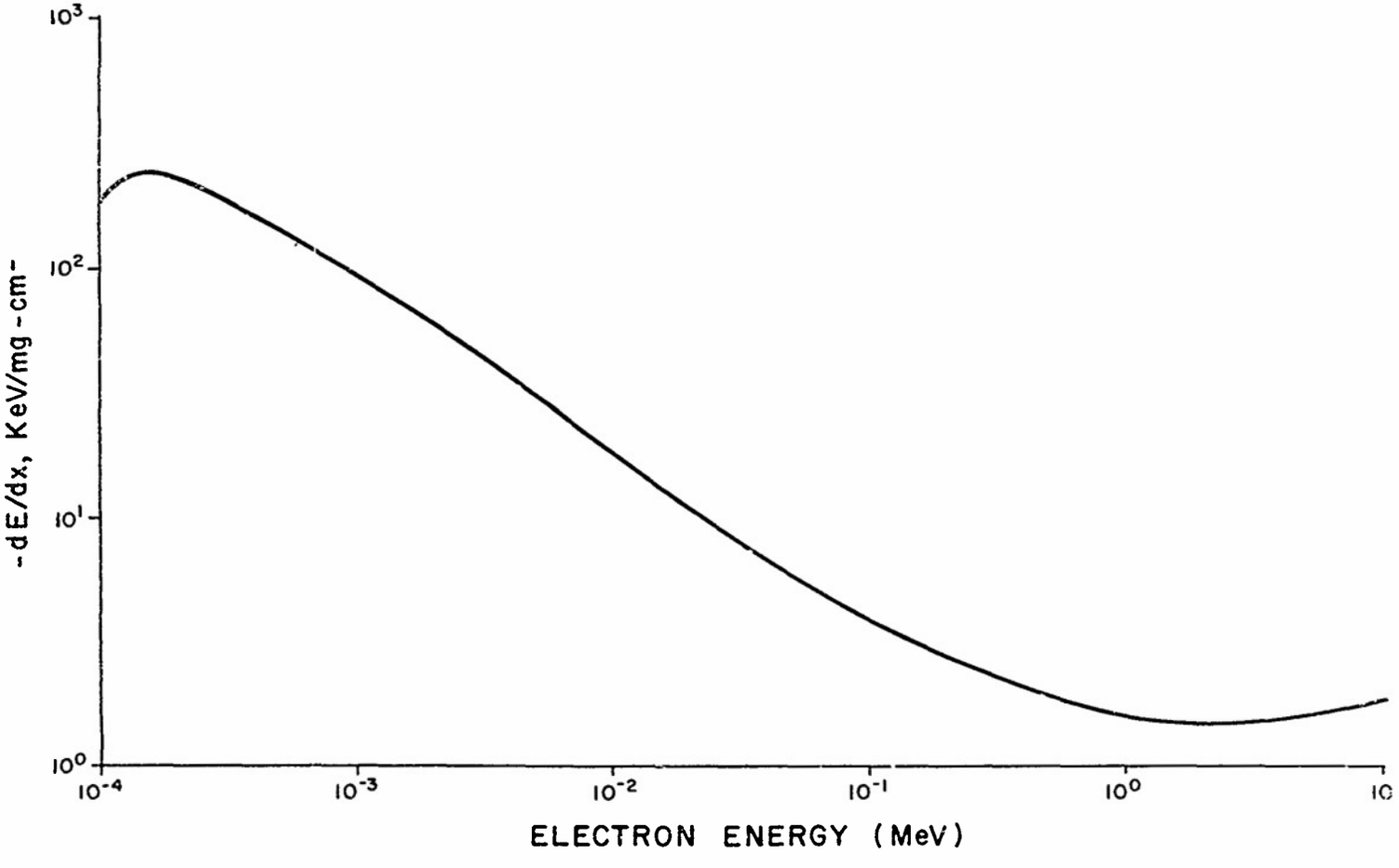

Figure V-3 — Electron Stopping Power in Air

Chapter VI

Measuring Radiation From Charged Particle Accelerators

R. D. Cooper, F. J. Mahoney, T. G. Martin

Introduction

Radiation measuring instruments are used with accelerators in at least three different ways. The most common use of such instruments is by an experimenter to measure radiation interactions and to obtain information. The devices used to make these measurements are usually found in or near the beam of the accelerator. A second major use for radiation detection and measuring instruments is in area monitoring in shielded areas and in nearby rooms, corridors, and labyrinths. These instruments are used for health physics purposes and are therefore germane to the discussion here. A third use of radiation measuring devices is in personnel dosimetry. Since these dosimeters must necessarily be rather simple, an understanding of the limitations on their readings should be kept in mind.

Since the literature on radiation measuring methods and the instruments that are used for this purpose is enormous, there will be no attempt here to repeat what is well-known and can easily be reviewed. Instead the emphasis will be placed on the differences between measuring accelerator produced radiation and the more common task of detecting and measuring radiation from radioactive isotopes. A general description will be given of the radiation sources with emphasis on the radiation measuring problems involved with each. Then a short discussion of the different detection methods and devices will attempt to show how the instruments can be used to measure accelerator produced radiation. A more detailed description of the major problems which arise in monitoring accelerator produced radiation will follow with emphasis on the quantities required to specify biological effect under these conditions. Finally there will be a discussion of the statistics of counting radiation from both continuous and pulsed sources to insure that proper corrections are made where necessary.

In order to monitor radiation levels in the areas around an accelerator it is necessary to measure gammas, neutrons, and most often a mixture of the two. Clearly one of the first problems which is met in accelerator installations is that of obtaining instruments sensitive to gamma rays or neutrons but not both. Besides routine area monitoring, instruments are required to continuously measure the activity in air and water effluents to insure that all systems are working properly.

The radiation from an accelerator source differs considerably in some cases from that produced by radioactive isotope sources. In the first place, the accelerator output is often pulsed or modulated in some way. As will be seen from the examples discussed in the next section, the lengths of the radiation pulses vary from as much as one-half second down to as little as 10^{-8} seconds.

A second major difference is that the direct beam of the accelerator is very concentrated in its spatial distribution and therefore neither primary nor secondary radiation is expected to be isotropically distributed as is the radiation from an isotope source. This anisotropy, just as in the case of very short pulses, can lead to saturation of detectors if the instruments are not used under proper conditions. Of the radiation produced by accelerators, only neutrons at medium energies are generally isotropic in distribution.

A third difference is that accelerator radiation fields are usually mixed fields. This is because neutrons are easily removed from nuclei either by high energy photons or by positively charged ions. Bremsstrahlung is also easily produced when charged particles are stopped, so a mixture of neutrons and gammas is commonly found. This fact must be taken into account when planning the instrumentation to be used in an accelerator installation.

Radiation Measuring Instruments

Before discussing the types of detection and measuring instruments with their advantages and disadvantages for accelerator use, the different sources will be described so that the particular problems of each can be pointed out.

Table VI-1 lists a number of radiation sources together with the primary radiation commonly emitted and the approximate pulse lengths. Radioisotopes and reactors give off radiation continuously with each particle or photon being emitted randomly in time. Electrostatic accelerators such as Van der Graaffs and Dynamatrons where one terminal is charged to a high potential also usually operate in the continuous mode. These can however be pulsed by using appropriate grids in front of the source of charged particles. Pulses of any length down to about 10 nanoseconds can be obtained in this way.

Circular particle accelerators such as cyclotrons, betatrons, and synchrotrons are usually pulsed devices. In the case of betatrons and synchrotrons the accelerating mechanism requires a modulation of the magnetic field which results in a pulsed beam. Cyclotrons are usually pulsed in order to make better use of the power available, since electronic tubes and devices are available to handle high peak power but are limited to moderate average power levels. In cases such as cyclotrons where microwave oscillators are used, there is a microstructure within the beam pulse as well.

Linear accelerators are pulsed for the reason described above, since high peak power klystrons are available but there are no continuous high power klystrons in use. Here again there is a microstructure at the microwave frequency within the beam pulse. Since for electron linacs the microwave frequency is often 3000 megahertz, the micropulse rate is 3×10^9 pulses per second with pulse lengths approximately 3×10^{-10} seconds. In general, this microstructure is too fast to affect counters, so it can be ignored except under very special conditions.

TABLE V-1 Sources of Nuclear Radiation

Radiation Source	Type of Radiation	Pulse Length
Radioisotope	β γ	Continuous Random
Reactor	neutron	Continuous Random
Pulsed Reactor	neutron	100 μsec-15 msec
Van der Graaff	e^-, positive ions	Continuous *
Dynamatron	e^-, positive ions	Continuous *
Cyclotron	positive ions	50-200 μsec †
Betatron	e^-	1-10 msec
Synchrotron	e^-, protons	100 μsec-50 msec †
Electron Linac	e^-	0.01-10 μsec †
Positive Ion Linac	positive ions	200-3000 μsec †
Pulsed neutron generator	neutrons	1-10 sec

* Can be pulsed

† Microstructure at RF frequencies

The instruments which are available for use in accelerator installations are, of course, the same devices that are available for any other nuclear measurement. The personnel dosimeters in common use such as film badges, thermoluminescent dosimeters, and pocket ion chambers are all used in and around accelerators frequently without a great deal of thought being given to what is being measured. Clearly, in mixed neutron fields and with high energy gammas, the personnel dosimeters give only information about the dose and can indicate little concerning the quality factor needed to determine the dose equivalent. In addition, charged particle equilibrium may not exist in many cases, so readings from this type of instrument must be used with great care.

As mentioned, for area monitors which are of primary interest here, the only types of radiation of importance are neutrons and gamma rays as long as the primary beam energy is below the meson production thresholds. The problem of determining how to measure this mixed field of radiation and what effect it would have on humans can be broken into the following specific problems:

a) The effects of instrument dead time on measurements of continuous and pulsed radiation.

b) The effect of the quality factor of the radiation.

c) The importance of charged particle equilibrium with the high energy gammas which may be present.

d) Miscellaneous instrumental effects such as saturation of a detector or the effect of a changing magnetic field of an accelerator on a detector.

During the remainder of this chapter these problems will be discussed in terms of the instruments which can be used for area monitoring near accelerators.

Table VI-2 lists the most commonly used nuclear detection and measuring instruments together with the primary factors which determine the dead time and typical dead times for each. These are instruments which are often used as area monitors and do not include those such as cloud chambers, bubble chambers and spark chambers which can detect several particles simultaneously and are primarily used within the radiation beam.

Most of the devices listed in this table are principally used as gamma-ray detectors. However, in most cases, they can be converted to measure neutrons by changing the gas or the wall material. Neutrons can often be measured, in these instruments by making use of the knock-on protons which occur in hydrogenous materials or by adding boron or lithium which produce very highly ionizing disintegration products after absorbing a neutron.

TABLE VI-2 Nuclear Radiation Detection Instruments

Detector	Dead Time Factors	Typical Dead Times
Ionization Chamber	Gas Pressure Geometry	5-10 μsec
Proportional Counter	Time Lag Gas, Voltage	1-5 μsec
Geiger Counter	Quenching Method	200-600 μsec
Scintillation Counter	Preamplifier Pulse Shaping	3-6 μsec
a. Organic Scintillator	Fluorescence Decay Time	0.01-0.1 μsec
b. Inorganic Scintillator	Fluorescence Decay Time	0.25-3 μsec
Cerenkov Counter	Photomultiplier Transit Time	2-20 nsec
Solid State Counter	Preamplifier and Amplifier Pulse Shaping	1-5 μsec

Ion chambers, proportional counters, and Geiger counters are all gas-filled devices which produce an output current or a pulse when radiation interacts with the gas in the chamber. Ion chambers and proportional counters produce a signal proportional to the radiation absorbed, while the Geiger counter produces the same size pulse for each quantum of radiation which interacts in the counter. The rate at which gas-filled counters can count depends upon the diffusion rate for electrons and ions since these charged particles produce a signal as they move through the electric field towards the wall. In a Geiger counter, an avalanche is started by the initial interaction, and the length of the pulse depends upon how quickly this avalanche can be stopped.

In measuring the dose at any point in a medium, an ionization device depends upon the Bragg-Gray relation

$$D_m = J_g \, W \, \frac{S_m}{S_g} \qquad \text{(VI-1)}$$

where

D_m = dose in medium (ergs/gm)

J_g = the number of ion pairs per gram of gas

W = the energy per ion pair (ergs/ion pair)

$\frac{S_m}{S_g}$ = the ration of stopping power in the material to that in the gas

This merely says that when the cavity is small, the gas is subject to the same ionizing particles as the material itself. Since the dose equivalent to humans is most often required in health physics application, tissue equivalent ion chambers and tissue equivalent gas have been developed. Thus, as the energy of the radiation changes, the signal from the ion chamber would continue to represent the effect on tissue.

A solid or a gas is tissue equivalent if its atomic composition is identical to that of human muscle. This composition is 10.2% hydrogen, 12.3% carbon, 3.5% nitrogen, 73% oxygen, and other atomic species about 2%. Most tissue equivalent such as that made by Shonka has the correct hydrogen and nitrogen values but replaces much of the oxygen by carbon. This leads to errors of less than 5%.

Table VI-2 indicates that the fastest radiation detector in common use is the Cerenkov counter where the dead time depends only upon the photomultiplier and preamplifier characteristics since the light output is essentially instantaneous. Some scintillators, particularly certain organic materials are also very fast, and the length of time during which the counter is dead (i.e., unable to accept new information) depends upon the pulse shaping done in the preamplifier and amplifier electronics.

Solid state detectors, developed only within the last decade, have been widely accepted because of their very good energy resolution. In general, this high energy resolution is not required for area monitoring, so this type detector is primarily used in nuclear experimental work.

To take advantage of the high energy resolution which can be obtained with these detectors, it is necessary to use pulse shaping with about a five microsecond pulse. Thus even though the actual collecting time of the electron hole pair is much shorter, the dead time of the system will be determined by the amplifier and preamplifier characteristics.

The effect of the finite dead time of these counters together with the pulsed nature of the radiation from many accelerators will be discussed further in a later section of this chapter. The beam pulses will be found to be a very important factor in the statistics of counting radiation from accelerators.

Measurement of Dose Equivalent

A number of neutron counters have been developed in which the neutron sensitivity varies with energy in approximately the same way that the dose equivalent in rems varies with energy in tissue. These are known as rem counters.

A device has been developed by Hurst[1] which measures fast neutron dose in a mixed field by summing pulse heights from a proportional counter and multiplying by the energy The gamma rays can be discriminated against almost completely since the pulses due to the recoil nuclei resulting from neutron collisions are so much larger than the electron produced pulses. Neutron tissue doses can be measured in gamma radiation fields as much as 10^5 higher.

Anderson and Braun[2] have developed a rem counter which is a cylindrical BF_3 proportional counter surrounded by polyethylene and boron plastic cylinders. They obtained an accuracy of ±10% in measuring dose equivalent of neutrons over the range 0.04 to 10 MeV.

Another method has been used by Goodman and Rossi[3] to measure the dose equivalent in mixed fields. They used a pair of ionization chambers, one of which was a tissue equivalent chamber and the other a neutron insensitive chamber. An approximation to the dose equivalent in a mixed neutron and gamma ray field can then be given by

$$DE = \Gamma + 10N \qquad \text{(VI-2)}$$

where

Γ = the gamma tissue dose in rads

N = the neutron tissue dose

10 = a conservative value for the quality factor

Such paired chambers could be very effective in determining the dose equivalent near accelerators.

There are many other specific instruments which are described in the literature for use in mixed neutron-gamma ray fields. The objective here is not to describe specific instruments but rather to emphasize that the quantity which must be determined is the dose equivalent. To measure this quantity, it is necessary either to measure the dose of each component separately and apply proper quality factors, or to make use of a scheme which will do this automatically such as measuring the kerma.

There is another problem which has been hinted at above and is particularly important around accelerators. This is the necessity for having charged particle equilibrium in the measuring instruments. In general, this is not difficult when measuring neutrons, because of the short range of the recoil atoms. Electrons produced by high energy gammas, however, can easily result in non-equilibrium conditions.

Maximum ranges of protons produced by neutrons of energy E and of electrons produced by gammas of energy E are given in Table VI-3 together with the mean free paths of the primary particles. It is clear that for gamma rays and neutrons the maximum ranges of the secondary particles are much less than the mean free paths of the primaries. Thus the intensity of the radiation does not vary greatly over volumes of the dimension of the maximum range of the secondaries, and so a good approximation to charged particle equilibrium exists in this case. When electrons are the primary particles, the secondaries can receive up to one-half of the energy in a single collision and electron equilibrium would not exist.

The final type of problem unique to measuring radiation near accelerators can be described as the effect of the environment on the detector and electronics. This environment often includes very intense, changing magnetic fields, pulsed RF fields, and low frequency electromagnetic disturbances synchronous with the pulsing of the accelerators.

A principle instrument strongly affected by magnetic and RF fields is the photomultiplier. Commercial mu metal shields, if properly used, will normally provide sufficient shielding against magnetic fields. To eliminate the effects of RF fields, aluminum foil or screening can be used. Low frequency electromagnetic fields are among the hardest to shield against. When small signals are being conducted over relatively large distances, great care has to be taken to assure that the cable shielding is well grounded and that there is a common ground for the equipment on each end. Grounding problems are nearly universal and often require considerable effort before good results are obtained.

Table VI-3 Maximum Ranges of Secondaries Produced by Gamma Rays and Neutrons[4]

E (MeV)	Max. Proton Range gcm^{-2}	Neutron MFP gcm^{-2}	Max. Electron Range gcm^{-2}	Gamma Ray MFP gcm^{-2}
0.1	1.7×10^{-4}	0.83	0.014	39
0.3	6.0×10^{-4}	1.7	0.083	32
1.0	2.9×10^{-3}	4.2	0.43	33
3.0	1.6×10^{-2}	6.7	1.47	44
10.0	1.4×10^{-1}	17	4.9	65
30.0	1.2	33	13.2	

Measurement of Photon Radiation

In this section, some of the factors which must be considered in measuring x-rays and gamma rays will be described. Particular problems which must be recognized include radiation of response with photon energy, directional sensitivity of response and the size of the sensitive operture, and finally variations in response due to physical factors such as temperature and humidity.

At energies below about 150 KeV the principal interaction mechanism is the photoelectric effect. The primary reason for variation of response at these low energies is due to lack of particle equilibrium. In a cavity ionization chamber the relative response falls off at low energies because of the effect of the thickness of the walls. Just above this energy the relative response can rise above unity because the effective atomic number of the walls exceeds that of air.

At energies between 150 KeV and 3 MeV air equivalent and tissue equivalent chambers give approximately the same results. However, at energies above 3 MeV the primary interactions mechanism is pair production with a Z^2 dependence on the detector material. Therefore it is necessary to make use of tissue equivalent chambers at these higher energies.

Variation in the directional response of instruments usually occurs at low energies where there is a detector with a window built into one end. Clearly if one of the thick walls faces the source of low energy gammas, particle equilibrium does not occur in the chamber. By making use of a point source of the low energy radiation, the directional sensitivity can be calibrated. Since the detector is usually calibrated with a broad beam of radiation, a beam very much smaller than the operature will give a lower response for the same radiation field within the beam. Therefore, both the detector operture and the effective size of the radiation field must be understood for proper use of a detector with a window.

Calibration of a detector is usually constant throughout the normal ranges of temperature and humidity found in a working area. However, the response of open air ionization chambers can be very dependent upon these physical parameters. A change in response of as much as 20 to 30% can accompany a large temperature change.

Measuring Neutrons

The neutron energy spectrum is usually divided into a thermal region between 0 and 0.5 eV, an intermediate region to 200 KeV, a fast region between 200 KeV and 20 MeV, and relativistic neutrons above this energy. When choosing an instrument to measure the intensity spectrum of neutrons as a function of energy, the interaction processes characteristic of these different energy regions are used to distinguish between the neutrons.

To measure thermal neutrons, nuclear reactions such as B^{10} (n,α) Li^7 or Li^6 (n,t) He^4 which have high cross sections at these low energies are used. For example, the

most commonly used thermal neutron detector is the BF_3 filled gas proportional counter. Lithium iodide scintillation crystals and lithium loaded glasses are also commonly used for thermal neutron measurements.

Intermediate energy neutrons are somewhat harder to measure because the direct detections of recoils does not work well, especially at lower energies. Most commonly these neutrons are moderated down to thermal energies and then detected by thermal neutron detectors of the type described above.

Fast neutrons are usually measured either by using foil activation techniques where a number of thresholds and sensitivities are available or a gas proportional counter where proton recoils provide the ionization. Both of these methods discriminate very well against gammas and therefore can be used in mixed fields.

Relativistic neutrons are usually measured by the amount of C^{11} formed in C^{12} by the (n, 2n) process. There are also foil activation and scintillation methods which can be used.

For radiation protection purposes, it is not enough to know the [illegible] neutrons as a function of energy. The quantity of interest as has been pointed out before is the dose equivalent. To obtain this, it is necessary to measure the dose in each energy region and multiply by the appropriate quality factor. The ICRU has recommended a quality factor of 2 for neutrons between thermal and 10 KeV. This then rises to a peak of about 11 near 500 KeV before falling back to about 6 between 10 and 20 MeV. Thus the intermediate and fast neutrons have a greater biological effect as would be expected.

Instruments which measure directly the dose equivalent over a wide range of neutrons energies are now available. The most commonly used of these consists of a moderator surrounding a spherical or cylindrical thermal neutron detector. With a moderator properly made, it has been possible to obtain rem-proportional response to intermediate energy neutrons to within ±10%.

Measurement of Radiation Counting Rates from a Continuous Source

The final two sections of this chapter will concentrate on the statistics of counting radiation, first from a continuous source, and then from a pulsed source. The problem was described above and typical pulse lengths of accelerators and dead times of counters were listed. The objective in this final part of the chapter is to work out the statistics under various conditions so that corrections can be made to measured counting rates. An understanding of these statistical facts is necessary in many cases in order to choose a detector with the most suitable dead time for a particular situation.

Counting apparatus can in general be divided into two types depending upon whether an event in the detector, during the dead time of a previous event, will extend the dead

time (paralyzable) or not (nonparalyzable). In a paralyzable counter, a time equal to the dead time which contains no events is required before the counter can recover. Figure VI-1 shows examples of paralyzable and nonparalyzable counting. Paralyzable counting equipment includes certain electronically quenched Geiger counters or electromechanical registers which limit the counting rate. Although such equipment is rarely used at the present time with pulsed sources, the dead time corrections will be worked out for completeness. Most modern radiation detection and measuring instruments including all those listed in Table VI-2 are of nonparalyzable type.

The measured number of counts per second, n, in a nonparalyzable counter with a dead time ρ represents the value obtained by subtracting the counts lost per second from the actual number of events in the detector per second, N. The counts lost can be found by multiplying the total fraction of each second during which the counter is dead, $n\rho$, times the actual event rate. Thus the measured counts per second is given by

$$n = N - Nn\rho \tag{VI-3}$$

Since we can measure n and ρ, the actual event rate can be found.

$$N = \frac{n}{1-n\rho} \tag{VI-4}$$

It is of particular significance for paralyzable counters that every counter actually tallies intervals between events rather than events themselves. By definition a paralyzable counter can only count intervals longer than its dead time ρ. It can be shown from probability theory[5] that the probability of an interval being ρ or longer is exp $(-N\rho)$. Consequently the measured count rate, that is the number of intervals longer than ρ, will be this factor times the actual number of events per second.

$$n = Ne^{-N\rho} \tag{VI-5}$$

In this case, the measured counts per second reaches a maximum at a particular value of N and then falls off to zero with increasing actual rate. This can be shown by differentiating the expression above with respect to N and setting it equal to zero. This results in the point of maximum n being where

$$N = \frac{1}{\rho} \tag{VI-6}$$

Substituting we find

$$n = \frac{1}{\rho\ e} \tag{VI-7}$$

which is the maximum counting rate. It is essential to realize that the actual event rate is double valued in n. Thus a single measurement of the counting rate n does not uniquely determine the actual rate.

Counting Radiation from Pulsed Sources

We will now determine the methods which can be used to count radiation delivered in repetitive pulses limiting the discussion to cases where the dead time is shorter than the interval between pulses. Figure VI-2 shows the two cases which will be considered. Other variations of the parameters involved can be worked out using the methods to be described here. The variables in these cases are defined as follows:

N	=	actual event rate within the pulse
N′	=	actual number of events occurring per second = $2\pi\ell$
n	=	measured count rate within the pulse
n′	=	measured counts per second = $n\pi\ell$
ρ	=	measuring system dead time
ℓ	=	radiation pulse length
d	=	time interval between pulses
π	=	number of radiation pulses per second

In case 1 the dead time of the counting system is longer than the radiation pulse but shorter than the interval between pulses. This situation occurs frequently when measuring radiation from a linear accelerator.

It is clear that the most important difference between the continuous and pulsed cases is that in the latter, events can only occur during a pulse assuming that the flight time to the detector can be neglected. From this obvious point, it follows that the total fraction of each second available for events to occur in the counting system is $\pi\ell$. A further conclusion which can be drawn is that the effective dead time in the pulsed cases are not necessarily equal to the instrument dead time and in fact are in many instances variable in length. It is just this variability which makes it impossible to apply directly the continuous case statistics to pulsed cases.

Since the effective dead time may be variable, methods must be developed which do not depend upon the length of the dead time. This will require the application of probability theory to predict whether an event does or does not occur within the radiation pulse.

In Case 1 with a nonparalyzable counter, an event which occurs in one pulse will turn off the counter for the remainder of that pulse but will have no effect on succeeding pulses. We have seen that the probability for an interval ℓ to contain no events when on the average there would be $N\ell$ events is $e^{-N\ell}$. The number of such intervals occurring per second is just this probability times the number of intervals possible each second, that is $\pi e^{-N\ell}$. The number of counts per second is then just the total number of intervals minus this number which contain no events.

$$N' = \pi - \pi e^{-N\ell} = \pi(1-e^{-N'/\pi}) \qquad \text{(VI-8)}$$

Case 1 with a paralyzable counting system is clearly equivalent to the case above as long as the dead time is less than the interval between pulses. Thus even though an event occurs at the end of a pulse, it is unable to extend the dead time into the next pulse.

As the actual number of events occurring per second increases toward infinity, the second term in the equation above becomes zero and the number of counts per second, as is expected, becomes the radiation source pulse rate.

$$n' = \pi \qquad \text{(VI-9)}$$

Thus Case 1 is considerably different from the continuous case since both paralyzable and nonparalyzable systems give the same results and the counting rate is a single-valued monotonically increasing function of the number of events per second.

Case 2 can obviously be much more easily identified with a continuous source. A count with a variable dead time can only occur in this case when an event is registered within a time ρ of the end of the pulse. If the effect of this one short dead time pulse is ignored, the counts per second can be easily found by modifying the results for the continuous case to take account of the fraction of time the radiation is on. For a nonparalyzable system, this results in

$$n' = N' (1-n'\rho/\pi\ell) \qquad \text{(VI-10)}$$

which as N' goes to infinity becomes

$$n' = \pi\ell/\rho \qquad \text{(VI-11)}$$

This is a good approximation for Case 2 nonparalyzable when ρ is very small compared to ℓ. As ρ becomes significant compared to ℓ, the effect of events occurring near the end of the pulse becomes more important.

As described above, the probability for an event to occur within a time ρ of the end of the pulse is $(1-e^{-N'\rho/\pi\ell})$ and the number per second is $\pi(1-e^{-N'\rho/\pi\ell})$. This, except for a correction term due to dead times from previous pulses which overlap into the time period of interest, is the number of counts with dead times less than ρ. A good approximation to the number of counts per second in this case is then given by

$$n' = \frac{\pi(\ell-\rho)N'}{\pi\ell+N'\rho} + \pi(1-e^{-N'\rho/\pi\ell}) \qquad \text{(VI-12)}$$

where the first term is due to counts with full dead time occurring in the first $\ell-\rho$ of each pulse and the second term is for counts with shortened dead time.

The saturation counting rate under this approximation is

$$n' = \frac{\pi(\ell-\rho)}{\rho} + \pi = \frac{\pi\ell}{\rho} \qquad \text{(VI-13)}$$

which is seen to be the same maximum value as found above.

No account has been taken here of the fact that each pulse can have only an integral number of counts. Thus even though ℓ/ρ may be fractional, the actual number of counts as N' goes to infinity becomes the next higher integer times the number of pulses per second. For example if ℓ/ρ is 2.3, the asymptotic value will be 3π. As long as $\ell>>\rho$ this is not a terribly important consideration.

When a paralyzable counting system is used in this same situation, it is necessary to again consider the counter as an interval counter. If an event occurs within a time ρ of the end of the pulse, the counter will be cut off by the interval between pulses. Any other event occurring within the pulse will have to be followed by an interval ρ with no event occurring to be tallied as a count. Therefore the total counts per second consists of two terms as follows

$$n' = \frac{\ell-\rho}{\ell} N'e^{-N'\rho/\pi\ell} + \pi(1-e^{-N'\rho/\pi\ell}) \qquad \text{(VI-14)}$$

As in the nonparalyzable case above, this result is only an approximation and does not take account of those cases where the dead time from a previous count cuts down on this time period ρ at the end of each pulse.

As is expected, when N' goes to infinity, the counting rate of the paralyzable counter will be $n' = \pi$ since the counter will be cut off at the end of each pulse.

The maximum counting rate can be found by calculating dn'/dN', setting equal to zero and substituting back into n'. When this is done assuming that $\rho/\ell<<1$, the maximum coating rate is

$$n' = \frac{\pi(\ell-\rho)}{\rho} 1/e + \pi(1-1/e) \qquad \text{(VI-15)}$$

This is greater than π as long as $\rho \ll \ell$, so as in other cases using paralyzable counting systems, it is necessary to know whether counting is being done above or below the peak value.

Figures VI-3, VI-4 and VI-5 show the way in which n' varies as a function of N' for the cases considered here. A summary of all of these relationships is given in Table VI-4.

Table VI-4 Summary of Relationships Between True and Measured Counting Rates

Nonparalyzable

Case	Dead Time Relationship	Count Rate	Max. Meas. Rate	Sat. Rate
Steady State	ρ	$n = N(1-n\rho)$	$n = 1/\rho$	$n = 1/\rho$
Case 1	$\ell<\rho<d$	$n' = \pi(1-e^{-N'/\pi})$	$n' = \pi$	$n' = \pi$
Case 2	$\rho<<\ell$	$n' = \frac{\pi(\ell-\rho)N'}{\pi\ell+N'\rho}$	$n' = \pi\ell/\rho$	$n' = \pi\ell/\rho$
	$\rho<d$	$+ \pi(1-e^{-N'\rho/\pi\ell})$		

Paralyzable

Case	Dead Time Relationship	Count Rate	Max. Meas. Rate	Sat. Rate
Steady State	ρ	$n' = Ne^{-N\rho}$	$n = 1/\rho e$	0
Case 1	$\ell<\rho< d$	$n' = \pi(1-e^{-N'/\pi})$	$n' = \pi$	$n' = \pi$
Case 2	$\rho<<\ell$	$n' = \frac{\ell-\rho}{\ell} N'e^{-N'\rho/\pi\ell}$	$n' = \frac{\pi(\ell-\rho)}{\rho e}$	$n' = \pi$
	$\rho<d$	$+ \pi(1-e^{-N'\rho/\pi\ell})$	$+ \pi(1-1/e)$	

References

1. G. S. Hurst, An Absolute Dosimeter for Fast Neutrons, Brit. J. Radiol. **27**, 353 (1954).

2. I. O. Anderson and J. Braun, A Neutron Ram Counter, Nukleonik **6**, 236, (1964).

3. L. J. Goodman and H. H. Rossi, The Measurement of Dose Equivalent using Paired Ionization Chambers, Health Phys. **14**, 168-170 (1968).

4. W. C. Roesch and F. H. Attix, Basic Concepts of Dosimeter, pp. 1-41 in Radiation Dosimetry, Academic Press (1968).

5. R. D. Evans, The Atomic Nucleus, p 785, McGraw-Hill, N.Y., N.Y. (1955).

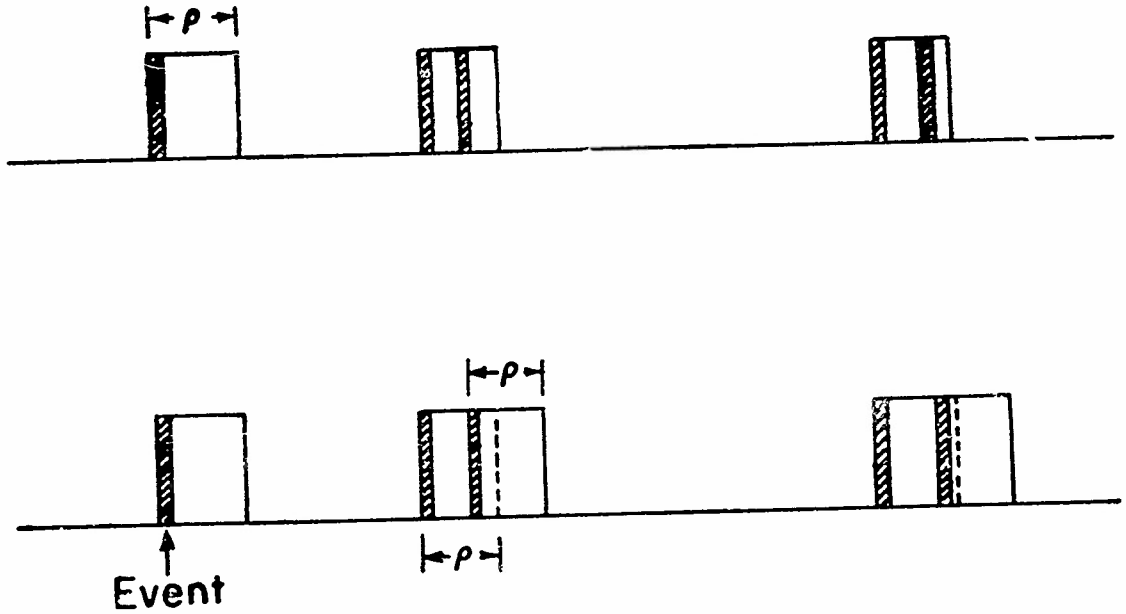

Types of Counting Apparatus

Figure VI-1

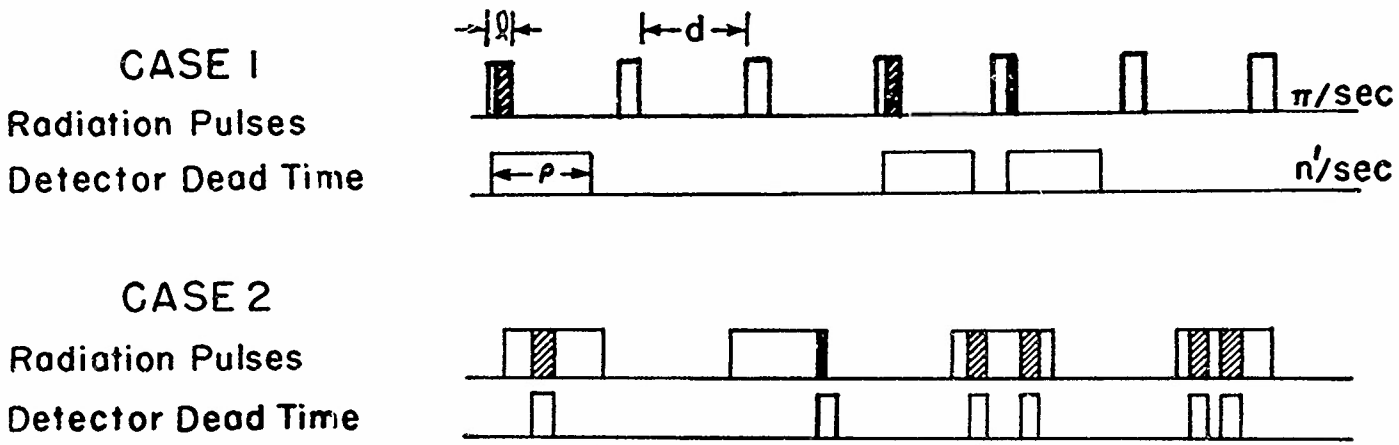

Detector Dead Time in Pulsed Radiation Measurements

Figure VI–2

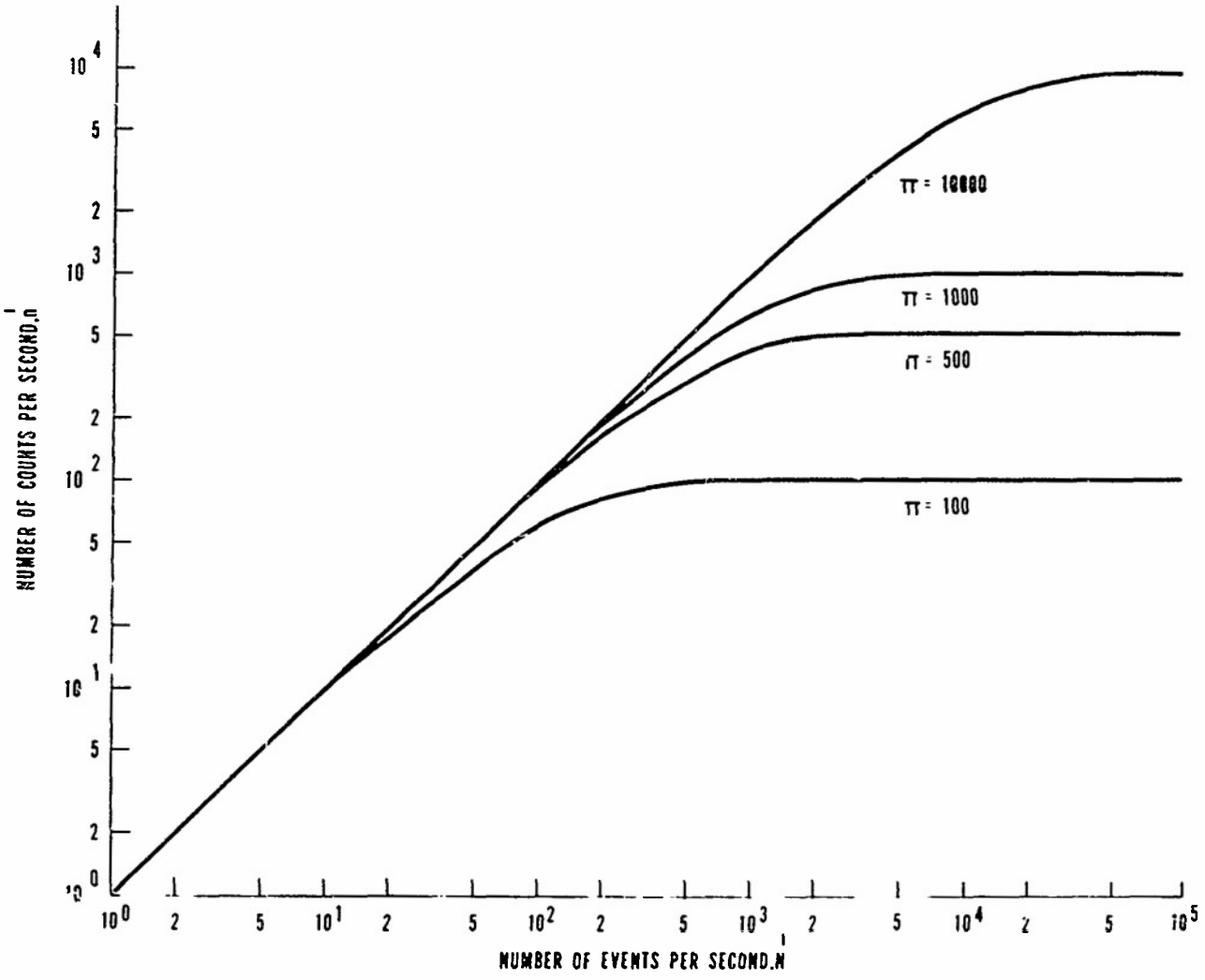

REPRESENTATIVE COUNTING RATES FOR CASE 1

Figure VI–3

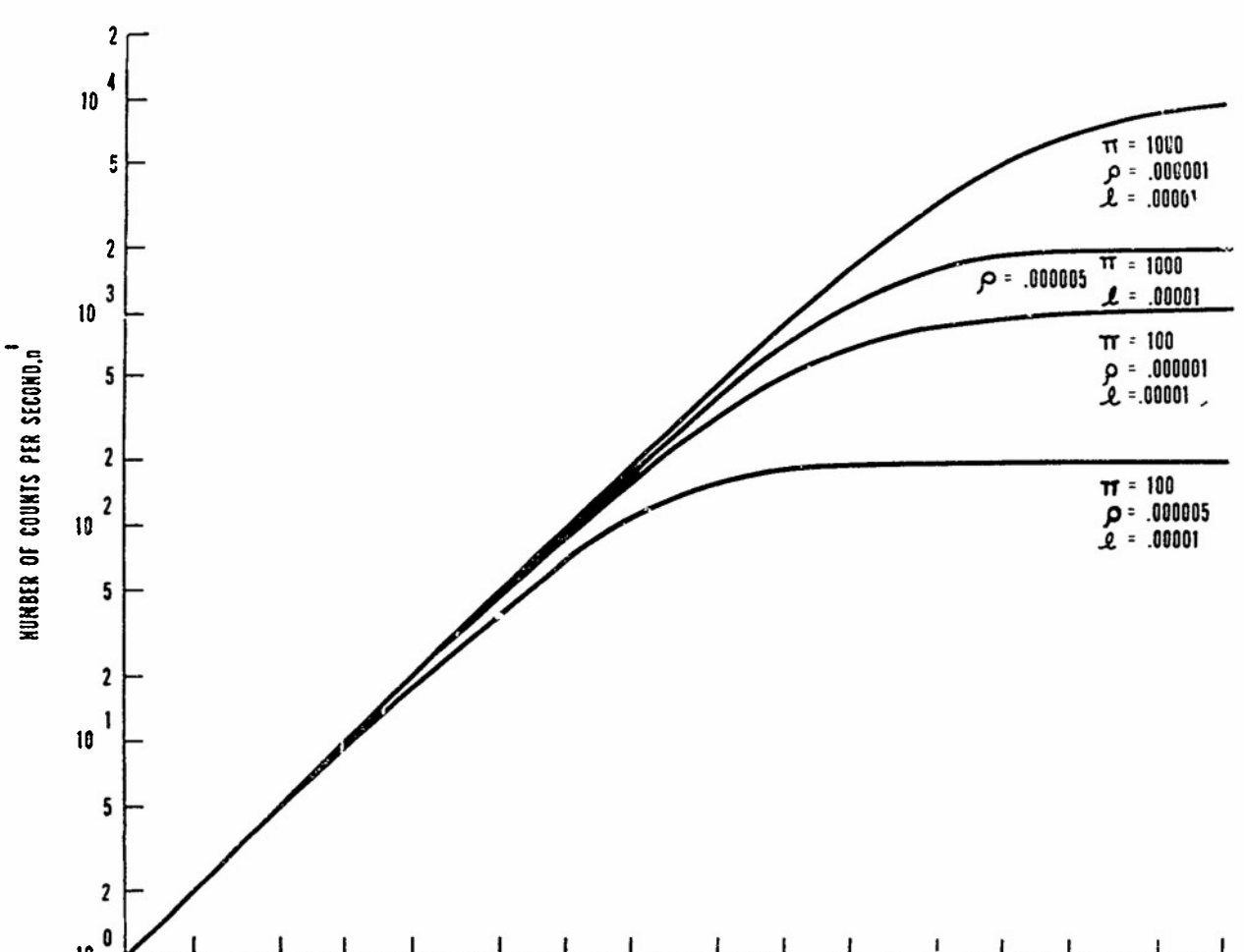

REPRESENTATIVE COUNTING RATES FOR
CASE 2 WITH NONPARALYZABLE COUNTER

Figure VI- 4

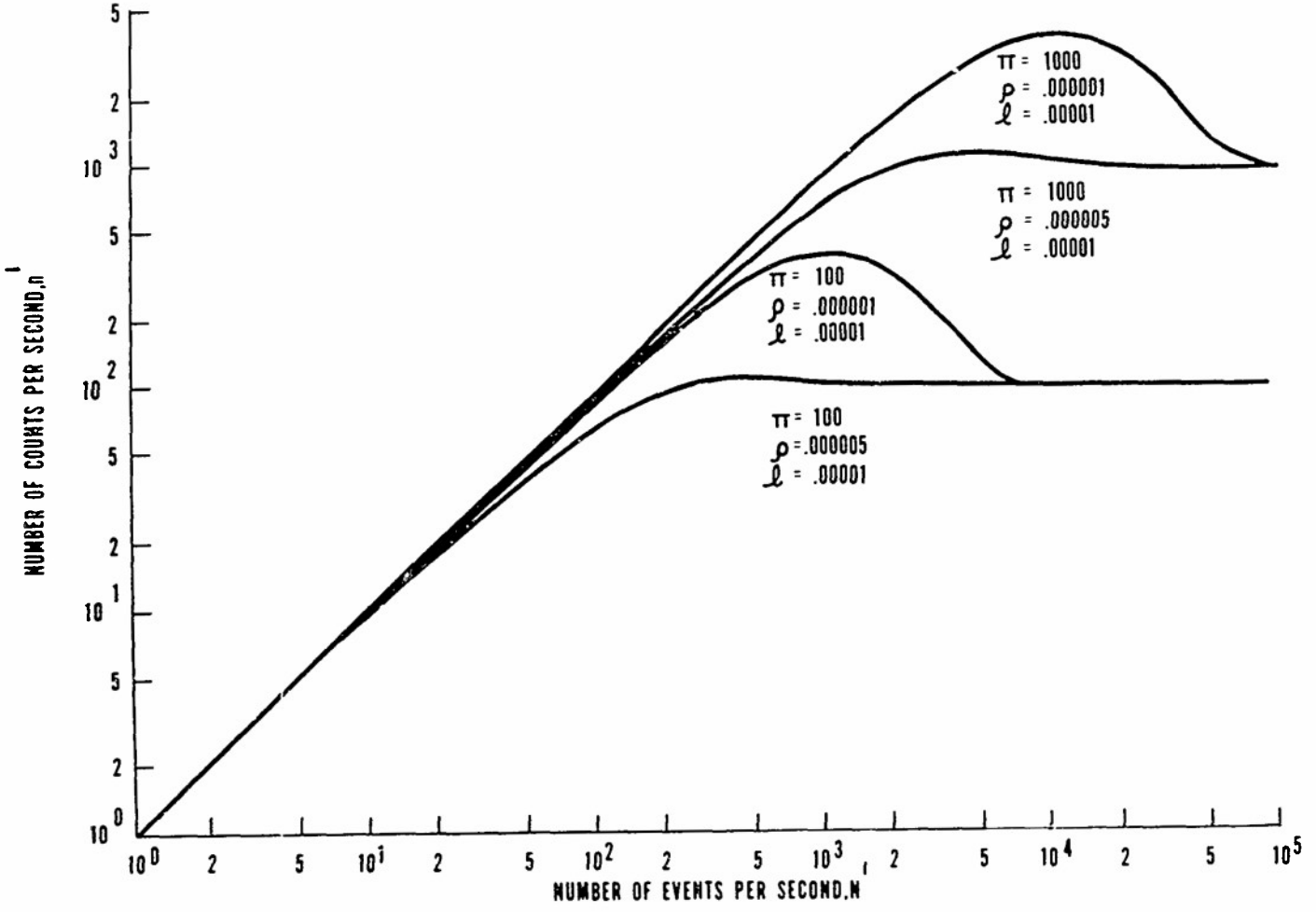

REPRESENTATIVE COUNTING
RATES FOR CASE 2 WITH PARALYZABLE COUNTER

Figure VI 5

Chapter VII

Access Limitation and Interlocks

Thomas G. Martin and Christopher W. Rees

Introduction

The most common cause of serious radiation exposures associated with accelerators, has been accidental (and sometimes intentional) entrance into the normally shielded target cell. No matter how effective the shielding of an accelerator facility is, if access to the beam area during operation is available the potential for a serious accident is enormous. It is therefore necessary to establish some means of access limitation. Methods used are nearly as varied as the number of accelerators in existence but they can generally be considered as physical barriers (doors, gates, pits) and electronic or electrical interlocks (photocells, keyed switches, microswitches, etc.). Generally both are used together. Possibly a discussion of electronic interlock system would better be located in Chapter VI, Measurement of Radiation but it is felt that the interlock is so intimately associated with access limitation that the discussion of one without the other might be lacking in continuity.

It is not the intent here to make a selection of a particular system or even to recommend a system for a specific purpose. The intent is merely to present some of the systems is use or proposed and to discuss some of their characteristics. As in the shielding discussions of Chapters II and III it again must be emphasized that the individual facility with all its peculiar problems must be examined and solutions evaluated on their own merit and applicability.

In the selection of access modes and interlock systems several important parameters must be kept in mind. This discussion will attempt to stimulate thought by enumerating some of these parameters though certainly not all. The need for "fail safe concepts" and "redundancy" is emphasized throughout this chapter.

The determination of shielding walls, ceilings and floors may be accomplished as discussed in Chapters II and III. Some detail however is presented in this chapter concerning the estimation of the shielding effectiveness of labyrinths or mazes as methods of access. It must be emphasized that the procedures described are approximations and detailed calculations of specific configurations as well as measurements after completion of construction are necessary.

Physical Barriers

Physical barriers must serve two purposes, shielding and access limitation. Careful consideration of the functions to be served and the layout of the overall facility can save significant costs in the construction of the accelerator shielding. Obviously where space and geometry permit, underground construction or use of existing terrain features

can provide highly economic shielding. Some accelerator facilities situated in remote locations can safely function with little or no shielding so long as radiation areas can be visually examined and monitored. This is an exception rather than the rule and in general shielding must be constructed. Concrete, because of its cost and structural capabilities, is the most generally acceptable choice.

After the selection of material to be used as shielding it is necessary to choose a method of access control. Glasgow and Haughian[1] have presented a representative picture of available shielding doors. Figure VII-1 (from this reference) indicates some of the more common types of shielding doors. Selection of a particular type of shielding door is dependent on several important factors, (e.g., the degree of shielding required and the availability of funds). Doors should be designed to provide shielding at least equivalent to the adjoining walls and to permit the passage of equipment large enough for experimental and operational setups.

The use of these generally massive doors introduces safety problems not generally associated with the radiation. Travel of these large doors is necessarily slow but the momentum is great. Stopping of these doors must be properly engineered to prevent trapping of personnel and/or possible cracking of other shielding walls due to repeated impact. Another consideration where the massive doors are concerned is that one must be able to open these doors even after a loss of power. Some manual method of opening the door from inside and outside must be included in the design. Hydraulic lowering of vertically mounted doors permits manual opening if power is lost. Horizontal movement is possible without power but is somewhat more involved. Similar comments may be made of the more sophisticated barrel and pivited types of doors.

Maze or Labyrinth

The shielding function of the door may be accomplished alternatively by a maze through the shielding wall (Fig. VII-1A) thus requiring only a light door or a gate to accomplish access limitation. Several important advantages may be derived by using this maze-gate combination since massive door movement is not a requirement. It presents disadvantages also because the maze frequently requires much more space and large equipment often may not fit through the maze. If necessary, delay naturally imposed by large door opening must be intentionally imposed on the gate-maze system.

The choice of the gate-maze type of access limitation requires an evaluation of the effectiveness of the proposed maze in preventing radiation hazards. Naturally no "line of sight" path for radiation would be permitted yet it is also necessary that the scatter path through the maze be considered. Considerable research has been done in an attempt to quantify the effect of ducts and voids through shields.[2] In general this problem is one of geometry. All possible paths cannot be considered although Monte Carlo methods do give reasonable approximations of the "all paths" problem. Reasonable approximations of the effect of multiple scattering surfaces may be obtained also if the energy per solid angle resulting from Compton scattering from the first "line of sight" surface the maze

is followed through the maze as illustrated in Fig. VII-2. Moyer[4] estimated that for a 90° scattering of X-rays it is conservative to assume that 0.05 of the incident energy would be scattered into one steradian in the new direction. Considering only 90° scattering results in a conservative estimate when compared with the experimental work reviewed by Selph and Claiborne[1] and Huddleston and Wilcoxson[5]. The intensity at the end of a series of scattering surfaces could then be represented as:

$$I_p = \frac{I_1}{r_n^2} \left[\frac{S_j r_{n-1}}{\prod_{\substack{r_i=1 \\ S_j=1}}} \right] \frac{0.05 S_j \cos 45°}{r_i^2} \qquad \text{(VII-1)}$$

where

I_p = intensity of radiation at point p (MeV/cm^2-sec, r/hr, mr/hr, etc)

I_1 = intensity at target in direction r (MeV/cm^2-sec, r/hr mr/hr, etc)

r_1 = distance from target to scatter area S_1 (cm, ft, etc)

r_i = distance between scatter areas (cm, ft, etc)

S_j = projected scatter areas (cm^2, ft^2, etc)

r_n = distance from last scatter area to point of interest

Some examples of this approximation is as follows:

Consider a 6' x 6' three legged maze such as illustrated in Fig. V-2 and an exposure dose rate of 7.1 x 10^5 mr/hr. Constructing a line through the maze with the shortest r values and 90° angles we arrive at v and s solves as follows:

r_1 = 9.5 ft $\qquad$ S_1 = 8 x 6 = 48

r_2 = 21 $\qquad$ S_2 = 6.5 x 6 = 39

r_3 = 8

therefore:

$$I_p = \frac{(7.1 \times 10^5}{(8)^2} \left[\frac{(0.05)(48)(0.707)}{(9.5)^2} \right] \frac{(0.05)(39)(0.707)}{(21)^2}$$

= 0.65 mr/hr

This calculated value agrees reasonably well with the measured value of 1 mr/hr (cobalt-60 radiation) reported by Terrell et al. [6]

Fig. V-3 illustrates somewhat more complex maze with the source of Xray flux being a 24 MeV electron linac.[7] From Fig. VII-3 the following values are approximated:

$r_1 = 40$ ft $\qquad S_1 = (5.5)(11) = 60.5$ ft

$r_2 = 24 \qquad S_2 = (7)(11) = 77$

$r_3 = 17 \qquad S_3 = (7)(11) = 77$

$r_4 = 28.5 \qquad S_4 = (8)(11) = 88$

$r_5 = 8$

for a dose rate in the direction of the labrinth of 4×10^{4} mr/hr we have

$$I_p = \frac{4\times10}{64}\left[\frac{(0.05)(60.5)(0.707)}{1600}\right]\left[\frac{(0.05)(77)(0.707)}{576}\right]\left[\frac{(0.05)(77)(0.707)}{289}\right]\left[\frac{(0.05)(88)(0.707)}{812.25}\right]$$

$I_p = 1.4 \times 10^{-2}$ mr/hr as an xray component of the dose rate at the entrance to the labyrinth.

With an energy of 24 MeV and a high Z target it would of course be necessary to calculate also the contribution to the dose rate by neutrons.

Although the neutron flux scattered through a maze presents a more complex problem, a similar approach may be used. The assumption that the energy of the neutrons entering the maze remains uneffected by the several collisions (reflections) may result in a too conservative estimate of the dose rate reduction afforded by the labyrinth. Careful studies have been made and experimental determination have shown reasonable correlation between the albedo-Monte Carlo calculations and experiments[2,3,5]. This geometric approximation tends to be conservative.

The scattering of thermal neutrons is more probable then fast neutrons and somewhat easier to correct (e.g. Boron loaded concrete on the surface of the shield wall will increase the probability of absorption, decreasing the probability of scatter in reflection).

The flux of neutrons at a point p could be approximated by:

$$\phi_p = \frac{\phi s}{2\, r_n^2} \prod_{i=1}^{n} \beta\Omega_i \qquad \text{(VII-2)}$$

where

ϕ_s = source strength in n/sec

β = albedo for neutrons (from 0.66 for thermal neutrons to approx. 0.05 for fast neutrons)

Ω = solid angle intercepted by the surface area of next reflection i.e.,

i.e., $\Omega = \frac{S_i\ (cm^2)}{4\pi r_i^2}$

r_i = distance from source to 1st surface or surface to next surface (distance between scatter areas)

r_n = distance from last scatter area to point of interest

Again using figures VII 2 and VII 3 as example labyrinths, approximations of the expected neutron fluxes are as follows:

From Fig. V-2 with $O_s = 5.0 \times 10^7$ n/sec

$r = 9.5$ ft $\qquad \Omega \cdot = \frac{8x6}{4\ \pi\ (9.5)^2} = 4\ .23x10^{-2}$

$r_2 = 21$

$r_3 = 8$ (=244cm) $\qquad \Omega_2 = \frac{6.5 \times 6}{4\ \pi\ (21)^2} = 7.04x10^{-3}$

$\phi_p = \phi_s B\ \frac{\Omega_1 B \Omega_2}{4\pi r_3^{\ 2}}$

and using an albedo of 0.4 which is relatively conservative for fast neutron

$\phi_p = \frac{(5x10^7)(0.4^2)(4.23x10^{-2})(7.04x10^{-3})}{4 \cdot\ \pi\ (\cdot 244)^2}$

$\phi_p = 3.2x10^{-3}$ n/cm^2 · sec

and from fig VII-3 with a source strength of 2×10^{13} n/sec we have

$r_1 = 40$ ft $\qquad \Omega_1 = 60.5/4\pi(40)^2 = 3.0 \times 10^{-1}$

$r_2 = 24 \qquad \Omega_2 = 77/4\pi(24)^2 = 1.1 \times 10^{-2}$

$r_3 = 17 \qquad \Omega_3 = 77/4\pi(17)^2 = 2.1 \times 10^{-2}$

$r_4 = 28.5 \qquad \Omega_4 = 88/4\pi(28.5)^2 = 8.6 \times 10^{-1}$

$r_5 = 8 = (244\text{cm})$

$$\phi_p = \frac{2\times10^{13}}{4\pi(244)^2} \left[(0.4)^4 (3.0\times10^{-1})(1.1\times10^{-2})(2.1\times10^{-2})(8.6\times10^{-1})\right]$$

$\phi_p = 4.07$ n/cm^2 · sec

Interlocks

In addition to physical barriers, it is frequently necessary to further protect personnel from serious exposure by interrupting the beam automatically upon the creation of a potentially dangerous condition such as the opening of a cell door, entrance of personnel into a high radiation area, or loss of exhaust system.

The basic philosophy of interlocking is to avoid serious consequences from a minor lapse of memory, or danger to a wandering visitor. Therefore, it is of prime importance that any interlock system be as simple as practical. The personnel should be subjected to a minimum of hindrance and aggravation while utilizing the system. The temptation to short circuit the system or some of its components should be as small as possible, if the system is to perform its function effectively. On the other hand it should never be convenient for an operator or an experimentor to remake an open interlock without someone actually going to the position of the break and, if the hazard no longer exists, reestablishing the interlock.

Although each individual case must be considered on its own merits and problems, some general comments apply to all facilities. In view of the serious consequences which could result from an interlock system failure, it is essential that the components of the system be selected with the same care as the protection system itself. For example, only heavy duty industrial type limit switches should be employed, avoiding light duty switches to insure durability and reliability.

It is likewise important to consider the effect of the radiation and atmospheric conditions on the interlock components.

Radiation sensitivity of electronic components such as the various semiconductor devices (transitors, diodes integrated circuits, etc) dictates that circuits imploying them should not be exposed to high levels of radiation. Dielectric and insulating materials, however, must be on occasion subjected to extremely high doses of radiation at detector positions located in target rooms and at beam ports. Table VII-1 shows some examples of insulating materials and their relative radiation resistance. In addition, interlock failure may result from corrosion of contacts exposed to the highly oxidizing gas, ozone. All of this indicates the importance of frequent testing and routine maintenance of all interlock systems.

The complexity of the facility, the flexibility required, the intended mission, and the degree of hazard are typical examples of the considerations which will determine the choice of interlock system. Small single port Cockcroft Walton neutron generators may require only a simple door switch interlock with a "machine on" light and a radiation monitor. However, a large research facility, such as a linear accelerator or tandem Van de Graaff, with many ports and target rooms might require a computer logic type of system. Even industrial irradiation facilities where routines are established may have to move demountable shielding walls or modify access barriers to enable processing of a new geometry of product. Such operations present a genuine challenge to the flexibility of an interlock system.

Several types of circuitry are in use which employ computer logic. One such system is that described by Horrigan, et al.[10] This system in use at the University of Toronto employs an "exclusive OR" gate arrangement for mutually exclusive conditions. Operation in a mode other than that authorized is prevented by either the lack of input or the presence of contradictory input. The operating mode is established by plugging in the desired printed circuit board, which completes the proper interlock interconnections.

This system consists of a dual network of diode transistor logic gates which feed two cascaded interlock relays. Inputs for the gates come from microswitches or relay contacts on the interlocked equipment. The logic gates are commercially available plug-in modules constructed of discrete components, rather than integrated circuits. This is advantageous because discrete component modules are generally more rugged and tolerant of overload and transients than integrated circuits, and are easier to modify or repair. The application of modular units makes the system flexible, and allows simple trouble shooting and module replacement by the normal operating staff.

A disadvantage of using logic gates, however, is that major repairs or modifications must be done by highly skilled personnel. Further, the interlock switches and wiring of this system had to be located in separate enclosures to prevent burnout of the system by accidental cross-connection with unrelated electrical circuits.

Another effective system is that described by Seitz, et al.[11], at the Los Alamos Tandem Accelerator Facility. There are 18 experimental beam tubes permitting multiple use of the facility, and 2 accelerators, a vertical and a tandem which may be operated

Table VII-1

Relative Radiation Resistance of Insulating Materials [9]

Material	Gamma Dose	Neutron Fluence
Phenolic, Glass laminate	$> 1 \times 10^{10}$	$> 5 \times 10^{18}$
Phenolic, Asbestos filled	$> 1 \times 10^{10}$	$> 5 \times 10^{18}$
Phenolic, unfilled	1×10^{7}	4×10^{15}
Epoxy	5×10^{9}	2×10^{18}
Polyurethane	$> 1 \times 10^{10}$	$> 5 \times 10^{18}$
Polyester, glass filled	5×10^{9}	2×10^{18}
Diallyl Phthalate	$> 1 \times 10^{10}$	$> 5 \times 10^{18}$
Polyester, unfilled	1×10^{6}	4×10^{14}
Mylar	8×10^{7}	2×10^{16}
Silicone (glass filled)	5×10^{9}	2×10^{18}
Melamine-formaldehyde	2×10^{7}	8×10^{15}
Polystyrene	5×10^{9}	2×10^{18}
Polyvinyl chloride	1×10^{8}	4×10^{16}
Teflon	5×10^{4}	2×10^{12}
Natural Rubber	4×10^{7}	2×10^{16}
Neoprene Rubber	3×10^{6}	1×10^{15}
Quartz	$> 5 \times 10^{12}$	$> 1 \times 10^{21}$
Aluminum Oxide	1×10^{12}	4×10^{20}
Beryllium Oxide	3×10^{11}	1×10^{20}

either together or separately. There is a set of punched cards which are coded to allow the accelerators and the access doors to operate in specific modes, and selection of a particular coded card allows the operator to interlock the operation of the accelerator (s) and any applicable area doors, thus permitting access only to areas desired.

Each door operates a single pole, double-throw stitch, and the door switches required for a chosen mode are connected to the electronics through a punched-card actuated switch When a door is closed a closed contact of the door switch applies power to light a green lamp, indicating "door closed". Opening the door removes power from the green lamp and closes the other contact of the door switch. This second contact applies power which activates a momentary gong, indicating the opening of a door; and triggers the turn on of a silicon-controlled rectifier (SCR) and a yellow lamp, indicating "door open". A relay, also pulled in by the turn-on of selected SCR's, removes power from the accelerator circuitry and lowers the accelerator voltage.

This system provides a method of selecting required controlled access for various modes of operation. The application of SCR's provides memory so that the door open indication does not reset when the door is closed but remains until the operator actuates a reset button, allowing the SCR's to turn off. The operator is kept informed as he has a map indicating the positions of the doors which are controlled for a particular mode.

Some possible interlock system failures may include loss of power, broken wires, and component failures such as sticky relays and dirty or broken switches which fail to make contact. As an example, if the door switch in the above system were to fail to make contact when the door was opened, or if the wire connected to that contact was to break, then the "door open" signal could not trigger on either the SCR and accelerator voltage relay, or the warning gong. Another possibility might be if the accelerator voltage relay were to stick and fail to pull in even though its coil was energized by the SCR.

As in any circuit, when a fail-safe interlock malfunctions, the system ceases to function properly. However, instead of either shutting off an accelerator unnecessarily or allowing unprotected operation as a result of the specific circuit failure; the anticipated malfunctions will all result in shutting off the interlocked function.

Although only those failures which are anticipated may be guarded against, there are some well known common failure modes. Such failures include a loss of continuity as by damaged or broken wires, or switches and relays which will not make contact even though closed.

Generally, a break in a circuit, is a more likely occurance than an additional short-circuiting connection, so a fail-safe design may typically use a complete path or presence of a signal to permit accelerator operation and an open circuit or loss of signal to disable operation. As an example, accelerator operation could continue only so long as a relay remained energized, and would stop when the relay dropped out because of loss of exitation.

A definite disadvantage of fail-safe design is that system failures will halt operations even when no actual safety hazard exists. Furthermore, such a system limits the designer's approach and technique, as well as his choice of components. However, there are some fail active components, such as pressure-sensitive floor pads, which have sufficient utility to warrant inclusion in an otherwise fail-safe design. For interlocks, however, the loss of operating time must be preferred to the loss of safety.

Periods requiring that the normal interlock system be by-passed will certainly occur. Therefore, specific procedures must be available to allow this by-pass to be accomplished without damage to the normal operation and to provide positive checks to insure that the normal interlock system is activated and functioning before returning to normal operation.

Horrigan, et al.[10] refers to a by-pass system which requires 2 key switches, with the additional key held by the Radiation Safety Officer. This system uses a dual input which prevents the single key from disabling an interlock which affects personnel safety without the additional input provided by the Radiation Safety Officer's key.

Emergency-stop Switches

Thought must be given to the location and identification of emergency-stop switches. In some facilities it is necessary to install these switches in temporary positions such that protection is available for a transient condition governed by a particular experimental setup. The purpose and function of these switches should be immediately evident to everyone, employee and visitor alike, likely to be present in the facility. Because the degree of danger varies at different locations within a facility some locations may only require a switch which will disable a particular magnet of the beam transport system to prevent carrying the beam into the area in question, other locations will require switches which shut the beam down completely.

Because of this variety of function, and because there will also be emergency stop switches controlling electrical power to experiments and shielding doors, as well as portions of the accelerator itself, the identification of these switches is a demanding task. A person overlooked during the search before lockup must be able to positively defeat the beam instead of ineffectively shutting down some unassociated apparatus. On the other hand, the person must not hesitate to operate the emergency-stop switch for fear of being criticized for mistakenly shutting down some other apparatus, such as a vacuum system.

The number of stations required to perform a safety survey before startup is determined not only by the size of the controlled areas but also their complexity. After completion of the lockup procedure the person who has performed the survey should have seen every position capable of hiding a man. Since most accelerator facilities become more complex as time goes by, it becomes increasingly important that no person be overlooked during the search before lockup. Incidents of overlooking workmen involved in some sort of maintenance in a usually unoccupied location are all too common although serious accidents have been few.

Alarms and Indicator Lights

Large and complex facilities should present at frequent locations a system which will quickly display the status of the interlock system at any particular moment. Researchers and other users of the facility should find this information easily obtainable in order to perform their duties with justifiable confidence.

Rich and Kase[12] in their description of the accelerator safety program at Lawrence Radiation Laboratory refer to their standardized audible alarms as follows:

Radiation – Chimes

Beam On – "ooga" or "dive" horn

Evacuation – steady klaxon

Other facilities find other arrangements more suitable for their own particular needs, therefore it is evident that whatever system is chosen its success depends in large measure on the education of and acceptance by the user personnel.

Taped voice announcements can be used advantageously to keep the staff informed about the operational conditions. Confusion with meanings of various audible alarms can be avoided by routine test alarms at programmed times. Too frequent tests, however, may do more harm than good (cry wolf).

The standarization of audible alarms suggests also the need for the standardization of visual alarms as well. Signs and lights should clearly indicate their purpose. Positive wording in one area and negative in another leads to confusion.

Colors of lights should represent constant situations. The use of red to indicate a hazardous condition and green to indicate a safe condition is popular but not universally accepted. Magenta lights are sometimes used to indicate exits. It is important that all ambiguity be resolved in the selection of visual alarms.

The SLAC warning lights described by Babcock et al[13] use yellow to mean beam is off (but residual radioactivity may remain), steady magenta means a potential beam on condition; and flashing magenta means beam is on. Similarly, for the Klystron gallery, green means variable voltage substation on, Klystrons potentially operable; and flashing red means one or more Klystrons on.

Conclusion

"Fail-Safe" techniques are essential and should be used in all situations where practical Occasionally the value of a particular experiment is so high that the cost of full time guards at all possible entrances to hazardous areas may be justified rather than risking the loss of the data by an accidental break in the interlock or power loss during the run. Extreme care must be taken in making this type of judgment since a change in mind later frequently results in a temporary operation under highly dangerous conditions.

Morse[14] refers to "nuisance modifications" to increase awareness. It is an unfortunate situation that such a thing should be necessary yet it does serve its intended purpose. The philosophy stated by Morse et al. does establish a good basis in the design of a system of protection. The two statements are:

1. Human safety should not be entrusted to one or more persons following a written routine.

2. Even mechanized systems become routine after a time and hence may lose their effectiveness.

The system incoporated at RPI[14], which allows for fast entrance and exit for research operations, accounts for only one of the two principle problems, that of rapid access for a particular experiment. The second problem, which is not described in this reference, is also worth note. This is the necessity of establishing a fixed procedure for "by passing" an interlock system. Experience has shown that there will be times when maintenance or special experimental setups will require a machine to be run under other than ideal conditions. More important than the description of the procedure for establishing a by pass is a definite procedure, with redundancy, for insuring that the by-pass condition is corrected before release for routine operation.

References

1. Glasgow, L. R. and Haughian, J. M., Shielding Doors, First National Particle Accelerator Conference, March 10-12, 1965.

2. Jaeger, R. G., Editor in Chief, Engineering Compendium on Radiation Shielding, Chapter 8 (Several authors), Ducts and Voids in Shields, Vol. 1, Springer-Verlag, New York (1968).

3. Selph, W. E. and Claiborne, H. C. Methods for Calculating Effects of Ducts, Access Ways, and Holes in Radiation Shields ORNL-RSIC-20 (1968).

4. Moyer, B. J., Radiation and Shielding Estimates for Target Facility of FMC-Varian Accelerators, 15 Dec (1957).

5. Huddleston, C. M. and Wilcoxson W. L. Gamma-Ray Streaming Through Ducts. Naval Civil Engineering Laboratory Report NCEL-TR-289 (Feb 1964)

6. Terrell, C. W., Jerri, A. J., and Lyday, R. O., Jr., Radiation Streaming in Ducts and Shelter Entrance-ways, Armour Research Foundation Report ARF 1158-A02-7 (April 1962).

7. Associated Nucleanics, Inc. Report AN127 Design Report on Radiation Shielding for Quartermaster Radiation Laboratory Contract No. AT (30-1)-2718 (1961).

8. Cain, W. R., Calculations of Thermal-Neutron Flux Distributions in Concrete-Walled Ducts Using an Albedo-Model with Monte Carlo Techniques, Oak Ridge National Laboratory Report, ORNL 3513 (1964).

9. Hanks, C L., and Hammon, D. J , Radiation Effects Design Handbook, Section 3, Electrical Insulating Materials and Capacitors. NASA CR-1787 (July 1971).

10. Horrigan, E. W., Millar, R. T. and Schwedtmann, K., The University of Toronto Solid State Linac Interlock System, Proceedings of 1969 Particle Accelerator Conference, Wash., D. C., 5-7 March (1969).

11. Seitz, T. P., Lang, H. J. and Henkel, R. L., Door Alarm and Interlock System at the Los Alamos Tandem Accelerator Facility, LA 4262, Nov (1969).

12. Rich, B. L., and Kase, K. R., Lawrence Radiation Laboratory Accelerator Safety, California Univ., Livermore, UCRL-71706, Oct (1969).

13. Babcock, G., Breymayer, K. E., Busick, D. C., Crook, K., Jenkins, T. M., Mallory, K. B., McCall, R., Reagen, D.C., and Warren, G. Protection Systems, Chapter 21 The Stanford Two-Mile Accelerator R-B. Neal, Editor, W.A. Benjamin Inc., New York (1968).

14. Morse, D.S., Haken, J., and Ryan, R.M., New Personnel Interlock System and Procedures for the RPI Lab., Proceedings of the 1969 Particle Accelerator Conference, Wash., D.C., 5-7 Mar (1969).

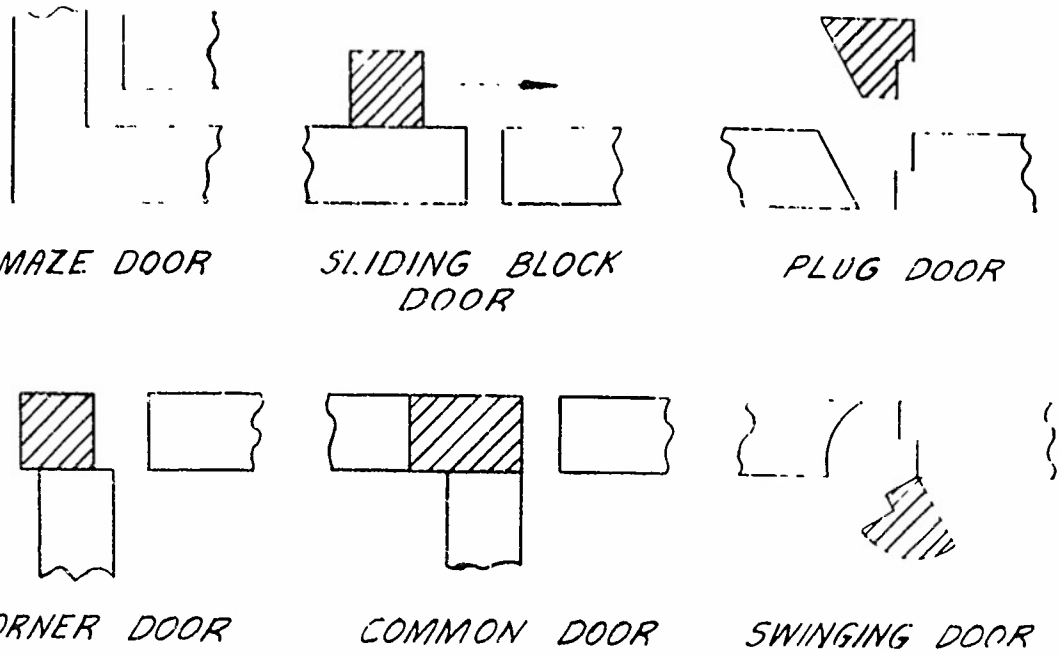

Figure VII-1 — Examples of Shielding doors[1]

Figure VII-2 – Example 1 labyrinth for calculation three legged

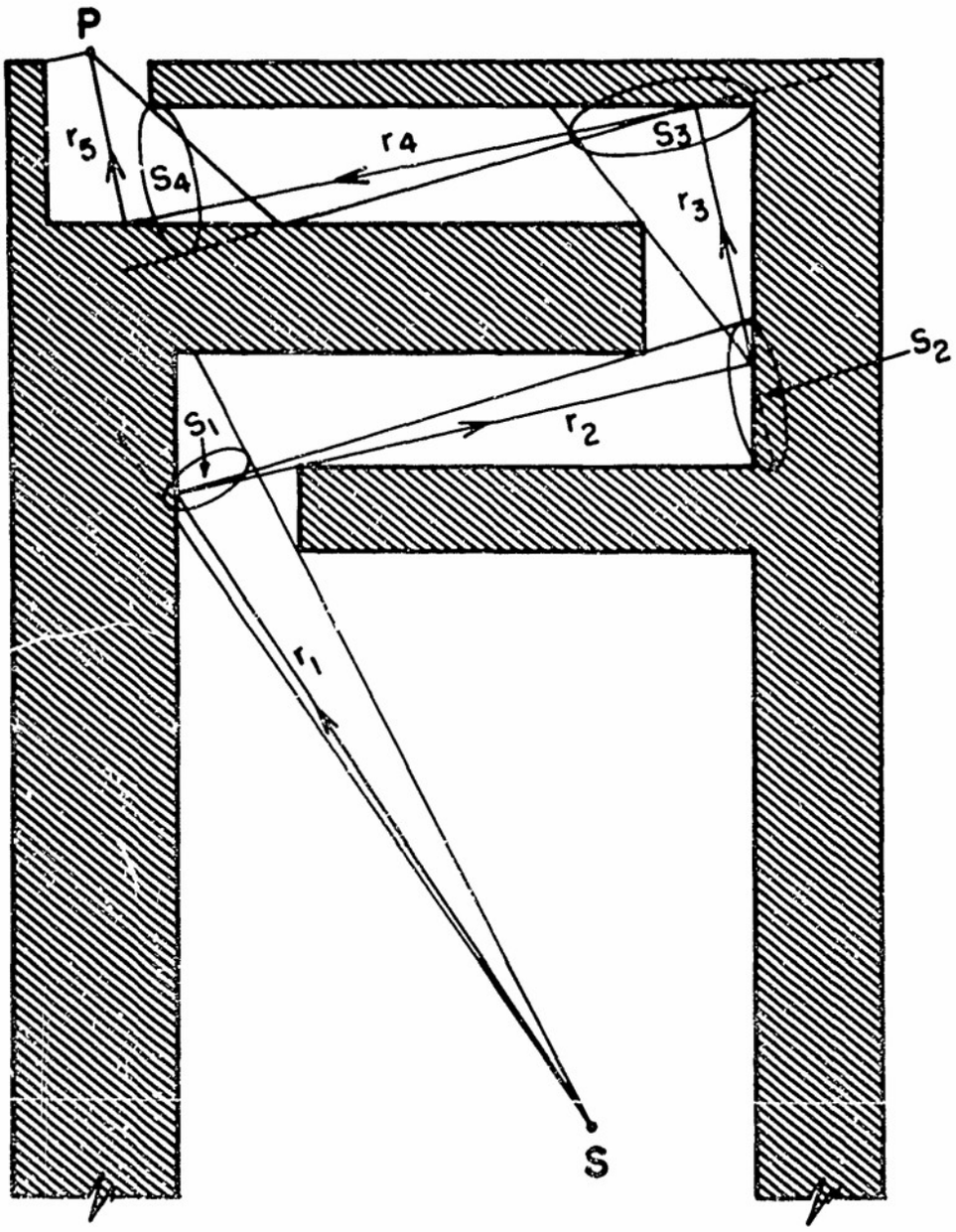

Figure VII-3 — Example 2 labyrinth for calculation

VIII Waste-effluents

Thomas G. Martin

Introduction

Waste disposal is one of the most difficult and critical problems facing the nuclear field. No attempt will be made here to decide on the final disposition of any radioactive or other toxic wastes. Release of small amounts of radioactive material to the environs is generally accepted as a necessary evil but the term "small" is subject to redefinition at frequent intervals. The recommendations of the International Commission on Radiological Protection, National Committee on Radiation Protection, Federal Radiation Council and the Atomic Energy Commission as well as other regulatory and health agencies are the bases for the decision on magnitude of release.

Solid Radioactive Waste

Solid radioactive waste such as activated targets and shielding blocks, filters and ion exchange resin or contaminated laboratory equipment present problems which are generally handled by collection, packaging, and shipment for disposal through commercial channels. Little can be said here except a short review of existing regulations concerning the packaging and shipment of radioactive material.

Under Title 49 of the Code of the Federal Register 1, Chapter 1, Department of Transportation; Hazardous Material Regulations Board, regulations are set forth for the control of hazards associated with the shipment of radioactive material in the United States. Several Definitions from this regulation are of interest for accelerator facilities.

Table VIII-1 assigns a transport group number to a large number of radionuclides. This table is subject of course to revision and is published here merely as a reference, therefore, decisions of actual assignment must be made with reference to current regulations. Transport groups are assigned considering radiotoxicity and relative potential hazard in transportation.

"Large Quantities of Radioactive Material" may be defined as quantities of radioactivity which exceed the values listed in Table VIII-2.

Table VIII-3 lists the maximum allowable amounts of the various transport groups in the Type A and B packaging.

"Type A packaging" means packaging which is adequate to prevent loss or dispersal of the radioactive contents and also maintains the integrity of the shielding designed into the package. Type A packages must withstand a series of tests designed to simulate normal transportation stresses. These tests include; a 30 minute heavy water spray, a free drop

Table VIII-1

Transport Groups of Radionuclides

Element[1]	Radionuclide[3]	Transport Group I	II	III	IV	V	VI	VII
Actinium (89)	Ac-227	X						
	Ac-228	X						
Americium (95)	Am-241	X						
	Am-243	X						
Antimony (51)	Sb-122				X			
	Sb-124			X				
	Sb-125			X				
Argon (18)	Ar-37						X	
	Ar-41		X					
	Ar-41 (uncompressed)[2]					X		
Arsenic (33)	As-73				X			
	As-74				X			
	As-76				X			
	As-77				X			
Astatine (85)	At-211			X				
Barium (56)	Ba-131				X			
	Ba-133		X					
	Ba-140			X				
Berkelium (97)	Bk-249	X						
Beryllium (4)	Be-7				X			
Bismuth (83)	Bi-206				X			
	Bi-207			X				
	Bi 210		X					
	Bi-212			X				
Bromine (35)	Br-82				X			
Cadmium (48)	Cd-109				X			
	Cd-115m			X				
	Cd-115				X			

Table VIII-1 (cont'd)

Transport Groups of Radionuclides

Element[1]	Radionuclides[3]	Transport Group I	II	III	IV	V	VI	VIII
Calcium (20)	Ca-45				X			
	Ca-47				X			
Californium (98)	Cf-249	X						
	Cf-250	X						
	Cf-252	X						
Carbon (6)	C-14				X			
Cerium (58)	Ce-141				X			
	Ce-143				X			
	Ce-144			X				
Cesium (55)	CS-131				X			
	Cs-134m			X				
	Cs-134			X				
	Cs-135				X			
	Cs-136				X			
	Cs-137			X				
Chlorine (17)	Cl-36			X				
	Cl-38				X			
Chromium (24)	Cr-51				X			
Cobalt (27)	Co-56			X				
	Co-57				X			
	Co-58m				X			
	Co-58				X			
	Co-60			X				
Copper (29)	Cu-64				X			
Curium (96)	Cm-242	X						
	Cm-243	X						
	Cm-244	X						
	Cm-245	X						
	Cm-246	X						
Dysprosium (66)	Dy-154			X				
	Dy-165				X			
	Dy-166				X			

Table VIII-1 (cont'd)

Transport Groups of Radionuclides

Element[1]	Radionuclides[3]	Transport Group I	II	III	IV	V	VI	VII
Erbium (68)	Er-169				X			
	Er-171				X			
Europium (63)	Eu-150			X				
	Eu-152m				X			
	Eu-152			X				
	Eu-154		X					
	Eu-155				X			
Fluorine (9)	F-18				X			
Gadolinium (64)	Gd-153				X			
	Gd-159				X			
Gallium (31)	Ga-67			X				
	Ga-72				X			
Germanium (32)	Ge-71				X			
Gold (79)	Au-193			X				
	Au-194			X				
	Au-195			X				
	Au-196				X			
	Au-198				X			
	Au-199				X			
Hafnium (72)	Hf-181				X			
Holmium (67)	Ho-166				X			
Hydrogen (1)	H-3 (see tritium)				X			
Idium (49)	In-113m				X			
	In-114m			X				
	In-115m				X			
	In 115				X			
Iodine (53)	I-124			X				
	I-125			X				
	I-126			X				
	I-129			X				

Table VIII-1

Transport Groups of Radionuclides

Element[1]	Radionuclide[3]	Transport Group I	II	III	IV	V	VI	VII
Iodine (53)	I-131			X				
	I-132				X			
	I-133			X				
	I-134				X			
	I-135				X			
Iridium (77)	Ir-190				X			
	Ir-192			X				
	Ir-194				X			
Iron (26)	Fe-55				X			
	Fe-59				X			
Krypton (36)	Kr-85m			X				
	Kr-85m (uncompressed)[2]					X		
	Kr-85			X				
	Kr-85 (uncompressed)[2]						X	
	Kr-87		X					
	Kr-87 (uncompressed)[2]					X		
Lanthanum (57)	La-140				X			
Lead (82)	Pb-203				X			
	Pb-210		X					
	Pb-212		X					
Lutecium (71)	Lu-172			X				
	Lu-177				X			
Magnesium (12)	Mg-28			X				
Manganese (25)	Mn-52				X			
	Mn-54				X			
	Mn-56				X			
Mercury (80)	Hg 197m				X			
	Hg-197				X			
	Hg-203				X			

Table VIII-1 (cont'd)

Transport Groups of Radionuclides

Element[1]	Radionuclide[3]	Transport Group I	II	III	IV	V	VI	VII
Mixed Fission Products	MF-P		X					
Molybdenum (42)	Mo-99				X			
Neodymium (60)	Nd-147				X			
	Nd-149				X			
Neptunium (93)	Np-237	X						
	Np-239	X						
Nickel (28)	Ni-56			X				
	Ni-59				X			
	Ni-63				X			
	Ni-65				X			
Niobium (41)	Nb-93m				X			
	Nb-95				X			
	Nb-97				X			
Osmium (76)	OS-185				X			
	OS-191m				X			
	OS-191				X			
	OS-193				X			
Palladium (46)	Pd-103				X			
	Pd-109				X			
Phosphonus (15)	P-32				X			
Platinum (78)	Pt-1'				X			
	Pt-193				X			
	Pt-193m				X			
	Pt-197m				X			
	Pt-197				X			

Table VIII-1 (cont'd)

Transport Groups of Radionuclides

Element[1]	Radionuclide[3]	Transport Group I	II	III	IV	V	VI	VII
Plutonium (94)	Pu-238	X						
	Pu-239	X						
	Pu-240	X						
	Pu-241	X						
	Pu-242	X						
Polonium (84)	Po-210	X						
Potassium (19)	K-42				X			
	K-43			X				
Praseodymium (59)	Pr-142				X			
	Pr-143				X			
Promethium (61)	Pm-147				X			
	Pm-149				X			
Protactinium (91)	Pa-230	X						
	Pa-231	X						
	Pa-233		X					
Radium (88)	Ra-223		X					
	Ra-224		X					
	Ra-226	X						
	Ra-228	X						
Radon (86)	Rn-220				X			
	Rn-222		X					
Rhenium (75)	Re-183				X			
	Re-186				X			
	Re-187				X			
	Re-188				X			
	Re Natural				X			
Rhodium (45)	Rh-103m				X			
	Rh-105				X			
Rubidium (37)	Rb-86				X			
	Rb-87				X			
	Rb-Natural				X			

Table VIII-1 (cont'd)

Transport Groups of Radionuclides

Element[1]	Radionuclide[3]	Transport Group I	II	III	IV	V	VI	VII
Ruthenium (44)	Ru-97				X			
	Ru-103				X			
	Ru-105				X			
	Ru-106			X				
Samarium (62)	Sm-145			X				
	Sm-147			X				
	Sm-151				X			
	Sm-153				X			
Scandium (21)	Sc-46			X				
	Sc-47				X			
	Sc-48				X			
Selenium (34)	Se-75				X			
Silicon (14)	Si-31				X			
Silver (47)	Ag-105				X			
	Ag-110m			X				
	Ag-111				X			
Sodium (11)	Na-22			X				
	Na-24				X			
Strontium (38)	Sr-85m				X			
	Sr-85				X			
	Sr-89			X				
	Sr-90		X					
	Sr-91			X				
	Sr-92				X			
Sulphur (16)	S-35				X			
Tantalum (73)	Ta-182			X				
Technectium (43)	Tc-96m				X			
	Tc-96				X			
	Tc-97m				X			
	Tc-97				X			
	Tc-99m				X			
	Tc-99				X			

Table VIII-1 (cont'd)

Transport Groups of Radionuclides

Element[1]	Radionuclide[3]	Transport Group I	II	III	IV	V	VI	VII
Tellurium (52)	Te-125m				X			
	Te-127m				X			
	Te-127				X			
	Te-129m			X				
	Te-129				X			
	Te-131m			X				
	Te-132				X			
Terbium (65)	Tb-160			X				
Thallium (81)	Tl-200				X			
	Tl-201				X			
	Tl-202				X			
	Tl-204			X				
Thorium (90)	Th 227		X					
	Th-228	X						
	Th-230	X						
	Th 231	X						
	Th-232			X				
	Th-234		X					
	Th Natural			X				
Thulium (69)	Tm-168			X				
	Tm-170			X				
	Tm-171				X			
Tin (50)	Sn-113				X			
	Sn-117m			X				
	Sn-121			X				
	Sn-125				X			
Tritium (1)	H-3 (as a gas, as luminous paint or adsorbed on solid material)				X			X
Tungsten (74)	W-181				X			
	W-185				X			
	W-187				X			

Table VIII-1

Transport Groups of Radionuclides

		Transport Group						
Uranium (92)	U-230							
	U-232	X						
	U-233[4]		X					
	U-234		X					
	U-235[4]			X				
	U-236		X					
	U-238			X				
	U Natural			X				
	U Enriched[4]			X				
	U-Depleted			X				
Vanadium (23)	V-48				X			
	V-49			X				
Xeon (54)	Xe-125			X				
	Xe-131m			X				
	Xe-131m (uncompressed)[2]					X		
	Xe-133			X				
	Xe-133 (uncompressed)[2]							X
	Xe-135		X					
	Xe-135 (uncompressed)[2]					X		
Ytterbium (70)	Yb-175				X			
Yttrium (39)	Y-88			X				
	Y-90				X			
	Y-91m			X				
	Y-91			X				
	Y-92				X			
	Y-93				X			
Zinc (30)	Zn-65				X			
	Zn-69m				X			
	Zn-69				X			
Zirconium (40)	Zr-93				X			
	Zr-95			X				
	Zr-97				X			

[1] Atomic Number shown in parenthesis
[2] Uncompressed means at a pressure not exceeding 14.7 p.s.i. (absolute)
[3] Atomic weight shown after the radionuclide symbol
[4] Fissile radioactive material

1 1/2 to 2 1/2 hours after the spray through 4 feet onto a flat unyielding surface, a free drop through one foot onto each corner, a 13 pound steel cylinder with hemispherical end dropped onto the package through 40 inches and a compression load of five times the weight of the package or 2 psi times the maximum horizontal cross section whichever is greater.

Table VIII - 2

Large Quantity Radioactive Material

Transport Group	Maximum Amount of Radioactivity
I or II	20 Ci
III or IV	200 Ci
V	5000 Ci
VI or VII	50000 Ci
Special Form	5000 Ci

Table VIII - 3

Maximum Amounts of Radioactivity in Type A and B Packaging

Transport Group	Type A Quantity (Ci)	Type B Quantity (Ci)
I	0.001	20
II	0.05	20
III	3	200
IV	20	200
V	20	5000
VI or VII	1000	50000
Special form	20	5000

Type B packaging must meet the same tests as Type A and in addition be able to survive the "hypothetical accident" without release of activity or increase of radiation level to more than 1 rem/hr. The tests of this "hypothetical accident" are: a free drop of 30 feet, a drop of 40 inches onto a 6 inch diameter bar, and 1475°F for 30 minutes without cooling for three hours.

"Special Form Radioactive Material" means that if this material is released from the package there would be little probability of contamination even though radiation may still present a hazard (e.g. sealed sources).

"Transport index" is defined as the number placed on a package to designate the degree of control which must be exercised during transportation. This index is determined by the highest radiation dose rate in millirem/hr at 3 feet from any accessible external surface. (e.g. a package with a radiation level of 10 mrem/hr at 3 feet would be assigned a transport index of 10).

All radioactive material except where exempted must be packaged such that the following general packaging requirements are satisfied.

The outside of the package must have some sort of a seal which will indicate if the package had been illicitly opened.

Packages must be at least 4 inches on its smallest dimension and capable of maintaining leak tightness under the stresses normally expected in transportation and capable of passing the tests required of Type A packaging.

Shielding required to meet the maximum permissable external radiation limits must be uneffected by the stress normally expected in transportation.

Heat produced by the radioactive material must not result in a surface temperature in excess of 122°F when fully loaded or in the case of sole occupancy of the vehicle not more than 180°F.

There must be no significant removable radioactive surface contamination. "Significant" is defined as in excess of 10^{-11} Ci/cm^2 of β–γ and 10^{-12} Ci/cm^2 of α for all contaminants except natural uranium and thorium.

Packages must be shielded and braced to prevent radiation dose rate from exceeding 200 mrem/hr at any point on the external surface and the transport index from exceeding 10. If the radioactive material is shipped on a vehicle which is in use solely by the consignor then the external radiation levels may not exceed any of the following:

1. 1000 mrem/hr at 3 feet from the surface of the package in a closed vehicle.
2. 200 mrem/hr at any point in the ouside surface of the vehicle.
3. 10 mrem/hr at 6 feet from any external surface of the vehicle and
4. 2 mrem/hr in any normally occupied position in the vehicle.

Frequently the radioactive waste to be disposed of from accelerator facility will fall within the definition of Low Specific Activity Material as outlined in Table VIII-4. This type of material may include low level radioactivity on waste matter such as glassware, paper towels, cardboard boxes as well as target coolants, and wash water from low level decontamination projects. These quantities are exempt from the general packaging regulation just summarized provided compliance with the following rules:

1. Materials must be packaged to prohibit leakage under normal transportation conditions in packages which will pass the tests required of Type A or Type B packaging.
2. No significant removable surface contamination.
3. Packages must be labeled with Radioactive material labels (see Fig. VIII 1).

When shipped on vehicles which are used solely by the consignor low specific activity radioactive materials are exempt from packaging and labeling requirements provided the compliance with the following rules:

1. Materials must be packaged to prohibit leakage under normal transportation conditions.
2. No significant removable contamination.
3. External radiation levels do not exceed those described under the general packaging requirements.
4. Shipments must be loaded by the consignor and unloaded by the consignee from the same vehicle.
5. There must be no loose radioactivity in the vehicle.
6. Vehicles carrying material which requires a Yellow-III radioactivity label (see Fig VIII-1c) must be placarded with RADIOACTIVE on the front, both sides and the rear. The black 4 inch letters are on a yellow background.
7. The outside of each package must be marked "Radioactive - LSA".

The labels required in shipping the radioactive waste material are shown in Fig. VIII-1. Which label is required is determined by the transport index (Table VIII-5).

Radioactive white label (see Fig VIII-1a) is used on packages containing radioactive material which has no external radiation in excess of 0.5 mrem/hr.

Table VIII - 4

Low Specific Activity Material

Transport Group	Amount of Radioactivity
I	0.1 μ Ci
II	5 μ Ci
III or IV	300 μ Ci

TABLE VIII - 5

Labels for Radioactive Material Shipments

Label	Surface Dose Rate	Transport Index	Limitations
Radioactive White - I	< 0.5		
Radioactive Yellow - II	$\geqslant 0.5$ and < 10	< 0.5	
Radioactive Yellow - III	$\geqslant 10$	$\geqslant 0.5$	Also any package containing "Large Quantity of Radioactive Material (see definitions)

Radioactive Yellow-II label is used when external radiation on the surface exceeds 0.5 mrem/hr, but less than 10 and the transport index does not exceed 0.5.

Radioactive Yellow-III label is used when the external radiation level is more than 10 and the transport index exceeds 0.5.

Liquid Radioactive Wastes

The sources of liquid waste are numerous in many accelerator facilities; however, principally they are target and accelerator guide coolants, beam dumps and effluents from the laboratory facilities associated with the accelerator. Frequently liquid effluents are monitored in several different ways. Due to the requirements for highly purified (distilled or deionized) water in the cooling lines of the accelerator and the target assemblies, some

sort of water processing facility is incorporated in the system. By installing a radiation sensitive device in the flow of this water, the build up of induced radioactivity may be monitored. For example, a photofission target which might rupture could result in a rapid increase in the radioactivity in the coolant which would be designed to cause an alarm and possible break an interlock which would shut down the accelerator.

Monitoring need not be "in line", water samples routinely collected and analyzed, can accomplish the same goal for example using liquid scintillation counting, one could analyze samples of water to monitor the integrity of a titanium tritide (d, n) target which is cooled by the water.

Liquid waste presents several problems in its disposal. Frequently it may be convenient to use one of the several techniques for converting liquid to solid waste thus making it easier to handle and more acceptable to commercial disposal firms. No completely satisfactory techniques exists to solidify and thus immobilize the radioactive waste, yet by evaporation (of nonvolatile) and solidfying as a concrete or a ceramic small quantities of radioactive liquids can be handled without too much difficulty. Dilution to concentrations which are of levels which may be safely (and legally) released into sewer systems is the most generally accepted technique. This approach is reasonable in most accelerator facilities provided a dependable technique is available to prevent the release of the unusually high radioactivity which may result from the rupture of a target or other unscheduled events.

One procedure used successfully is the "hold up tank". The waste is released only after radioassay of the waste water is performed and assurance given that levels do not exceed permissible concentration.

Concentration of radioactivity which are permissible to release into either sewer systems or the atmosphere are subject to regulation by many different agencies. Most frequently these concentration guides are established based on the recommendations of the NCRP, ICRP, FRC and AEC; however, prior to establishing a release program local regulations must be considered and incorporated into that program.

Shipping of liquid radioactive wastes for disposal is subject to the same requirements as solid wastes. Also liquid radioactive material must be packaged in leak resistant inner containers in addition the package must be able to prevent loss or dispersal of the material after a 30 foot drop test or contain enough absorbent material to absorb at least twice the amount of liquid contained and not allow the radiation level on the outside surface of the package to exceed 1 rem/hr.

Gaseous and Airborne Radioactivity

Gaseous and airborne radioactive wastes are problems common to nearly all accelerator facilities therefore the treatment of these wastes is the principal area of interest. The induced radioactivity and toxic gases must be properly handled in disposal such that no person will be excessively exposed.

The use of microfilters in the exhaust systems has long been an effective means of preventing the release of unwanted particulate contamination to the atmosphere. Associated with such a system are excellent means of monitoring the effective life of such filters. Serious charges in the pressure differential on the up and down stream sides indicate that the filter has either clogged or ruptured. Levels of radioactivity may be continuously monitored by simply locating a suitable detector (e.g.. ion chamber, scintillation counter) in a location near the face of the filter bank. In this manner the release of particulate contamination can be readily prevented. The sources of this particulate radioactive contamination are discussed in more detail in Chapter IV. Elaborate air cleaning systems have been designed and should be considered when the levels of contamination are significantly high and particle size such that simple filtration is ineffective.

The production of radioactive isotopes of oxygen and nitrogen in the air is of prime importance in the establishment of cell ventilation and occupancy criteria. Exhaust rates and delayed entrance requirements are determined based on levels of ^{15}O and ^{13}N expected in the cell atmosphere.

Modes of production, depending on accelerator type, will be principally either (n,2n) and (γ,n). The cross section for $^{14}N(n,2n)^{13}N$ for 14 MeV neutrons is 6 mbarn and for $^{16}O(n,2n)^{15}O$ is very small favoring $^{16}O(n,p)^{16}N$. ^{16}N has a 7.1 second half-life and therefore need not be considered in the disposal aspect. If air is being circulated, this could be significant in ducting.

The threshold for (γ,n) reactions are of sufficient magnitude to make the production of ^{13}N and ^{15}O of concern only to electron accelerators of energies in excess of 15-20 MeV.

The modes and rates of production of radioactivity may be calculated as described in Chapter IV under circulating fluids-air and water. Equations IV 5 through IV 7 permit the estimation of the amount of radioactivity in the air and IV-8 allows the calculation of approximate delay time required before entry into the target area. It is at this point that the future disposition of this radioactivity becomes of concern.

The release of the activated products into the atmosphere requires assurance that exposure to the general public be within the safety restrictions imposed by the present state of knowledge of the effects of radiation on mankind (and of course Federal, State and Local regulations).

Toxic Gas - Ozone and Oxides of Nitrogen

Although not treated in Chapter IV the problem of production and treatment of toxic gases is similar to that of radioactive gases. In the irradiation of air ozone and oxides of nitrogen are formed. Ozone is produced in the largest quantities and may be considered to be the most toxic.

G-values for the X and electron radiation induced formation of ozone have been reported over a broad range of values however work done recently by Ghormley et al.[2] indicate a confident Xray value of 13.8 ± 0.7 molecules of O_3/100 e.v. in the radiolysis of oxygen. This value is used here. Correction for percentage of oxygen in air is incorporated in the constant in addition to the necessary units conversion.

The concentration of ozone produced in the beam may be predicted in order to determine the time which should elapse before personnel may enter the target cell Brynjolfsson and Martin[3] described ozone concentrations with equations VIII-1, VIII 2 and VIII-3. The production rate:

$$c_o = \frac{600.G_{O_3} \cdot i \cdot d}{V} \qquad \text{(VIII-1)}$$

where

c_o = production rate of ozone in the target cell (cm^3/sec m^3)

G_{O_3} = number of ozone molecules formed per 100 eV of radiation energy absorbed

i = electron beam current – Amperes

d = path length of beam in air (m)

V = volume of target cell (m^3)

During operation of the accelerator the amount of ozone in the cell may be approximated by

$$C = \frac{c}{v/V + 1/\alpha} \left(1 - e^{-[v/V \cdot 1/\alpha]\, t}\right) \qquad \text{(VIII-2)}$$

where

C = concentration of ozone in the cell (ppm)

c = production rate of ozone (Eq. (VIII-1))

v = exhaust rate of the cell (m^3/sec) during irradiation

α = lifetime of O_3 molecule (sec)

t = irradiation time (sec)

After shut-off both the exhaust rate and the rate constant ($1/\alpha$) are sometimes different than during irradiation. Then we have[2]

$$C_1 = C e^{-[v_1/V + 1/\alpha_1]t_1} \qquad \text{(VIII-3)}$$

where

C_1 = ozone concentration at t_1 sec after shut-off (ppm)

v_1 = exhaust rate after shut-off (m^3/sec)

α_1 = molecular lifetime without irradiation (sec)

Though ozone is not radioactive, the rate at which it decomposes to form O_2 and various oxides may be described as a first order reaction and is a function of its concentration, the concentration of other reactants and the surfaces available to aid the reactions. Therefore firm values for α are not available for all possible situations. George, et al.[4] noted an approximate "half-life" for the ozone in their measurements at Rensselaer and Yale of 35 minutes. Similar time was noted by the author at the U. S. Army Natick Laboratories Linac which yields an α_1 of 3.03×10^3 sec. If this value is also used in the calculations of C the results will be conservative because it is most likely that O_3 will decompose more readily with irradiation than without.

Equations IV-8 and Figure VIII-1[2] permit the estimation of time required for ^{13}N and O_3 concentration to decrease to 2 pCi/ml and 0.1 ppm respectively.

Example Calculation:

In order to determine the delay necessary before entering the radiation cell based on an ozone concentration of 0.1 ppm the following calculation can be made:

Parameters

path length = 2 meters

beam current = 0.5 mA

cell exhaust = $5m^3/sec$

ozone lifetime = 3000 sec

cell volume = $600m^3$

$$\frac{id}{v+V/\alpha} = \frac{(5\times10^{-4})\ (2)}{5+600/3000} = 1.92\times10^{-4}$$

$$\frac{v_I}{V} + \frac{1}{\alpha_I} = \frac{5}{600} + \frac{1}{3000} = 8.66\times10^{-3}$$

from figure IV-8 the delay required would be approximately 6 minutes.

Tritium from Targets

Most accelerators designed primarily as neutron generators produce the neutrons by accelerating a beam of deuterium ions into a target containing tritium. Leakage of the tritium from the target produces some radiological hazard. Such leakage can result from breakage as well as intentional vacuum loss for maintenance or target change.

Since tritium is also knocked out of the target during irradiation there is significant build-up in the vacuum system and release through pump exhausts. (Nellis, et al.[5] have noted that target deterioration of T/Ti target is brought about by actual loss of tritium during bombardment and that most of this tritium is in gaseous form.) Except for pumps only minor tritium contamination is found in the accelerator parts. Ion pumps tend to capture the tritium; oil pumps exhaust it. The deuterium-tritium reaction accounts for much less than 1% of the total tritium lost from the target therefore the build-up in the vacuum system is substantial because approximately 0.3 curie of tritium is displaced from the target per coulomb of deuterium beam.

In order to minimize the probability of large scale contamination in the target room, it is advantageous, whenever possible, to "pig" the target and exhaust the "pig" directly into the stack.[6] (Pigging is essentially constructing a small enclosure around the target and controlling the exhaust of that small volume in preference to the larger target room volume). This approach is effective for all types of target which may result in radioactive contamination of the target room.

In order to measure exhausting tritium a stack monitor consisting of a single ion chamber, a log picoameter, an airflow indicator, strip recorder, and an alarm is used in the stacks of the chemistry laboratory at LRL.[7]

Room monitors with alarm capabilities and ranges of full scale reading to 10 to 10^7 $\mu Ci/m^3$ are satisfactory and should be used where possible tritium leakage exists.

Routine use of portable air sampling survey instruments and wipe tests measured using liquid scintillation techniques will insure prompt detection of leaks.

Jacobs[8] reports that for routine tritium monitoring in air the ionization chamber with gamma compensation is simple, rugged and satisfactory.

Exhaust Characteristics

In determining the adequacy of a ventilation system it is necessary to determine not only the amount of contaminated waste discharged in the effluent but also the expected distribution of the waste after release to the environment. This distribution is seriously subject to the whims of meterological change. From a conservative point it may be evaluated under worst possible atmospheric conditions or at least the worst likely atmospheric conditions.

Considerable work has been done in establishing techniques for estimating dispersion of effluents by those concerned with air pollution and industrial plant siting. Reference[9] has been used to prepare Figures VIII-4, VIII-5, and VIII-6. The general equation for ground level concentrations at x meters from the exhaust is:

$$X(x,y,o) = \frac{Q}{\pi \sigma_y \sigma_z \bar{u}} e^{-\frac{h^2}{2\sigma_z^2} + \frac{y^2}{2\sigma_y^2}} \qquad \text{(VIII-4)}$$

where

X is in curies/m^3 (or g/m^3)

h = effective stack height (meters)

y = distance from axis of wind direction (m)

σ_y = crosswind plume standard deviation (Figure VIII-2)

σ_z = vertical plume standard deviation (Figure VIII-3)

$\bar{u}$ = mean wind speed at height of stack (m/sec)

x = downwind distance (m)

Q = release rate (Ci/sec) calculated from A_0 and A_1 in Chapter IV

Figures VIII-2 and VIII-3 are plotted for several stability conditions. The term "stability" as used in meteorology describes generally the tendency of the atmosphere to resist or enhance vertical motion. The temperature profile is used as an indicator of stability. A decrease in ambient temperature with height of 1C°/100 m indicates neutral conditions. More than 1C°/100 m tends toward unstable conditions and less towards stable conditions.

In order to determine a minimum stack height which will result in the required dilution some information must be known of the behavior of the plume. Moses, et al [10] have presented a comprehensive review of the several "height of rise" formulae. In spite of the large amount of research done in the field there exists some serious imprecision in the definitions of important terms. "Height-of-rise" is singled out by Moses, et al as one important term lacking specific definition.

Heat, a factor of great significance in the effectiveness of power plant stacks may be essentially neglected when considering the exhaust facilities of accelerators. That is the large temperature differential which would result in an increase in the bouyancy of the plume from the power plant stack. Without this temperature differential, the effective stack height is determined entirely by the stack dimensions, the discharge velocity, and the effect of the wind on the plume. Most formulas for the estimation of the effective stack height tend to underestimate which results in a conservative safety factor in the determination of ground level concentrations.

Moses, et al.[10] in their revue left no doubt that effective calculation of plume heights still requires some "black magic" yet within a factor of about 2, for the type of stack most likely required for an accelerator facility effective stack height for exhausts having little temperature excess may be calculated by:

$$h = h_s + D\left(\frac{v}{\bar{u}}\right)^{1.4}$$

where

h_s = actual stack height (m)

D = diameter of stack (m)

v = velocity of stack discharge (m/sec)

$\bar{u}$ = mean wind speed at height of stack (m/sec)

The maximum concentrations at any point x meters from the stack downwind may then the estimated by the following equation for a given set of meteorological conditions.

$$X(x,o,o) = \frac{2Q}{e\pi uh^2} \cdot \frac{\sigma_z}{\sigma_y} \qquad \text{(VIII-6)}$$

where X is concentration at x meters from the stack. ($\mu Ci/m^3$, mg/m^3, ppm, etc.).

Example Problem

Let us consider the example electron accelerator used in Chapter IV. What would the predicted maximum concentration of Nitrogen-13 be and where would it occur given the following parameters:

Energy of electrons		=	18 MeV
Current	i	=	10^{-1} amps
Beampath	d	=	5 m
Cell volume	V	=	560 m^3
Cell exhaust	v	=	4 m^3/sec
Stack height	h_s	=	25 m
Stack diameter	D	=	1 m
Average Wind Speed	$\bar{u}$	=	10 m/sec
Nitrogen-13 life time		=	1.67×10^{-3} sec

Unstable conditions.

Initially the stack exhaust rate of N^{13} must be calculated.

$$A_o = \frac{a_o}{v/V+1/\beta} \quad (1-e^{-[v/V+1/\beta]\,t_i})$$

$$= \frac{0.206}{0.0083} \quad (1)$$

$$= 24.8\ \mu Ci/m^3$$

therefore

$$Q = A_o v = (24.8)\ (4) = 99.2\ \mu Ci/sec$$

The effective stack height is

$$h = h + D\left(\frac{V}{\bar{u}}\right)^{1.4}$$

$$h = 25 + 1\ \left(\frac{4}{10}\right)^{1.4} = 25.28\ m$$

Since maximum ground concentration will exist at a downwind distance at which

$$\sigma_z = \frac{h}{2} = \frac{25.28}{2} = 17.9$$

$$\sigma_z = 18 \text{ at } 101 \text{ m}$$

$$\sigma_y = 18 \text{ at } 100 \text{ m}$$

Or using Figures VIII-4, VIII-5, or VIII-6 depending on stability conditions for

$$h - 25, \left.\frac{uX}{Q}\right|_{max} \text{ occurs at } x = 100 \text{ meters}$$

then

$$X_{max} = \frac{2Q}{e\pi\bar{u}h^2}\ \frac{\sigma_z}{\sigma_y}$$

$$X_{max} = 3.75 \times 10^{-3}\ \mu Ci/m^3$$

This is the predicted maximum concentration of N^{13} occurring at ground level from the 25 m stack. This concentration should occur at about 100 meters.

In addition to the exhaust rate and cross wind velocity other factors have significant effects on the behavior of the stack effluent (plume). The two most important factors are the temperature profile of the surrounding atmosphere and the presence of terrain irregularities or buildings.

The temperature profile has reasonable predictable effects on the plume and should be considered carefully in the location and design of stacks. Smoke studies made at Brookhaven National Laboratory[11] showed that under certain temperature inversion conditions the maximum concentration predicted by equation VIII-6 would be as much as 20 times too low for short periods of time.

In order to properly plan for the exhaust requirements of a particular facility it is necessary to learn the normal meteorological conditions which prevail as well as the frequency of variation from the normal.

In addition, although there is no completely suitable mathematical treatment available to determine the effect of random hills, valleys and neighboring building on the effluent of stacks, the effect is significant enough to warrant consideration in the determination of the stack location and characteristics. The airflow around large buildings in the vicinity of a stack will distract the plume even though the plume does not actually contact the building. The aerodynamic problem becomes more serious when the height of surrounding buildings is significant in comparison to the height of the stack.

Small accelerator facilities will seldom require the detailed meteorological surveys and reports necessary for reactors, power plants, etc., yet in order to insure the maximum safety some knowledge of the behavior of stack effluents is absolutely necessary.

There are many sources of climatological data which may be used in the study of the characteristics of a particular site. The best would of course be long term measurements made at the site but this is seldom available. Short-term measurements are necessary but should not be the basis for all situation estimates.

The U. S. Weather Bureau publishes data collected in approximately 12,000 observing stations and similar information is available in many other countries.

References

1. Code of Federal Regulations Title 49, Chapter I, parts 173 and 174. (Revised Jan 1, 1969).

2. Ghormley, J. A., Hochanadel, C. J. and Boyle, J. W., ORNL-P-4089 (1968).

3. Brynjolfsson, A., and Martin, T. G., Bremsstrahlung Production and Shielding of Static and Linear Electron Accelerators Below 50 MeV. Toxic Gas Production, Required Exhaust Rates, Int. J Radiation and Isotopes Vol 22, pp 29-40 (Jan 1971)

4. George, A. C., Breslin, A. J. Haskins, J. W., and Ryan, R. M , Proc. of USAEC First Symposium on Accelerator Radiation Dosimetry and Experience at Brookhaven National Laboratory, Nov 3-5, 1965, CONF 651109 (TID 4500), p. 539 (1965)

5. Nellis, D. O., Hudspeth, E. L., Morgan, I. L., Buchanan, P S , and Boggs, R F , Tritium Contamination in Particle Accelerator Operation, U. S Dept H E W , P H S , Pub. No. 999-RH (1967).

6. Ramler, W., Argonne National Laboratory personal communication

7. Silver, W. J. and Chew, M. H., Health Physics Aspects of Tritium Control at the Lawrence Radiation Laboratory, Livermore, UCRL-71327 (1969).

8. Jacobs, D. G., Sources of Tritium and its Behavior Upon Release to the Environment, TID-24635 (1968).

9. Smith, M. (Editor), Recommended Guide for the Prediction of the Dispersion of Airbourne Effluents, ASME, New York (1968).

10. Moses, H., Strom, G. H. and Carsen, J. E., Effects of Meteorological and Engineering Factors on Stack Plume Rise, Nuclear Safety 6. No. 1, p. 1-19 (1964)

11. Lowry, P. H., Microclimate Factors in Smoke Pollution from Tall Stacks, Meteorol Monographs 1(4): 26 (1961).

a

b

c

Radioactive Material Labels

Figure VIII-1 — a. "Radioactive White - I" label for radioactive material. White with red I on the lower half
b. "Radioactive Yellow - II" label. Upper half of the label is yellow, lower half is white with red II on the lower half.
c. "Radioactive Yellow - III" label. Upper half is yellow and the lower half is white with a red III on the lower half.

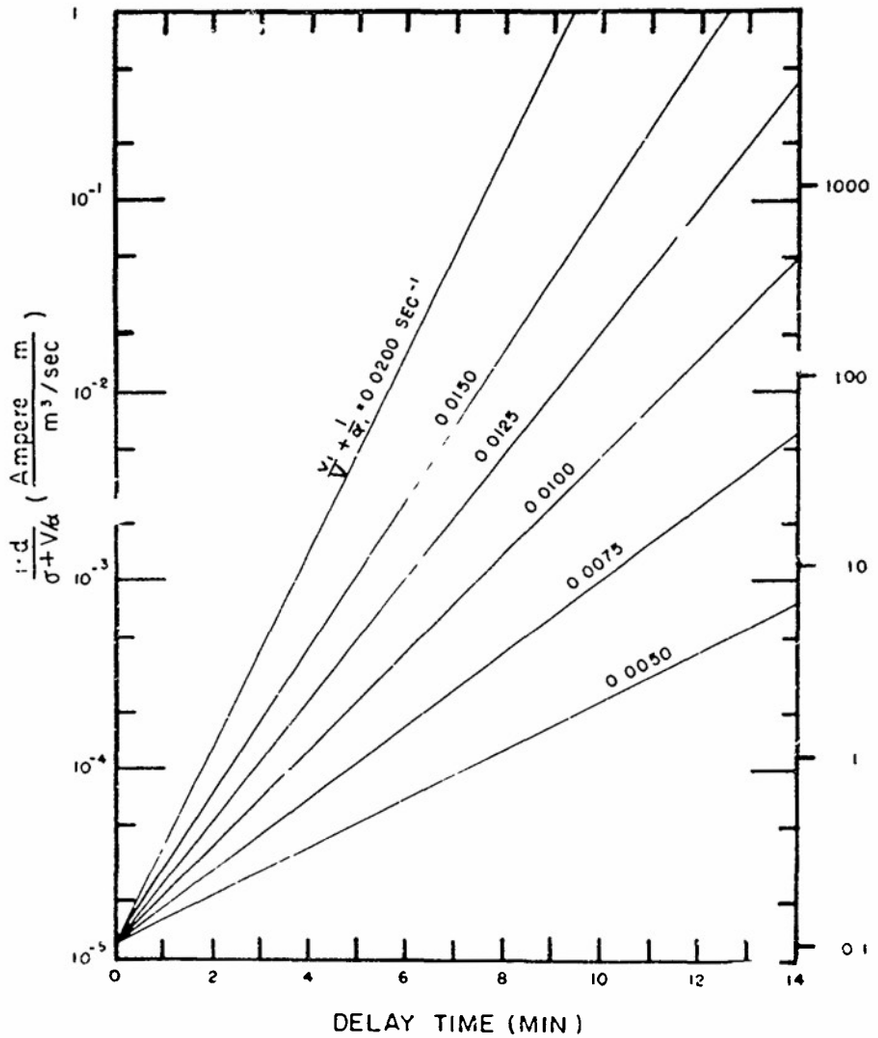

Figure VIII 2 Ozone concentration after shut off of the accelerator The abscissa indicates the time for decrease of O_3 concentration to 0 1 ppm plotted against a function of the rate of ozone production and the [illegible]

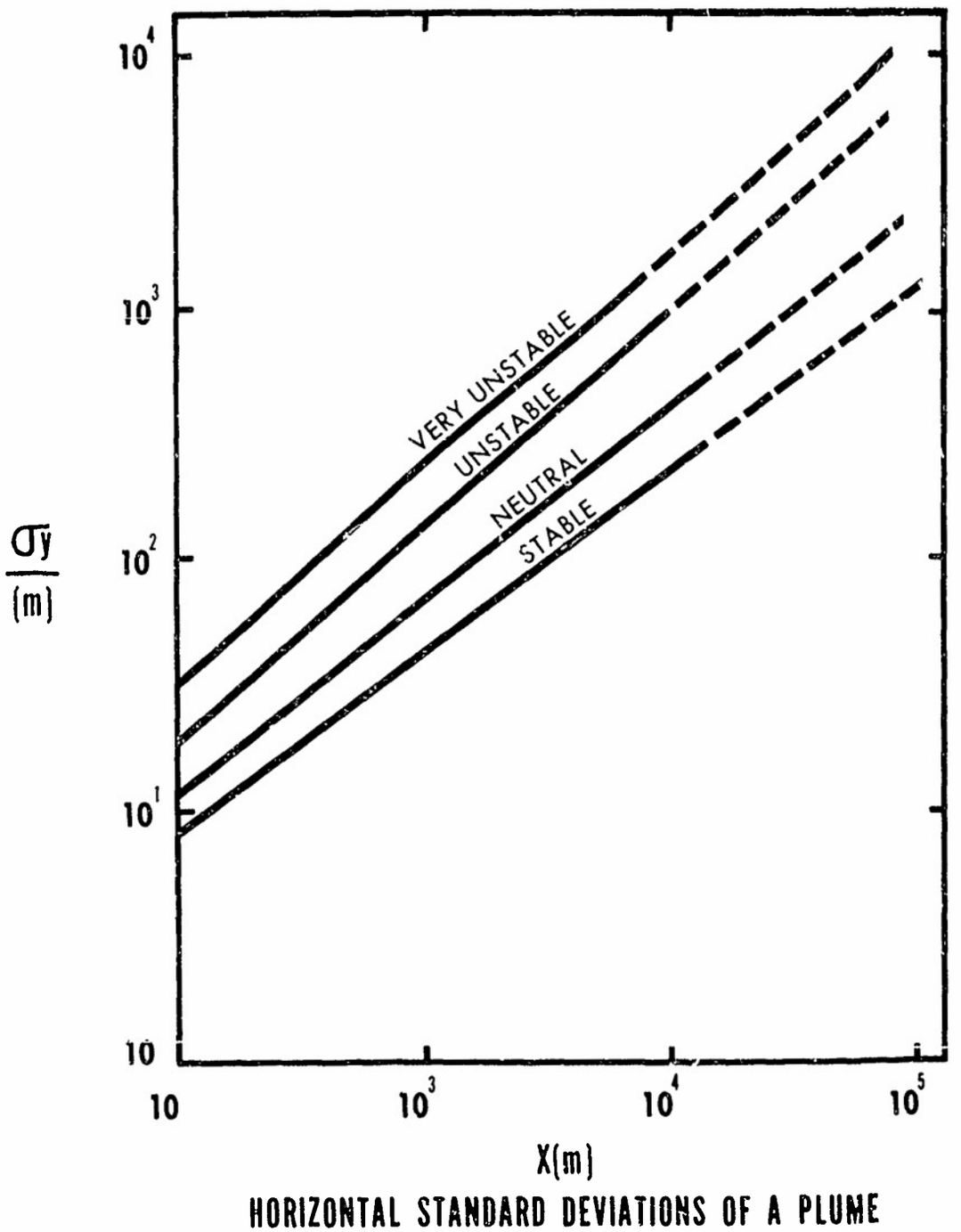

Figure VIII-3 — Horizontal standard deviations of a plume vs. distance from the stack. The dashed lines indicate that the relations are unreliable beyond 10,000 m. (Reprinted with Permission of the American Society of Mechanical Engineers.)

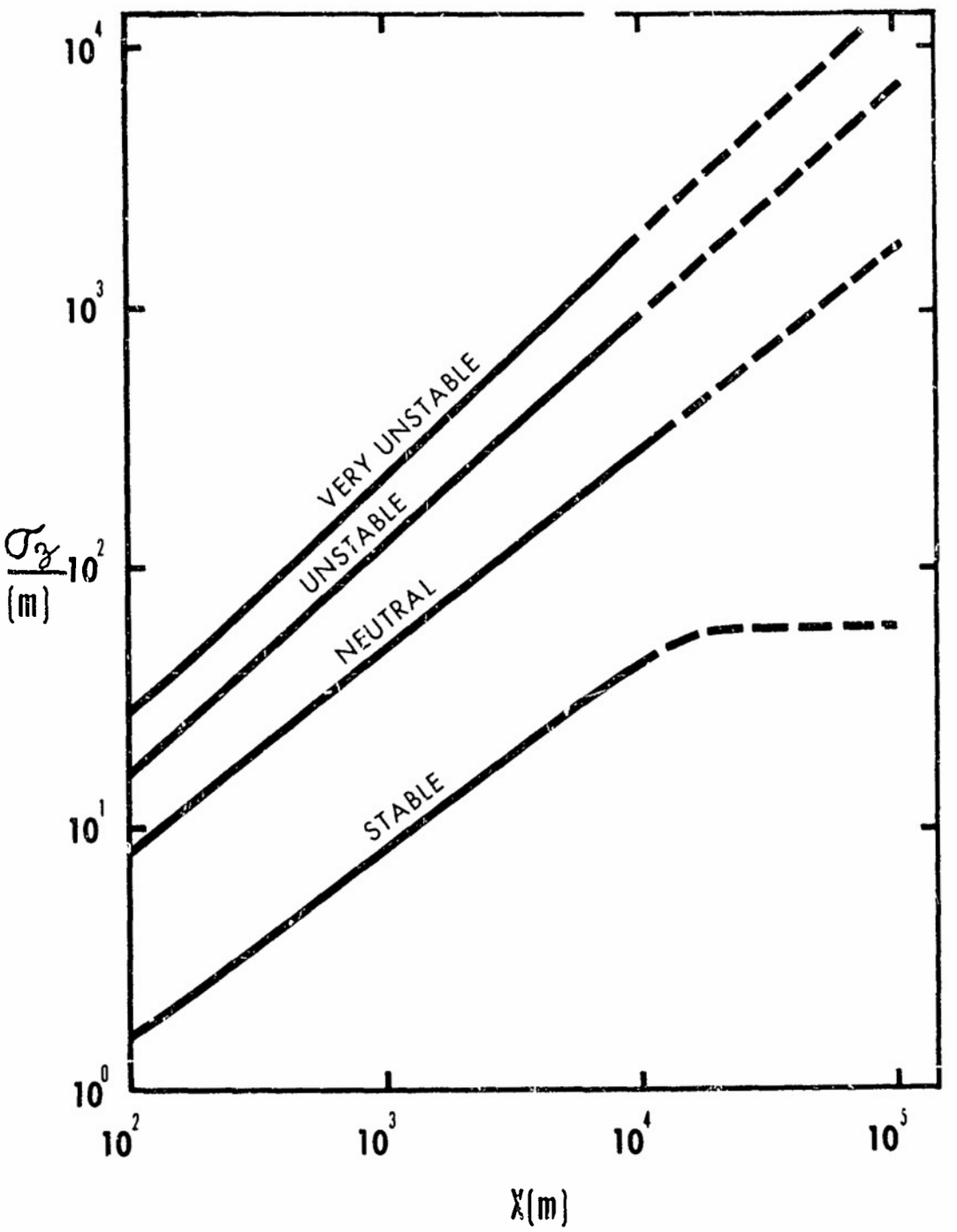

VERTICAL STANDARD DEVIATIONS OF A PLUME

Figure VIII-4 - Vertical standard deviations of a plume corresponding to those in Figure VIII-2. (Reprinted with the permission of the American Society of Mechanical Engineers.)

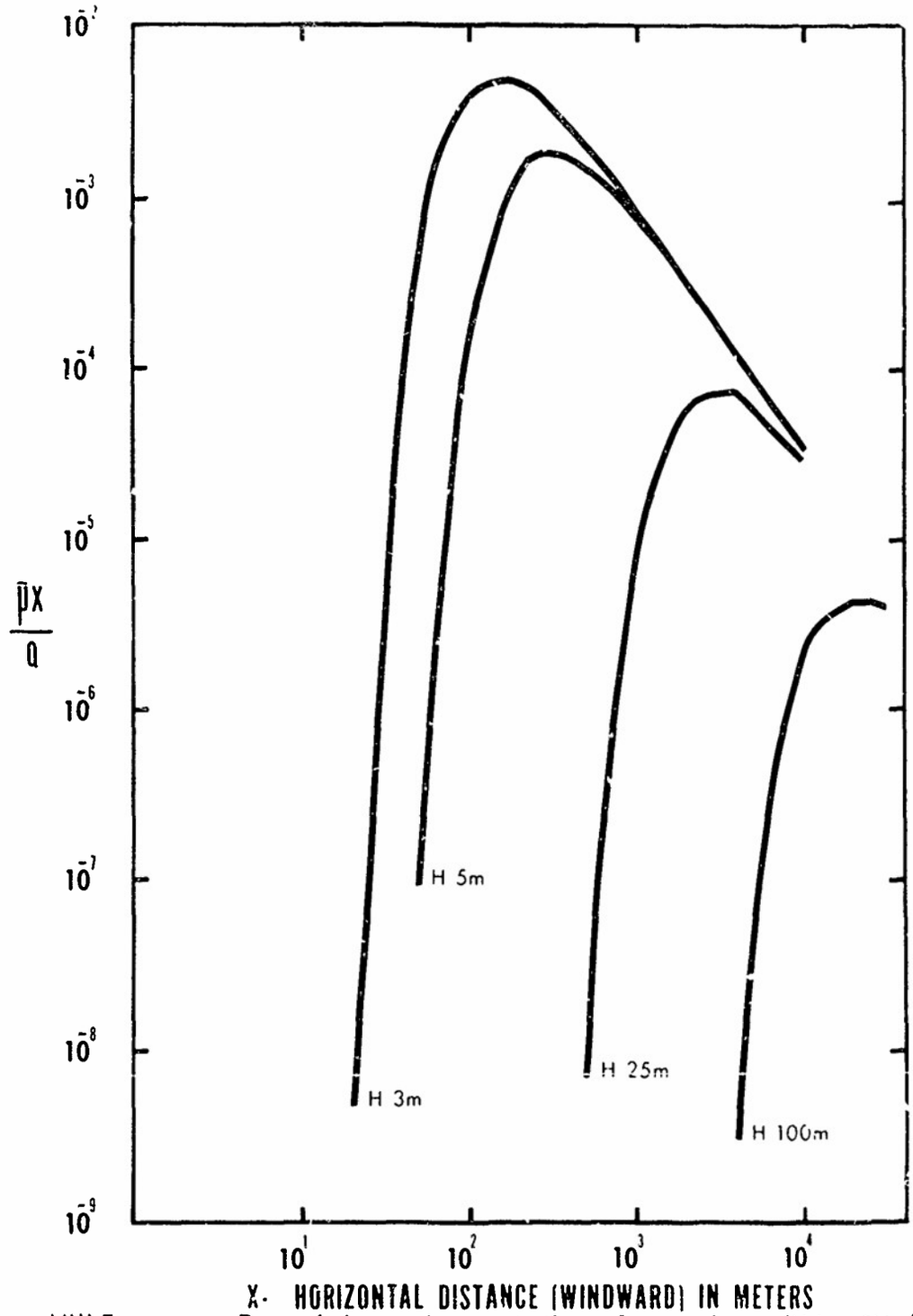

Figure VIII-5 — Downwind ground concentrations of contaminants (X in $\mu Ci/m^3$, g/m^3 etc.) The abcissa shows the distance from stack and the ordinate shows a function of the contaminant exhaust rate ($\mu Ci/sec$, g/sec, etc.) and the average wind speed (m/sec). plotted for several stack heights under stable conditions.

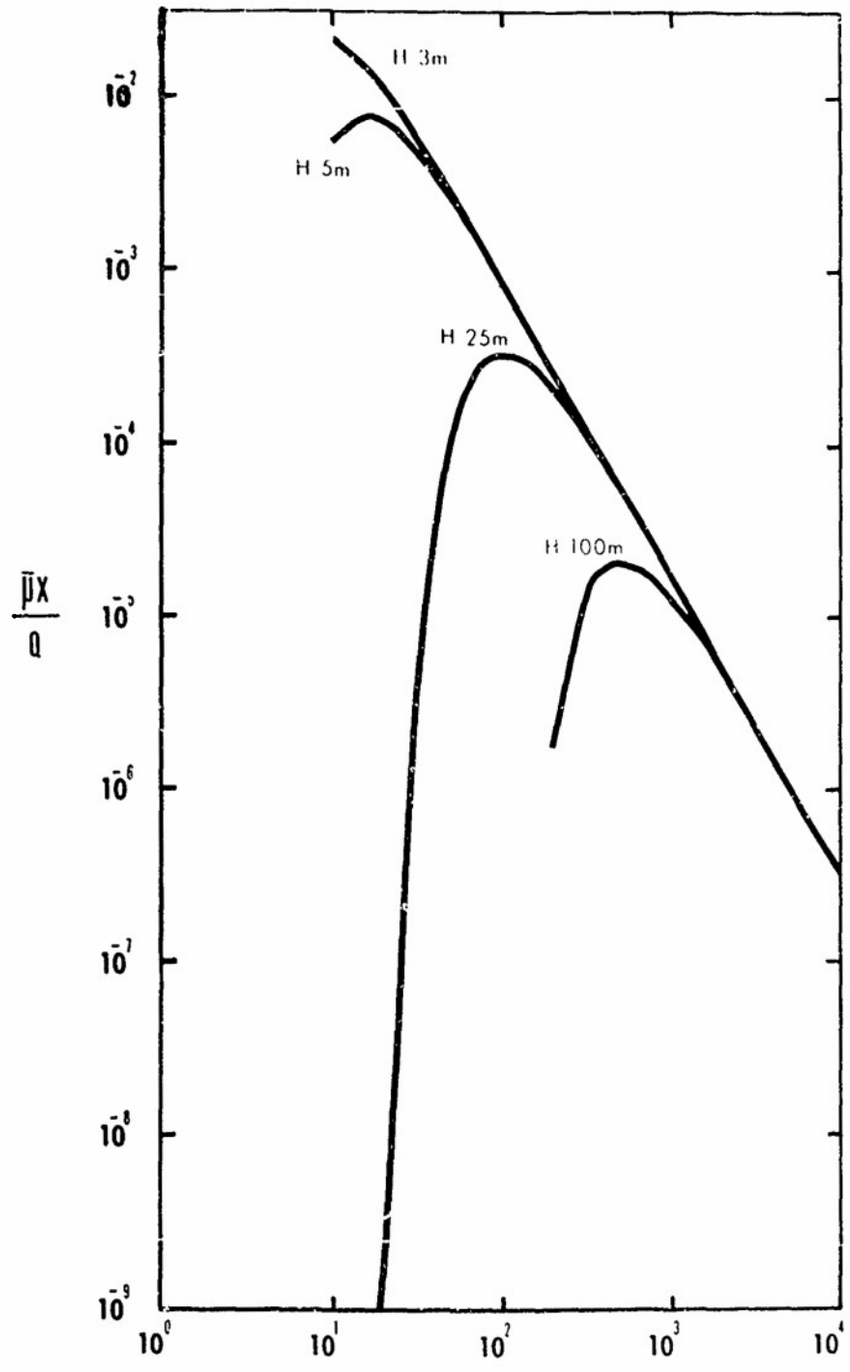

Figure VIII-6 -- Downwind ground concentrations of contaminant (X in $\mu Ci/m^3$, g/m^3, etc.). The abcissa shows the distance from the stack and the ordinate shows a function of the contaminant exhaust rate ($\mu Ci/sec$, g/sec, etc.) and the average wind speed (m/sec), plotted for several stack heights under unstable conditions.

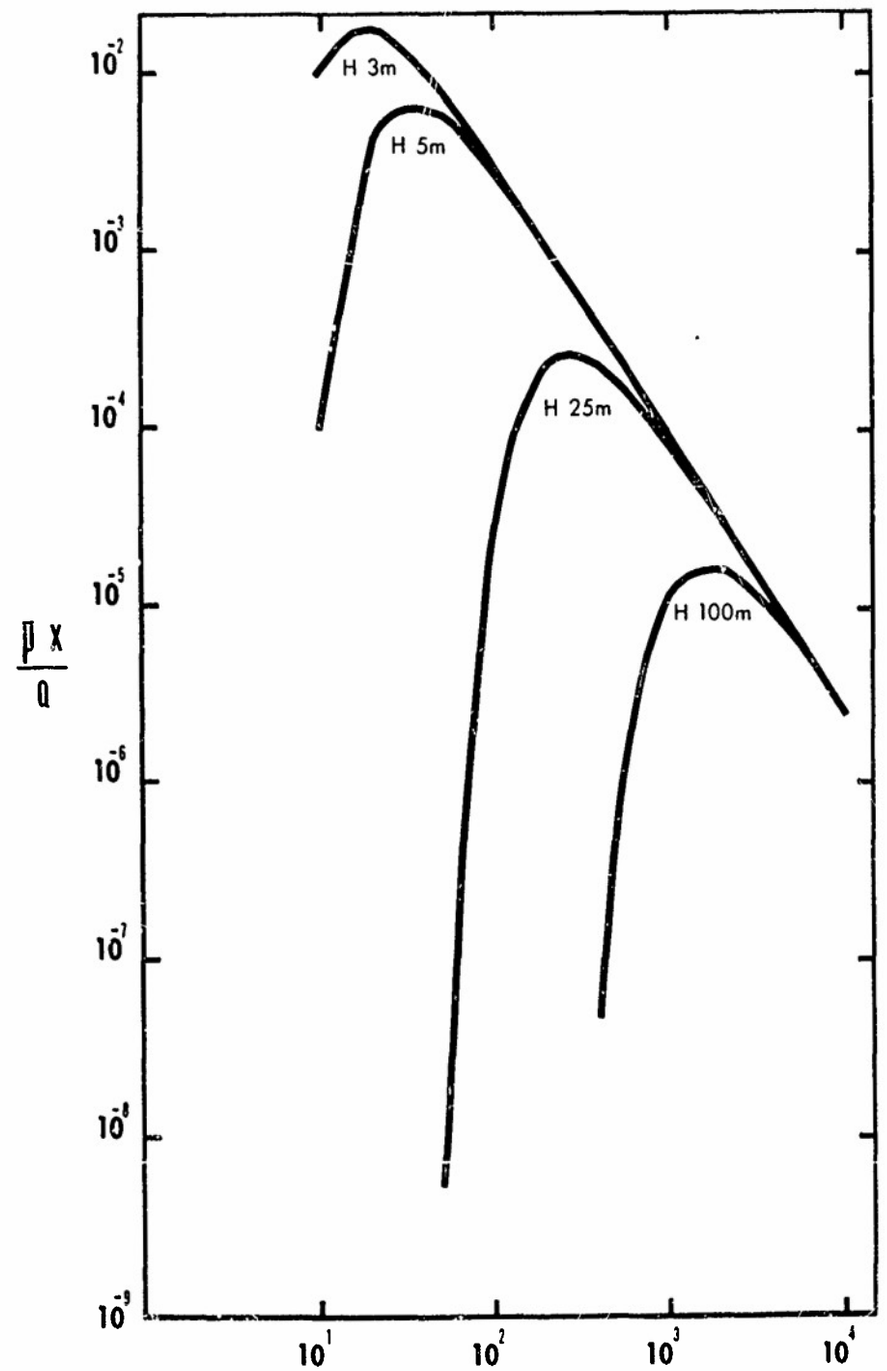

Figure VIII-7 — Downwind ground concentrations of contaminant (X in $\mu Ci/m^3$, g/m^3, etc.). The abcissa shows the distance from the stack and the ordinate shows a function of the contaminant exhaust rate ($\mu Ci/sec$, g/sec, etc.) and the average wind speed (m/sec), plotted for several stack heights under neutral conditions.

INDEX